1985

The reduction of transition metal complexes by tris(bipyridyl)ruthenium(1+) ion, chromium(II) ion, and the 1-hydroxy-1-methylethyl radical

Philip Connolly II
Iowa State University

Connolly, Philip, II

THE REDUCTION OF TRANSITION METAL COMPLEXES BY TRIS(BIPYRIDYL)RUTHENIUM(1+) ION, CHROMIUM(II) ION, AND THE 1-HYDROXY-1-METHYLETHYL RADICAL

Iowa State University PH.D. 1985

PLEASE NOTE:

In all cases this material has been filmed in the best possible way from the available copy. Problems encountered with this document have been identified here with a check mark ✓.

1. Glossy photographs or pages _____
2. Colored illustrations, paper or print _____
3. Photographs with dark background _____
4. Illustrations are poor copy _____
5. Pages with black marks, not original copy ✓
6. Print shows through as there is text on both sides of page _____
7. Indistinct, broken or small print on several pages ✓
8. Print exceeds margin requirements _____
9. Tightly bound copy with print lost in spine _____
10. Computer printout pages with indistinct print _____
11. Page(s) _____ lacking when material received, and not available from school or author.
12. Page(s) _____ seem to be missing in numbering only as text follows.
13. Two pages numbered _____. Text follows.
14. Curling and wrinkled pages _____
15. Dissertation contains pages with print at a slant, filmed as received _____
16. Other _____

University
Microfilms
International

The reduction of transition metal complexes by tris(bipyridyl)ruthenium(1+) ion, chromium(II) ion, and the 1-hydroxy-1-methylethyl radical

by

Philip Connolly II

A Dissertation Submitted to the
Graduate Faculty in Partial Fulfillment of the
Requirements for the Degree of
DOCTOR OF PHILOSOPHY

Department: Chemistry
Major: Inorganic Chemistry

Approved:

Signature was redacted for privacy.

In Charge of Major Work

Signature was redacted for privacy.

For the Major Department

Signature was redacted for privacy.

For the Graduate College

Iowa State University
Ames, Iowa

1985

TABLE OF CONTENTS

LIST OF FIGURES

LIST OF TABLES

DEDICATION

To Jeanne, my loving and sometimes patient wife, without her this work could never have been done. Also, to my parents Philip and Annette, for their love, support, and dedication to the education of their children.

GENERAL INTRODUCTION

Chapter I describes the kinetics and mechanism of the reduction of some transition metal complexes by tris-(bipyridyl)ruthenium(1+) ion. This ion is generated on a microsecond time scale, using a laser flash apparatus. Among the several topics discussed are: the mechanism for the reduction of some pyridinechromium(III) complexes, the possibility of a long-lived pentaaquo(organo)chromium(1+) ion, and the reaction of benzyl radical with europium(II) ion.

Chapter II presents the first known homogeneous catalytic production of hydrogen from chromium(II) or europium(II) ion solutions. The kinetics and mechanism of this reaction will be discussed in terms of Michaelis-Menten enzyme kinetics.

Chapter III presents a new method for the generation of 1-hydroxy-1-methylethyl radical for kinetic measurements. The photochemically produced radical is reacted with several cobalt(III) complexes. The kinetics and mechanism of these reactions are discussed.

CHAPTER I. KINETICS AND MECHANISM OF ELECTRON TRANSFER TO TRANSITION METAL COMPLEXES BY PHOTOCHEMICALLY PRODUCED TRIS(BIPYRIDYL)RUTHENIUM(1+) ION

Introduction

The photochemistry of tris(bipyridyl)ruthenium(2+) ion and the reactivity of the excited state, $[Ru(bpy)_3^{2+}]^*$, have received much attention during the past decade[1-6]. The electronic configuration of the excited state most closely approximates a charge separated Ru(III) metal center and a ligand radical anion[2]. As such, the excited state is a strong oxidant ($E^\circ_{*/+}$ = 0.84 V)[2]. Thus, reduction of the charge transfer excited state can easily be effected using rather mild conditions. For example, the species of interest in this work, tris(bipyridyl)ruthenium(1+) ion, is readily produced by reduction of $[Ru(bpy)_3^{2+}]^*$ with a variety of reagents, including Eu^{2+} (most frequently employed here), $Ru(NH_3)_6^{2+}$, and ascorbate ion. $Ru(bpy)_3^+$ is a strongly reducing (E° = - 1.28 V)[2] complex containing ruthenium in the +2 oxidation state and a ligand radical anion.

Reductions of metal ion complexes are a topic of interest and have been investigated by our group[7-12]. The strongly reducing nature of the $Ru(bpy)_3^+$ ion and the photochemical means for its production has enabled the extension of these interests to systems not easily reduced and monitored.

One such set are some chromium(III) complexes, where there is a dearth of information concerning their reductions. Oxidations of pentaaquo(organo)chromium(2+) ions can occur directly as the case of the reaction of Fe^{3+} with 2-hydroxy-2-propylchromium(2+) ion[13] or indirectly via homolytic cleavage of the chromium-carbon bond[14]. Reductions, on the other hand, have not been investigated.

Other chromium complexes of interest are pentaaquo-pyridinechromium(III) ion, $(H_2O)_5CrNC_5H_5^{3+}$, and analogues. Questions regarding the participation of the pyridine π system during the reaction and the effect of pyridine substituents on the rate need to be answered. A broader question must also be addressed: does electron transfer to the chromium complex occur via a ligated pyridine radical or does the electron transfer directly to the metal center?

Experimental

Photochemical Experiments The flash photolysis experiments were performed on a laser system modelled after one in the literature[15]. Figure I-1 shows a schematic diagram of the system used in this work. The excitation light was provided by a Phase-R model DL-1100 pulsed dye laser. Pulse widths of approximately 0.6 microseconds fwhm are obtained with this flash lamp pumped laser system. The dye used in these experiments was coumarin 460 (1.5×10^{-4} M in methanol), which emits light at 461 nm (±20 nm fwhm). The laser beam

impinges on the sample at right angles to the monitoring beam, which was provided by a 50 W quartz-halogen lamp that was filtered to remove light below 480 nm. A 75 W xenon arc lamp, unfiltered, was used to monitor absorption changes in the ultra-violet. The signal beam was passed through an Instruments SA grating monochromator and was detected with a Hamamatsu R928 photomultiplier tube. The electronic signal was collected, digitized, and displayed using a Nicolet model 2090-3A digital oscilloscope with a model 206-1 plug-in unit.

High transient concentrations of $Ru(bpy)_3^+$ were produced by flashing deaerated solutions containing 0.1 M $EuCl_2$[16,17], $(3-4)x10^{-5}$ M $Ru(bpy)_3Cl_2$, 0.25 M HCl, the complex to be studied, and enough NaCl to adjust the ionic strength to

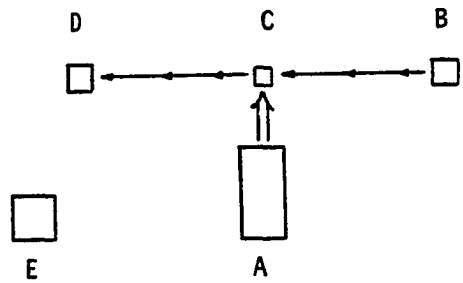

Figure I-1. A schematic diagram for the dye laser flash photolysis system where the components are: A) laser head, B) 50 W quartz-halogen lamp or 75 W Xe arc lamp, C) cell holder, D) grating monochromator and photomultiplier tube, E) Nicolet digital oscilloscope and Apple computer

1.00 M. Immediately prior to the photolysis of the reaction solution, the complex of interest was injected into a cell containing the remaining reagents and mixed by a stream of argon. The cell was protected from room light by aluminum foil.

The progress of the reaction can be followed at 510 nm, where $\Delta\varepsilon^{18} = 1.25 \times 10^4\ M^{-1}cm^{-1}$. Typically, there was a 200-300 millivolt change in PMT output, that was proportional to the transmittance change, during the course of the reaction. This corresponds to initial $Ru(bpy)_3^+$ concentrations of 20-30 μM.

Product Analyses Several of the products were analyzed by their UV-vis absorption spectra using either a Varian model Cary 219 spectrophotometer or a Perkin Elmer diode array spectrophotometer. Organic analyses were performed using a Hewlett Packard model 5790 gas chromatograph equipped with a six foot OV-101 column.

Reagents $EuCl_3$ -- A weighed quantity of Eu_2O_3, supplied by the Ames Laboratory, was dissolved in an excess of hydrochloric acid, such that the final concentrations were about 0.4 M for the Eu(III) and 0.25 M for the HCl.

$EuCl_2$ -- Europium(II) chloride solutions were prepared by zinc-amalgam reduction of the europium(III) chloride solution. The $EuCl_2$ solution was kept on the amalgam, protected from light, for at least two hours before it was used.

$Ru(bpy)_3Cl_2$ -- This salt, purchased from Aldrich Chemical

Company, was recrystallized once from warm water (ca 45°C) and then dried under a moderate vacuum. It was stored in the dark until used.

$Cr(ClO_4)_3$(hydrate) -- Chromium(III) perchlorate was prepared by the reduction of CrO_3 by H_2O_2 in perchloric acid. The product was recrystallized twice from dilute perchloric acid.

$Cr(ClO_4)_2$ -- Solutions of chromium(II) ion were prepared by zinc-amalgam reduction of the chromium(III) perchlorate solution.

$[(H_2O)_5Cr(4\text{-}(CH_2)C_5H_4NH)]Cl_3$ -- The 4-pyridiomethylchromium(2+) ion was prepared by a literature method[19]. 4-Bromomethylpyridinium bromide (0.191 g) was dissolved in 10 mL of 0.1 M HCl, deaerated, and treated with 20 mL of 0.112 M $Cr(H_2O)_6^{2+}$ solution (approximately a 30% excess). The excess chromium(II) ion was destroyed by passing a stream of pure O_2 through the reaction solution for about one minute. The product was then separated on a Sephadex SP C-25 cation exchange column, using acidified NaCl as the eluent. The concentration of the final product was determined spectrophotometrically: λ 225 nm (ε=6750 $M^{-1}cm^{-1}$), 308 (1.56×10^4), and 550 (92).

$[(H_2O)_5CrCH_2Ph]Cl_2$ -- The benzylchromium(2+) ion was prepared, as before[20], by injection of 9.8 mL of 0.112 M chromium(II) into a deaerated acetone solution containing 100

μL of $PhCH_2Br$. The solution was diluted five-fold with 0.01 M HCl, and separated by ion-exchange chromatography. The concentration of the benzylchromium was determined by its UV-visible spectrum: λ 355 nm (ε=2200 $M^{-1}cm^{-1}$), and 297 (6970).

$[(H_2O)_5CrCH_2OCH_3]Cl_2$ -- Methoxymethylchromium(2+) ion was prepared by the modified Fenton's reagent method[21]. Dimethyl ether was dissolved in a deaerated solution containing hydrogen peroxide and perchloric acid. A solution of chromium(II) ion was then injected and the product was separated and purified on Sephadex resin. The absorption spectrum for this complex show maxima at λ 530 nm (ε= 15.3 $M^{-1}cm^{-1}$) and 385 (404)[22].

$[(H_2O)_5CrCF_3]Cl_2$ -- The trifluoromethylchromium(2+) ion was prepared by the literature method[23]. Trifluoromethyl iodide was bubbled through 10 mL of 0.112 M chromous ion solution for 20 minutes. The solution was then allowed to stir under a positive pressure of CF_3I for 1.5 hours. The positive pressure of the CF_3I was then removed, and the solution was stirred for an additional 24 hours. The product was purified by ion-exchange. The UV-visible spectrum of this organochromium ion shows maxima at λ 380 nm (ε= 77.6 $M^{-1}cm^{-1}$) and 490 (43.2).

$[(H_2O)_5CrCHCl_2](Cl)_2$ -- The dichloromethylchromium(2+) ion was prepared by a modification of the literature method[24]. The reagents were deaerated separately and then combined in

the reaction vessel. Typically, 12 mL of H_2O, 10 mL of $CHCl_3$, and the required amount of perchloric acid to make the solution approximately 0.01 M in hydrogen ion, were combined in a 50 mL Erlenmeyer flask. With vigorous stirring, 1.4 mmol of chromium(II) solution are added. The solution turned, in stages, from blue to brown over the course of the reaction, which took approximately 2 hr. Chloroform was removed by rotary evaporation. An excess of $Hg(ClO_4)_2$ solution was then added and the reaction mixture allowed to stand for 30 mins, after which 4 mL of 2 M NaCl solution was then added and the precipitate formed left to settle for 20 mins. The precipitate was removed by filtration and the supernatant, after a four fold dilution, was loaded on a Sephadex SP C-25 ion exchange resin. The column is washed with 100 mL of 0.05 M HCl until a sulfide test for Hg^{2+} was negative. The organochromium ion was then eluted from the column with 0.25 M HCl. The complex was characterized by its UV-Visible spectrum: λ 514 nm (ε= 38.7$M^{-1}cm^{-1}$), 396 (157), and 266 (4290).

[cis-$(H_2O)_4Cr(py)_2]Cl_3$ -- The cis-(bispyridine)tetraaquo-chromium(3+) ion was prepared[25] by dissolving $[Cr(py)_2(H_2O)_2(OH)_2]Cl$ in excess HCl and removing, by filtration, the green precipitate ($Cr(py)_3Cl_3$). The solid sample, [cis-$Cr(py)_2(H_2O)_2(OH)_2]Cl$[26], was obtained from Andreja Bakac. The purple solution of the cis-$(H_2O)_4Cr(py)_2^{3+}$

ion was then ion-exchanged on Sephadex SP C-25 resin. The concentration of the final solution was obtained from its absorption spectrum: λ 533 nm (ε= 25.9 $M^{-1}cm^{-1}$), 393 (35.6), and 259 ($6.85x10^3$).

$[(H_2O)_5Crpy]Cl_3$ -- The monopyridinepentaaquochromium(3+) ion was prepared[27] by placing freshly ion-exchanged bis(pyridine)chromium(3+) in 1.0 M $HClO_4$ in a 75 °C water bath for 11.5 hours. The product was then purified by ion-exchange on Sephadex resin. The concentration of the monopyridine chromium complex was determined from its UV-visible absorption maxima[28]: λ 560 nm (ε= 18.2 $M^{-1}cm^{-1}$), 402 (20.8), and 260 ($3.46x10^3$).

$[(H_2O)_5Cr(NC_5H_4X)]Cl_3$ -- The substituted (X= Me, Cl, CN) pyridine complexes were prepared by modifications of the literature[28-30] preparations. These complexes were characterized by their UV-visible absorption spectra. Typically, 2 x 10^{-3} mols of CrO_3 and an equivalent amount of the desired pyridine were dissolved in 2 mL of water. This solution was cooled to 0 °C. 2 equivalents of 30% H_2O_2 (cooled to 0 °C) was then slowly added to the Cr(VI) solution; a blue paste formed during this procedure. Immediately following the addition of the H_2O_2, 7.5 equiv. of Fe^{2+} ion, in 11 equiv. of $HClO_4$, and cooled to 0 °C, were added. This usually caused the blue paste to float in the Fe^{2+} solution. The reaction flask was allowed to warm to room temperature, and, as this

occurred, the paste began to dissolve and the solution became purple. Approximately 10 minutes after the paste had dissolved the reaction solution was diluted four-fold with distilled water. The pyridine chromium complex was then placed onto a Dowex 50W-X8 ion-exchange resin and washed with 1000 - 1500 mL of 0.1 M NaSCN solution in 1 M HCl. The pyridine chromium complex was eluted with 3 M HCl. The UV-vis. absorption maxima (in nm followed by the extinction coefficients in parentheses) for the complexes are: 561(18.5), 402(20.6), 273(3.43×10^3) for the 3-chloropyridine complex, 561(19.0), 402(20.5), 265(3.38×10^3) for the 3-cyanopyridine complex, and 558(18.6), 402(20.8), 268(3.52×10^3) for the 4-methylpyridine complex.

$[Co(NH_3)_6]Cl_3$ and $[Co(en)_3]Cl_3$ -- Hexaamminecobalt(III) chloride[31] and tris(ethylenediammine)cobalt(III) chloride[32] were prepared following literature procedures, and were obtained from M. Steven McDowell[33].

$Co(sep)Cl_3$ -- The cobalt(III)sepulchrate was obtained as a gift to A. Bakac and J.H. Espenson from Alan Sargeson, and was prepared by the literature method[34].

$Yb(ClO_4)_3$ and $Sm(ClO_4)_3$ -- Ytterbium(III) and samarium(III) perchlorate solutions were previously prepared[35] by dissolving the corresponding oxide in perchloric acid.

$[Ni(tetramethylcyclam)](ClO_4)_2$ -- The $Ni(tmc)^{2+}$ was a gift from A. Bakac and was prepared by the literature methods[36,37].

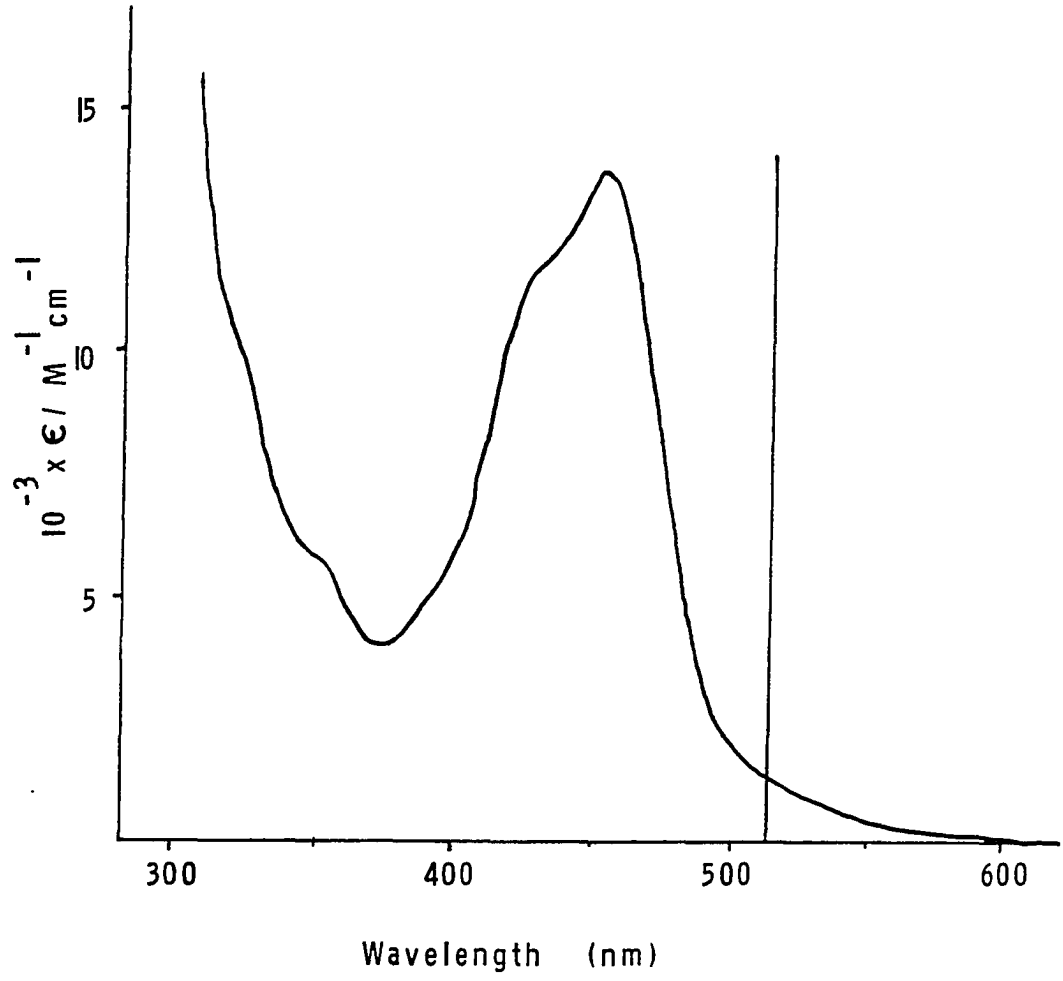

Figure I-2. The UV-visible spectrum of tris(bipyridyl)-ruthenium(II) chloride in water. The vertical line drawn at λ 510 nm shows the position of the absorption maximum for the tris(bipyridyl)-ruthenium(1+) ion; its length corresponds to the molar absorptivity at this wavelength

Results

Photochemistry and Kinetics The general photochemical sequence for the production and reactions of the tris(bipyridyl)ruthenium(1+) ion is represented in Scheme 1. The charge-transfer excited state of the $Ru(bpy)_3^{2+}$ ion is produced by irradiating the absorption band at 452 nm; an absorption spectrum for the ruthenium(II) complex is depicted in Figure I-2. This excited state is reductively quenched, with a rate constant k_q, to the $Ru(bpy)_3^{+}$ ion. The quencher used, for the most part, was the Eu^{2+} ion. If no other reactants are present in the system, the oxidized form of the quencher and the $Ru(bpy)_3^{+}$ ion simply revert to their original state by a back reaction, k_b. Systems containing an oxidizing substrate, M_{ox}, for the $Ru(bpy)_3^{+}$ ion can easily be monitored

Scheme 1

$$Ru(bpy)_3^{2+} \xrightarrow{h\nu} {}^*Ru(bpy)_3^{2+} \quad (1)$$

$${}^*Ru(bpy)_3^{2+} + Q \xrightarrow{k_q} Ru(bpy)_3^{+} + Q^{+} \quad (2)$$

$$Ru(bpy)_3^{+} + Q^{+} \xrightarrow{k_b} Ru(bpy)_3^{2+} + Q \quad (3)$$

$$Ru(bpy)_3^{+} + M_{ox} \xrightarrow{k_4} Ru(bpy)_3^{2+} + M_{red} \quad (4)$$

by virtue of the large molar absorbance of the ruthenium reactant at λ 510 nm ($\Delta\varepsilon$ = 1.25 x 10^4 M^{-1} cm^{-1})[18], provided that the reaction is faster than the back reaction. This condition was met for most of the reactions studied here. The complexes with the slower rates of reaction, however, are somewhat affected by the back reaction.

The rate constants for the reactions were obtained from an analysis of the decrease in absorbance at 510 nm vs. time data. The plots of log|Δ Abs| vs. time were linear, in most cases for more than 4 half lives, indicating a first order decay of the ruthenium(1+) complex. In the case of the reduction of benzylchromium(2+) ion, the plots were curved after one or two half-lives and better fits of the data were obtained by adjusting the infinity absorbance values. The first-order loss of $Ru(bpy)_3^+$ was confirmed by varying its initial concentration. The value of the observed rate constant was independent of these concentration changes.

$$-d[Ru(bpy)_3^+]/dt = k_4[M_{ox}][Ru(bpy)_3^+] \qquad (5)$$

$$k_{obs} = k_4[M_{ox}] \qquad (5a)$$

The observed rate constants for the decay of the $Ru(bpy)_3^+$ varied linearly with the concentration of the substrate, M_{ox}. Thus, the reaction between the ruthenium complex and M_{ox} follows the second-order rate law shown in eq 5. The plots of k_{obs} against $[M_{ox}]$, for reactions with second-order rate constants $>10^8$ $M^{-1}s^{-1}$, did not show an intercept. However, the 3-chloro-pyridine and 3-cyanopyridine chromium complexes and the slower reactions did. The intercept in the latter cases can be attributed to the back reaction between the oxidized quencher and the $Ru(bpy)_3^+$ ion.

Kinetic Results The concentration and observed rate constant data for each of the reactions reported here are collected in the Appendix I at the end of this chapter. In the main body of the text, only the already analyzed data will be presented.

Before the questions regarding the reactivity of the chromium(III) complexes can be answered, the general behavior of the $Ru(bpy)_3^+$ ion must be addressed. The reactions of the ruthenium(1+) complex with a number of substrates, most notably O_2 and $Co(bpy)_3^{3+}$ [38], Cu^{2+} [15], and Eu^{3+} [17], have been studied. The reported rate constants are 7.4×10^9, 1.6×10^9, 5.2×10^8, and 2.7×10^7 $M^{-1}s^{-1}$ respectively. To extend some of this work, we examined the reductions of some cobalt(III) complexes, Yb^{3+}, Sm^{3+}, and $Ni(tmc)^{2+}$.

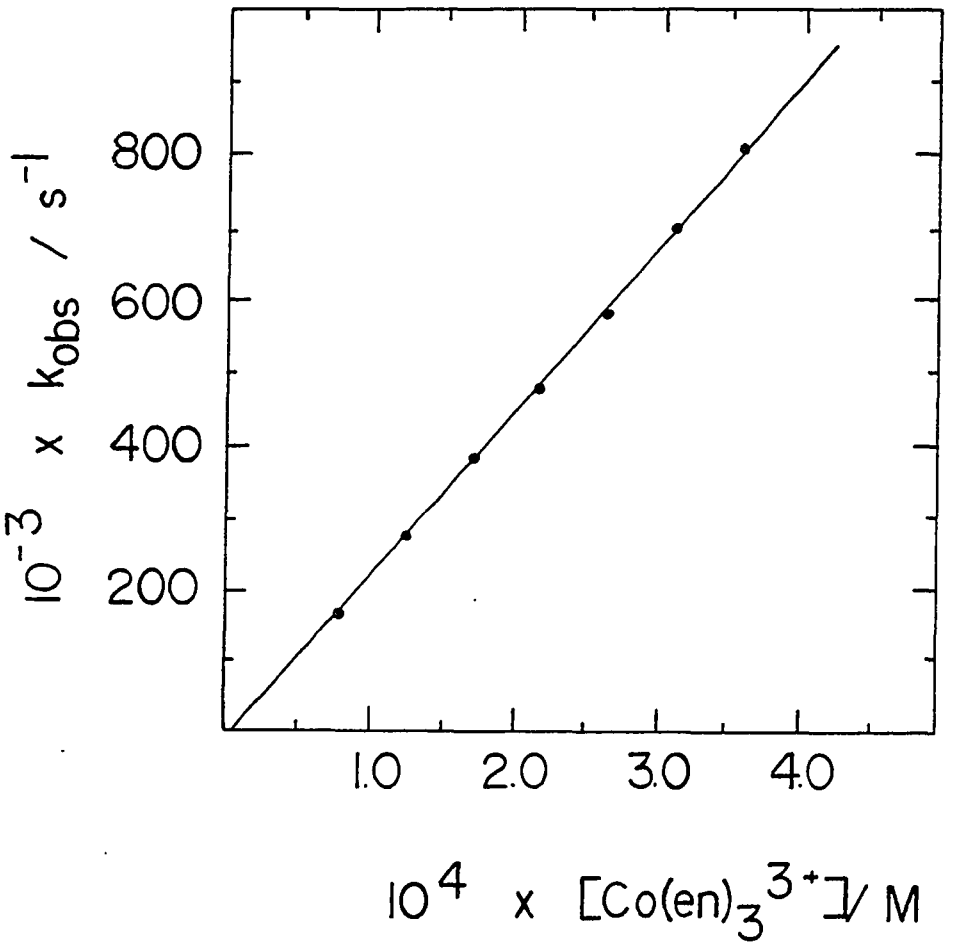

Figure I-3. The plot of the pseudo-first order rate constant for the reduction of tris(ethylenediaammine)-cobalt(III) chloride by $Ru(bpy)_3^{+}$ ion vs. the average concentration of $Co(en)_3^{3+}$. The second order rate constant is 2.29×10^9 $M^{-1}s^{-1}$

Cobalt(III) Complexes The reductions of several cobalt(III) complexes were studied. Figure I-3 shows a plot of the observed rate constants, k_{obs}, for the loss of $Ru(bpy)_3^{+}$ vs. the concentration of $Co(en)_3^{3+}$. The linear dependence of k_{obs} on the concentration of $Co(en)_3^{3+}$ confirms a second-order rate law (see eq 5) for the reaction. The rate constants for the reduction of this complex and other Co(III) complexes are all greater than 10^9 M^{-1} s^{-1} and are presented in Table I-1.

The value of the second-order rate constant for $Co(sep)^{3+}$ must be regarded as approximate since this cobalt complex

Table I-1. Rate Constants for the Reduction of Some Cobalt(III) Complexes[a,b]

Reactant	10^{-9} x k / M^{-1} s^{-1}
$Co(NH_3)_6^{3+}$	2.70(±0.08)
$Co(en)_3^{3+}$	2.29(±0.03)
$Co(sep)^{3+}$	>2
$MeCo(dmgBF_2)_2$	3.2 (±0.1)

[a]The pseudo-first-order rate constants for the individual kinetic runs are given as a function of the concentration of the reactants in Tables AI-1 through AI-4.

[b]T = 23 °C and I = 1.00 M.

reacts quite rapidly with the quencher[39], Eu^{2+}. The reaction can, however, be taken as real. The worst case scenario for this reaction is that the event monitored was simply the reduction of Eu^{3+} (formed in the complete reduction of $Co(sep)^{3+}$ by Eu^{2+}) by $Ru(bpy)_3^{+}$. If this were the case, however, even at the highest $Co(sep)^{3+}$ concentration used, 3×10^{-4} M, the maximum observed rate constant would be (2.7×10^{7} $M^{-1}s^{-1}$ [17]) x $[Eu^{3+}]$ = 8000 s^{-1}, significantly below the lowest observed value, 1.26×10^{5} s^{-1}.

Rare Earth Ions and $Ni(tmc)^{2+}$ Table I-2 gives the rate constants for the reduction of Yb^{3+}, Sm^{3+}, Eu^{3+}, and $Ni(tmc)^{2+}$ ions. The Eu^{3+} reduction was studied previously[17,40] and corroborated here. The trend in the rate constants between the rare earth ions, $Eu^{3+} > Yb^{3+} >> Sm^{3+}$, based on the values of their reduction potentials, is as expected. The reduction potentials are: -0.43 V[40], -1.15 V[41a], and -1.55 V[41b] for Eu^{3+}, Yb^{3+}, and Sm^{3+} respectively. In fact, no reaction is expected between Sm^{3+} and $Ru(bpy)_3^{+}$ since the reaction is thermodynamically forbidden ($K_{eq} = 10^{-4.6}$). Thus, the reaction observed with the Sm^{3+} is no more than the back reaction. Its particular usefulness in the context of this investigation is that it defines the limit above which an authentic reaction can be detected.

Chromium(III) Complexes The chromium(III) complexes can be divided into two groups depending upon the rates of their

reductions. The first group contains hexaaquochromium(III) ion and the organochromium(2+) ions. This set is distinguished from the set of pyridinechromium complexes by its relatively small rate constants (about 10^6 $M^{-1}s^{-1}$); the rate constants for the pyridinechromium complexes are around

Table I-2. Rate Constants for Reduction of Several Metal Ion Complexes at T = 23 °C [a]

Reactant	k / $M^{-1}s^{-1}$
Eu^{3+} [b]	2.7×10^7
Yb^{3+} [c]	$1.2(\pm 0.2) \times 10^5$
Sm^{3+} [d]	$< 2.0 \times 10^4$
$Ni(tmc)^{2+}$ [e]	$5.1(\pm 0.1) \times 10^8$

[a] The specific observed rate constant vs. concentration of reactant data are presented in Tables AI-17 and AI-18.

[b] I = 0.50 M ref 17 and 40.

[c] I = 1.1 M.

[d] I = 1.4M.

[e] $Ni(tmc)^{2+}$ is the 1,4,8,11-tetramethyl-1,4,8,11-tetraazacyclotetradecane complex of Ni(II). The quencher used in this experiment was the ascorbate anion at pH 11.1.

10^9 $M^{-1}s^{-1}$. Table I-3 contains the rate constants for the reduction of the various organochromium(III) complexes.

The reduction rate of $Cr(H_2O)_6^{3+}$ ion was found to be independent of the concentrations of both hydrogen and perchlorate ions. Figure I-4 is a plot of the pseudo-first order rate constant against the concentration of $Cr(H_2O)_6^{3+}$. The small intercept is due to the competition of the back reaction with the chromium(III) reduction, as discussed

Table I-3. Rate Constants for the Reduction of Some Organochromium(III) Complexes[a,b]

Reactant	10^{-7} x k / M^{-1} s^{-1}
$Cr(H_2O)_6^{3+}$	0.459(±0.009)
$(H_2O)_5CrCF_3^{2+}$	<0.05
$(H_2O)_5CrCH_2OCH_3^{2+}$	0.2 (±0.15)
$(H_2O)_5CrCHCl_2^{2+}$	2.12(±0.07)
$(H_2O)_5CrCH_2Ph^{2+}$	3.2 (±0.4)
$(H_2O)_5CrCH_2C_5H_4NH^{3+}$	139 (±2)

[a]The specific observed rate constant vs. the concentration of reactant data are presented in Tables AI-5 through AI-10.

[b]T = 23 °C and I = 1.00 M.

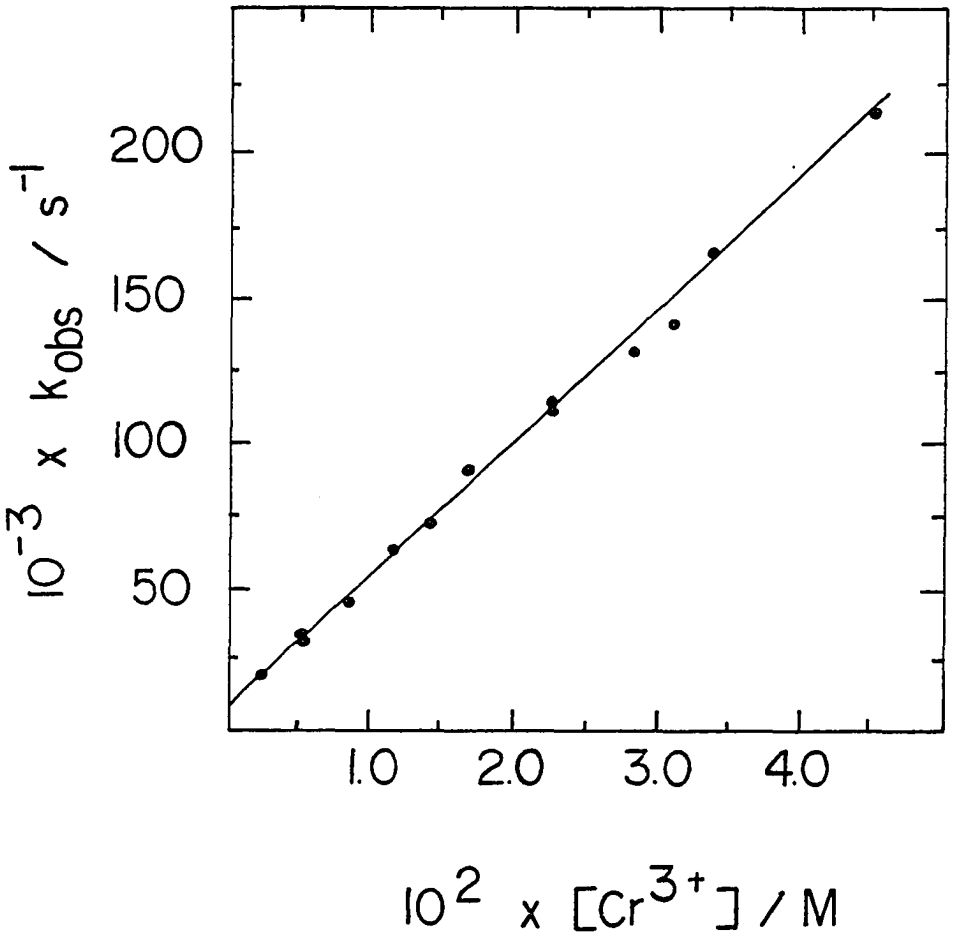

Figure I-4. The plot of the pseudo-first-order rate constant for the reduction of hexaaquochromium(III) ion by $Ru(bpy)_3^+$ vs. the concentration of $Cr(H_2O)_6^{3+}$. The value of the second-order rate constant is 4.6×10^6 $M^{-1}s^{-1}$. The small intercept is attributed to the "back" reaction between Eu^{3+} and $Ru(bpy)_3^+$ (see text)

previously. The rate constant for the reduction of $Cr(H_2O)_6^{3+}$ is $4.59(\pm0.09) \times 10^6$ $M^{-1}s^{-1}$.

Because the reduction of the organochromium complexes are relatively slow, these data are complicated by the back reaction between the Eu^{3+} ion and the $Ru(bpy)_3^{+}$ ion. Thus, these reactions are highly susceptible to small fluctuations in the quantity of Eu^{3+} present in the reaction solution. This was particularly evident in the reduction of the trifluoromethyl complex of chromium(III), where the reaction was at the limit of detection.

Coordination of a pyridine ligand to Cr^{3+} dramatically increases the reactivity of the complex. The rate constants for the reduction of the pyridinechromium complexes are given in Table I-4. The reaction of the pentaaquo(pyridine)-chromium(3+) ion follows a second-order rate law as the graph in Figure I-5 indicates. The rate constant for the reduction of $(H_2O)_5Crpy^{3+}$ is $5.5(\pm0.1) \times 10^8$ $M^{-1}s^{-1}$. Intercepts larger than expected were observed in the plots of the observed rate constants vs. the concentration of either the 3-cyanopyridine complex or the 3-chloropyridine complex (see Figure I-6). The value of the intercept and the second order rate constant were, however, independent of the $Ru(bpy)_3^{2+}$ and $Ru(bpy)_3^{+}$ concentrations.

In a search for a bound pyridyl radical to chromium, a 1 mM solution of the 3-cyanopyridine complex or the pyridine

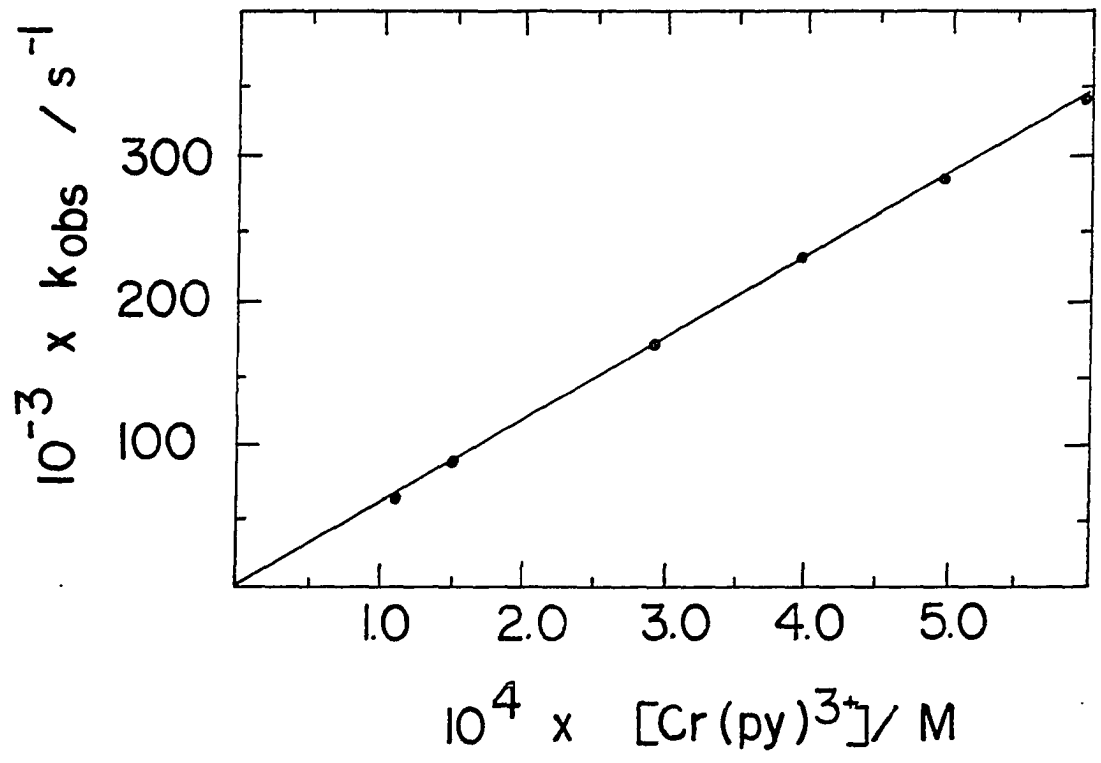

Figure I-5. The plot of the pseudo-first order rate constant for the reduction of pentaaquo(pyridine)-chromium(3+) ion by $Ru(bpy)_3^+$ vs. the average concentration of $(H_2O)_5Cr(py)^{3+}$. The second order rate constant for the reaction is 5.5×10^8 $M^{-1}s^{-1}$

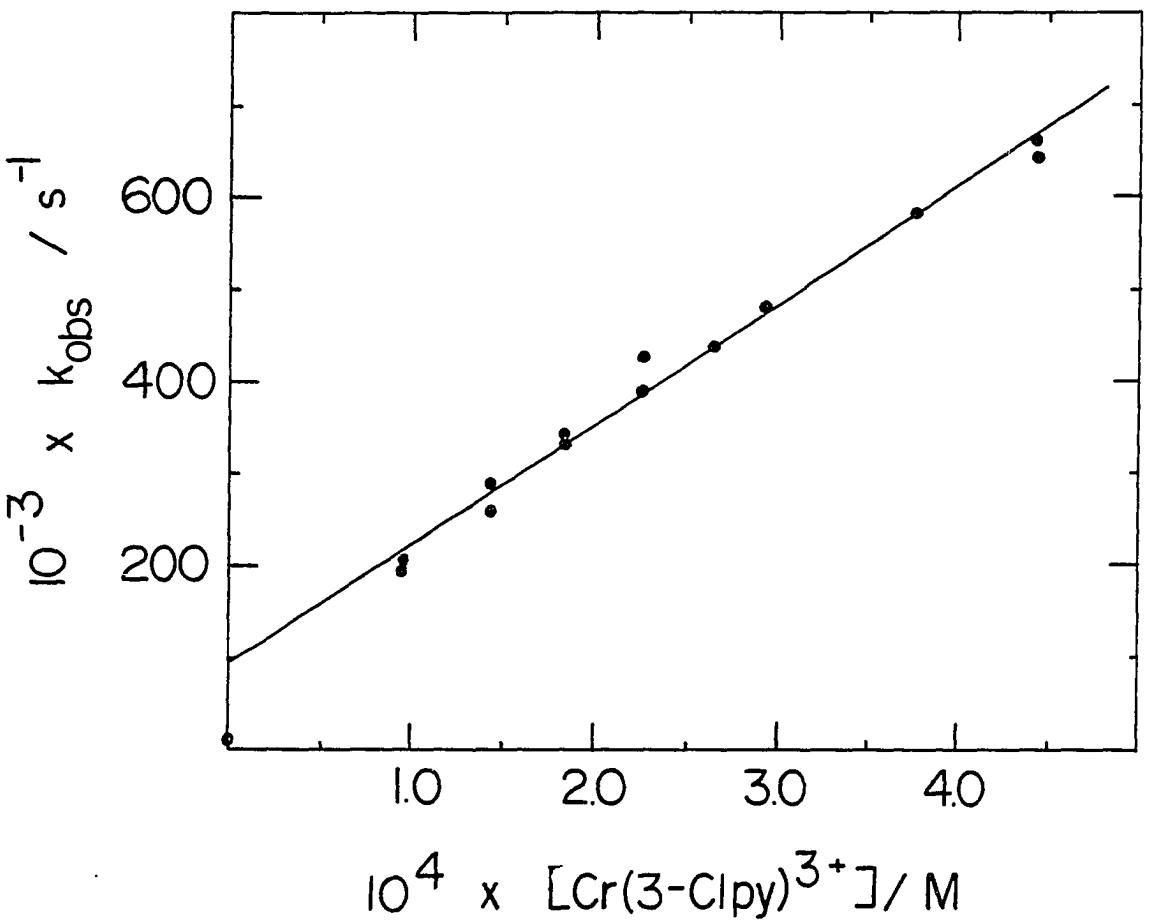

Figure I-6. The plot of the pseudo-first order rate constant for the reduction of pentaaquo(3-chloropyridine)-chromium(3+) ion by $Ru(bpy)_3^+$ vs. the average concentration of $(H_2O)_5Cr(3\text{-}Clpy)^{3+}$. The value of the second order rate constant is 1.29×10^9 $M^{-1}s^{-1}$. The point on the ordinate is the rate constant measured for the so-called back reaction, which is the expected intercept on this graph

Table I-4. Rate Constants for the Reduction of Some Pyridine Chromium Complexes[a,b]

Reactant	10^{-9} x k / M^{-1} s^{-1}
$(H_2O)_5Cr(4\text{-Mepy})^{3+}$	0.42(±0.01)
$(H_2O)_5Cr(py)^{3+}$	0.55(±0.01)
$(H_2O)_5Cr(3\text{-Clpy})^{3+}$	1.29(±0.04)
$(H_2O)_5Cr(3\text{-CNpy})^{3+}$	2.64(±0.07)
$(H_2O)_4Cr(py)_2^{3+}$	1.54(±0.03)
$(H_2O)_4Cr(bpy)^{3+}$	1.8 (±0.1)

[a]The observed rate constants and concentrations for each complex are presented in Tables AI-11 through AI-16.

[b]T = 23 °C and I = 1.00 M.

complex was reduced with $Ru(bpy)_3^+$. No longer-lived transients were observed in the region between 300 and 360 nm, where a pyridyl radical would be expected to absorb.[42]

Pyridinium and N-methylpyridinium ions do not react cleanly with the $Ru(bpy)_3^+$ ion. The reactions are fast, k's greater than 10^8 $M^{-1}s^{-1}$; however, they appear to be biphasic. This biphasic behavior was not observed in the reduction of the pyridinechromium complexes.

Product Analyses The reaction between $Cr(H_2O)_6^{3+}$ and $Ru(bpy)_3^{+}$ yielded Cr^{2+} as a product. After 45 minutes of irradiating the reaction mixture (Cr^{3+}, Eu^{2+}, and $Ru(bpy)_3^{+}$) with a 250 W sunlamp, an increase in absorbance above 700 nm could be observed. Cr^{2+} has a broad apsorption maximum in the region 690-740 nm (ε = 5 $M^{-1}cm^{-1}$), a region where all the other components of the system are nearly transparent. Chemical tests that could have been used to check the result and make it more quantitative were considered. Such tests for the presence of Cr^{2+} would entail its use as a reductant and are impractical because of the presence of a high amount of another strong reductant, the Eu^{2+} ion.

The pyridinium ion, released in the reduction of the $(H_2O)_5Cr(py)^{3+}$ ion, was determined by its UV spectrum[43] (λ 256 nm ε = 5290 $M^{-1}cm^{-1}$) after ion exchanging the reaction mixture. The reaction mixture, 1.5 mM $Cr(py)^{3+}$, 0.10 M Eu^{2+}, 3.6 μM $Ru(bpy)_3^{2+}$, and 0.19 M HCl, was flashed 100 times with the laser at 456 nm. Several fractions were collected from the ion-exchange column and the fraction with the most pyH^{+} ion had a concentration in excess of 2.3×10^{-4} M. The blank experiment, where the pyridinechromium complex and the Eu^{2+} ion were combined and allowed to stand for half an hour in the dark, produced no detectable pyH^{+}. Clearly, pyridine was released during the course of the reduction of the pyridinechromium complex.

No organic products could be detected in the reaction between the organochromium(III) ions and $Ru(bpy)_3^+$. The solutions were pulsed 100 times with the laser light, which should have produced approximately 1 mM solutions of products. The reaction solutions containing either $(H_2O)_5CrCH_2Ph^{2+}$ or $(H_2O)_5CrCHCl_2^{2+}$ were passed through Sephadex SP C-25 resin to hold the metal ions and pass any organic materials, if produced. Although there was a small amount of toluene detected in the reaction mixture from the benzylchromium(2+) ion reduction, it was barely above the amount present in a blank solution containing all ingredients except $Ru(bpy)_3^{2+}$. No dichloromethane was detected in the reduction of the $(H_2O)_5CrCHCl_2^{2+}$. It is also important to note that no Cr(III) products were observed on the Sephadex column. Since the product analysis was done in the presence of air, any Cr^{2+} produced would have been oxidized in the presence of the oxygen.

Reaction of Benzyl Radical with Europium(II) Ion

Benzylchromium(2+) ion undergoes a homolytic cleavage of the chromium-carbon bond (k_6 = 2.63 x 10^{-3} s^{-1} see eq 6).[44] The benzyl radical produced could react with Eu^{2+}. Since high concentrations of Eu^{2+} ion are used to quench $[Ru(bpy)_3^+]^*$, it was necessary to investigate the importance of the benzyl radical and Eu^{2+} reaction.

No reaction was observed in 600 s when benzylchromium(2+)

ion and Eu^{2+} were mixed at concentrations of 7.1×10^{-4} and 0.1 M respectively. The solution was maintained at 25.0(±0.1) °C and an ionic strength of 1.0 M adjusted with NaCl. Apparently, Eu^{2+}, unlike Cr^{2+}, is not an efficient scavenger for the benzyl radical. A limit for the reaction, however, can be estimated from these data.

The reaction can be represented by eq 6 and 7, where k_6 is given above and k_{-6}[45] is 8.5×10^7 $M^{-1}s^{-1}$. If the steady-state approximation is made for the benzyl radical and it is assumed that $k_7[Eu^{2+}] << k_{-6}[Cr^{2+}]$, then eq 8 can be derived. The upper limit for the extent of reaction is a loss of one percent of the initial benzylchromium(2+) concentration. After substitution of the extent of Eu^{3+} formation, the time of reaction, and the known rate constants into eq 8, the

$$CrCH_2Ph^{2+} \underset{k_{-6}}{\overset{k_6}{\rightleftharpoons}} Cr^{2+} + PhCH_2 \qquad (6)$$

$$PhCH_2 + Eu^{2+} \xrightarrow[H^+]{k_7} Eu^{3+} + PhCH_3 \qquad (7)$$

$$\frac{d[Eu^{3+}]}{dt} = \frac{\Delta[Eu^{3+}]}{\Delta t} = \frac{k_7 k_6 [CrCH_2Ph^{2+}][Eu^{2+}]}{k_{-6}[Cr^{2+}]} \qquad (8)$$

estimate $k_7 < 5 \times 10^6 \times [Cr^{2+}]$ is calculated. Since the quantity of Cr^{2+} produced must be less than one percent of the initial $[CrCH_2Ph^{2+}]$, an upper limit of $k_7 < 5\ M^{-1}s^{-1}$ is obtained. The Cr^{2+} ion is approximately 10^7 fold more reactive toward benzyl radical than the Eu^{2+} ion. The direction of the reactivity is not surprising since 2-hydroxy-2-propyl radical was found to be more reactive, by a factor of 340, towards chromium(II) than europium(II)[9].

Discussion

Marcus Theory Application of the Marcus cross relation (see eq 9) to the $Co(en)_3^{3+}$ reaction yields a calculated rate constant that agrees well, within a factor of 6, with the observed experimental value.

$$k_{ab} = (k_{aa}k_{bb}K_{ab}f)^{1/2}$$

$$\ln(f) = \frac{(\ln K_{ab})^2}{4\ln(k_{aa}k_{bb}/Z^2)} \qquad (9)$$

Based on the following parameters, k_{aa}[46] $= 10^8\ M^{-1}s^{-1}$, k_{bb}[47] $= 3.4 \times 10^{-5}$, and $K_{ab} = 2.73 \times 10^{18}$, the calculated value of the rate constant is $4.8 \times 10^8\ M^{-1}s^{-1}$. Considering the large thermodynamic driving forces for the reductions of these cobalt(III) complexes ($\Delta E° > 1$ V), it is not surprising that the rates of reaction are so large. Since $Ru(bpy)_3^+$, a Ru(II)

Table I-5. Thermodynamic and Kinetic Data for the Determination of the Ratio of the $Yb^{3+/2+}$ Exchange Rate and the $Eu^{3+/2+}$ Exchange Rate

Complex	E° [a]/ V	$\log(K_{ab})^{b}$	$\log(K_{ab})^{c}$	k_{bb}[d]/ $M^{-1}s^{-1}$
$Co(en)_3^{3+}$	-0.19	---	18.4	3.4×10^{-5}
Eu_{aq}^{3+}	-0.43	4.06	14.4	3.0×10^{-5}
Yb_{aq}^{3+}	-1.15	16.2	2.20	1.6×10^{-5}[e]

[a]The reduction potentials for the Co(III), Eu(III), and Yb(III) were taken from ref 39, 40, and 41a, respectively.

[b]This equilibrium constant is for the reaction between the dipositive rare earth ions and the $Co(en)_3^{3+}$ ion.

[c]This equilibrium constant is for the reaction between $Ru(bpy)_3^{+}$ and the Co(III), Eu(III), and Yb(III) ions, and is based on a reduction potential[2] of -1.28 V for the $Ru(bpy)_3^{+}$ ion.

[d]The self-exchange rates for the $Co(en)_3^{3+}$ and Eu^{3+} were taken from refs. 47 and 40, respectively.

[e]This value is 54 percent of the Eu^{3+} value, as determined by eq 10 using the $Co(en)_3^{3+}$ reaction with Yb^{2+} and with Eu^{2+}.

complex, and $Co(en)_3^{3+}$ are both substitution inert, and since there is good agreement between predicted and observed rate constants, the electron transfer reactions of the $Ru(bpy)_3^{+}$ ion most probably occur by an outer-sphere mechanism.

Use of the Marcus cross relation directly to analyze the Yb^{3+} reaction is not feasible since the self-exchange rate for the Yb^{3+}/Yb^{2+} couple, k_{YbYb}, is not known. A comparison of the Yb^{3+} reaction with the Eu^{3+} reaction, however, an approach previously applied[48] to the Yb(II) reductions of some cobalt(III) complexes, can be made.

The ratio of the Yb^{3+} and Eu^{3+} rate constants for the reaction with $Ru(bpy)_3^{+}$, k_{YbRu}/k_{EuRu}, is given by eq 10, and was obtained by dividing the Marcus cross relations (eq 9) for the two reactions. This equation provides a means of estimating k_{YbYb}/k_{EuEu} since other quantities are known or have cancelled. A recalculation of k_{YbYb}/k_{EuEu}[48] was made using data for the $Co(en)_3^{3+}$ reaction with Yb^{2+} [48]and with Eu^{2+} [49]. The recalculated value is $k_{YbYb}/k_{EuEu} = 0.54$. Table I-5 gives the relevant data used for these comparisons.

$$\frac{k_{YbRu}}{k_{EuRu}} = \left(\frac{k_{YbYb}}{k_{EuEu}}\right)^{1/2}\left(\frac{K_{YbRu}}{K_{EuRu}}\right)^{1/2}\left(\frac{f_{YbRu}}{f_{EuRu}}\right)^{1/2} \qquad (10)$$

The rate constant for the reduction of Yb^{3+} can then be calculated using eq 10 and the known rate constant[17,40] for Eu^{3+}. The calculated value is $k_{YbRu} = 3.7 \times 10^2$ $M^{-1}s^{-1}$ while the observed value is $1.2(\pm 0.2) \times 10^5$ $M^{-1}s^{-1}$. The agreement between the calculated value and the observed value is poor. Of course, eq 10 assumes all the reactions behave precisely according to Marcus theory, and thus, all of the deviations are forced into k_{YbRu}. In addition, Taube[50] has made a point about the discrepancies involved in applying the Marcus cross relation to the redox reactions of the lanthanides and actinides, and has suggested that the reactions are not adiabatic.

The rate of reduction of $Ni(tmc)^{2+}$ predicted by the Marcus cross relation is 2×10^6 $M^{-1}s^{-1}$, vs. the observed value of 5.1×10^8 $M^{-1}s^{-1}$. This prediction was based on a value of the $Ni(tmc)^{2+/+}$ exchange rate, $k_{NiNi} = 0.1$ $M^{-1}s^{-1}$, which was itself calculated[51] from one determination. The exchange rate, k_{NiNi}, was determined in neutral solution, whereas this work was done at pH 11.1. Since the $Ni(tmc)^{2+}$ partitions itself between 4, 5, and 6 coordinate forms depending on pH[52], the literature k_{NiNi} may not apply to this reaction. Nevertheless, the 250 fold difference between the observed and calculated rate constants seems high.

The rate constant for the reaction between the $Cr(H_2O)_6^{3+}$ ion and $Ru(bpy)_3^{+}$ is predicted quite well using the Marcus

cross relation. The calculated value of the rate constant is $< 2.7 \times 10^7$ $M^{-1}s^{-1}$, as compared with the observed value of 4.59×10^6 $M^{-1}s^{-1}$. This calculation was based on a $Cr^{3+/2+}$ self-exchange rate constant[53] of $< 1 \times 10^{-5}$ $M^{-1}s^{-1}$ and an equilibrium constant of 5.2×10^{14}.

Does a Long Lived Organochromium(1+) Ion Exist? The reduction of the organochromium complexes proceeds as described in eq 11. The expected route for the decomposition of CrR^+ was release of the organic group and Cr^{2+} (see eq 12), but no organic products were observed. The possibility that CrR^+ has other avenues of reactivity must be considered. CrR^+ can, in a formal sense, be considered a carbanion complex of Cr(II). As such, it is expected to be a strong reductant, even stronger than $Cr(H_2O)_6^{2+}$. Consequently, it could react with some oxidant present in the reaction solution, for example Eu^{3+}, and return to the original organochromium(2+) ion, as in eq 13. The likelihood of this happening depends

$$CrR^{2+} + RuL_3^{+} \longrightarrow CrR^{+} + RuL_3^{2+} \qquad (11)$$

$$CrR^{+} \xrightarrow[H^+]{k_{12}} RH + Cr^{2+} \qquad (12)$$

$$CrR^{+} + Eu^{3+} \xrightarrow{k_{13}} CrR^{2+} + Eu^{2+} \qquad (13)$$

upon whether the rate for reaction 13 is greater than the rate for reaction 12.

Ligand substitution at chromium(II) is normally considered to be an extremely facile process. The substitution of H_2O at $Cr(H_2O)_6^{2+}$ occurs by dissociation of a water ligand with a rate constant > 10^8 s^{-1}. CrR^+, however, can not adopt this mode for the substitution of the organic ligand since that would necessitate release of a carbanion into solution. Clearly, the mechanism for the substitution of the organic ligand on the CrR^+ complex must be different than the substitution of water on $Cr(H_2O)_6^{2+}$. The rates of substitution would also be different for these two complexes, with the loss of the organic group being slower than the loss of water. Support for this contention is obtained from the rates of ligand substitution at some $Ni(tmc)^{2+}$ complexes. The substitution of water at the axial positions on the $(H_2O)_2Ni(tmc)^{2+}$ complex occurs with a rate constant of k^{52b} = 2.1×10^7 s^{-1}. The solvolysis of $CH_3Ni(tmc)^+$ to methane and $(H_2O)_2Ni(tmc)^{2+}$, on the other hand, occurs only very slowly with a rate constant[12] of 4.1×10^{-3} s^{-1}. Thus, CrR^+ could easily have a lifetime long enough to enable it to undergo bimolecular reactions.

The suggestion that CrR^+ ions might have a lifetime long enough to do chemistry other than aquate opens some intriguing questions. How long would they exist in the absence of an

oxidizable substrate, what are their reduction potentials, and what are their spectral characteristics? In fact, the deviation from good pseudo-first-order kinetics in the reduction of benzylchromium(2+) ion could be explained by the concurrent loss of $(H_2O)_5CrCH_2Ph^+$ absorption.

An alternative explanation for the lack of reaction products was also considered; namely, that the reaction attributed to a reaction between CrR^{2+} and $Ru(bpy)_3^+$ was simply the back reaction. This can be discarded, however, because the organochromium(2+) ions do not react with Eu^{2+} to form Eu^{3+}.

Mechanism of Electron Transfer The reduction of the chromium(III) complexes, $(H_2O)_5CrL^{n+}$, by the tris(bipyridyl)-ruthenium(1+) ion show two distinct reactivity patterns. These patterns separate the chromium complexes into two groups: those with a pyridine coordinated to the chromium(III) and those not containing pyridine. The members of the latter group react with a rate that is not sensitive to the nature of the ligand, L. Thus, as one proceeds from $Cr(H_2O)_6^{3+}$ to $(H_2O)_5CrCH_2OCH_3^{2+}$ to $(H_2O)_5CrCH_2Ph^{2+}$ nonsystematic changes in the rate constants are observed, and more importantly, these rate constants are approximately equivalent.

The insensitivity of the rate constants toward L can be explained by the molecular orbital diagram in Figure I-7. The diagram is constructed by mixing the $3d_z2$ orbital on the chromium with the p_z orbital on the ligand, yielding a complex

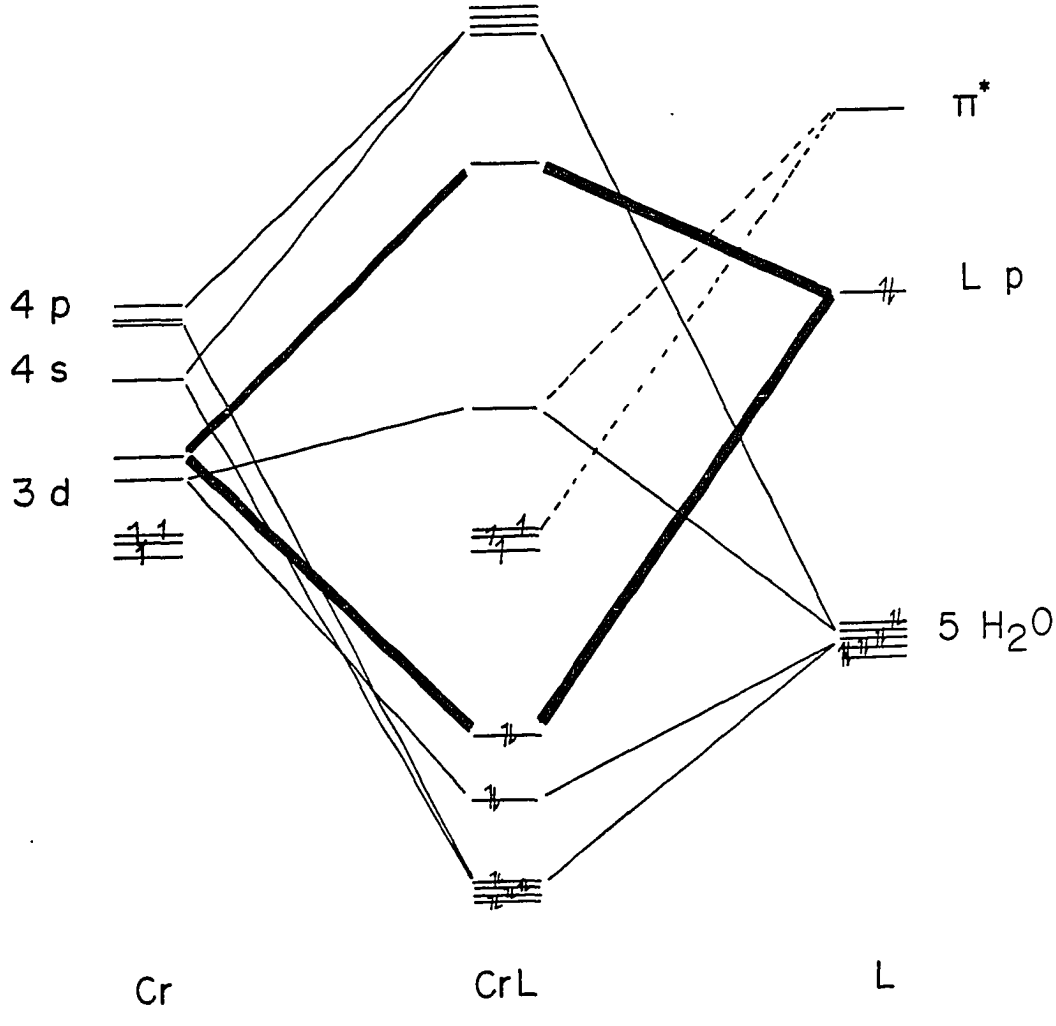

Figure I-7. Qualitative molecular orbital diagram for the chromium(III) complexes. The dashed line shows the interaction between a π^* orbital and the $d_{x^2-y^2}$ orbital possible only for the pyridine complexes. A π^* orbital does not exist for the alkyl groups bound to chromium

with local C_{4v} symmetry. The $3d_{xy}$, $3d_{xz}$, and $3d_{yz}$ orbitals (the t_{2g} in octahedral symmetry) form the three nonbonding highest occupied molecular orbitals (HOMO). These three d orbitals along with the $3d_{x^2-y^2}$ (which forms the LUMO and is one of the $^*e_g$ orbitals in octahedral symmetry) do not have the proper symmetry to mix with the p_z orbital on the ligand.

The incoming electron would enter one of the $^*e_g$ orbitals so as to form the ground state electronic configuration of chromium(II). Thus, the accepting orbital in the reduction of $(H_2O)_5CrL^{n+}$ complexes is the LUMO derived from the $d_{x^2-y^2}$ atomic orbital on chromium. Since the energy of the LUMO is relatively insensitive to the nature of L, the rates of reduction of these chromium complexes should not vary widely with the identity of this ligand.

The marked rate enhancement and the systematic deviations in the rate constants observed with the various pyridine complexes can be explained by the same molecular orbital scheme, with the addition of a new interaction. The LUMO, derived from the $d_{x^2-y^2}$ orbital in C_{2v} symmetry, has a_1 symmetry and can mix with the lowest energy π^* orbital on the pyridine. The result of this interaction is a lowering in energy of the LUMO, thus facilitating the electron transfer from the $Ru(bpy)_3^+$ to the chromium(III) complex. In addition, the energy levels of the π^* orbitals on the pyridine are dependent upon the nature of the various substituents

resulting in a systematic rate variation. This mechanism for the reduction of the pyridine chromium complexes is the same as the resonance mechanism[3,54] for electron transfer.

An alternative explanation for the magnitude and trend in the rate constants for the reduction of the pyridine complexes is that only the pyridine itself is reduced. The evidence obtained to date, however, does not support this theory, as is discussed below.

Figure I-8 shows a plot of log(k) vs. the Hammett substituent constant, σ, for the reduction of the substituted pyridine chromium complexes. The rate constants increase as the electron withdrawing ability of the substituent increases. The slope of the line is equal to the reaction constant, ρ, as defined in eq 14.

$$\log(k) = \rho\sigma + \log(k_o) \qquad 14$$

The small value of ρ, 1.1, reflects the small electronic requirements of the reaction. The positive ρ indicates that a negative charge is building in the transition state, consistent with a reduction reaction.

Table I-6 lists various ρ values for the reaction of some "pyridinium" ions with a series of reductants. Inspection of this table immediately reveals two reaction patterns for the reduction of these ions. $C_5H_5NH^+$ and $C_5H_5NCH_3^+$ have ρ values of about 9. If the pyridine is ligated to a metal ion

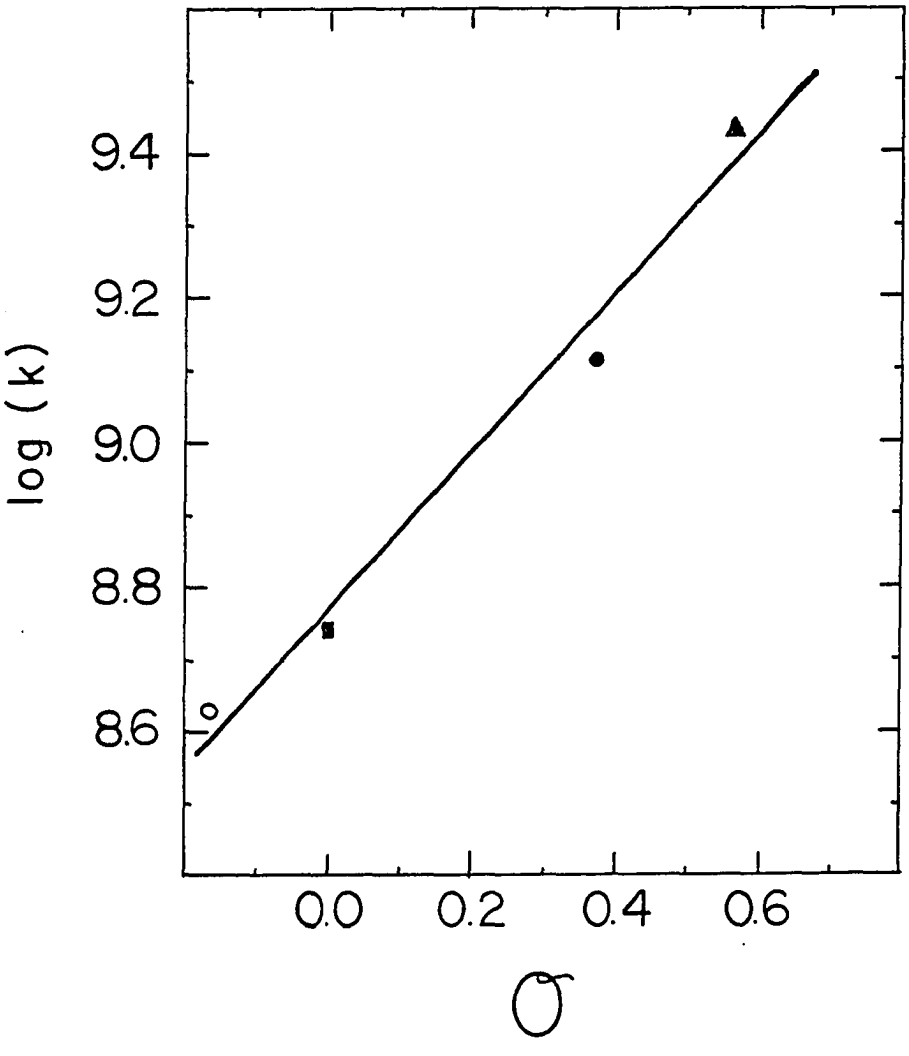

Figure I-8. A linear free energy analysis of substituent effects on the rate of reduction of the substituted $(H_2O)_5Cr(NC_5H_4X)^{3+}$ complexes by $Ru(bpy)_3^{+}$ according to the Hammett equation. The symbols used are:(o) X = 4-Me, (■) X = H, (●) X = 3-Cl, (▲) X = 3-CN. The value of the reaction constant, ρ, is 1.1

complex, however, a large decrease in the reaction constant is observed, and ρ becomes about 1.5.[55] These results for the pyridine metal complexes agree with a resonance mechanism for electron transfer, since changes in the ligand result in small changes in the rate constant. In the resonance mechanism,

Table I-6. Reaction Constants for the Reduction of $M^{n+}NC_5H_5$

Reductant	M^{n+}	Reaction Constant	Reference
R[a]	H^+	8.5	56
R[a]	CH_3^+	9.0	56
*$[Ru(bpy)_2(CN)_2]$[b]	CH_3^+	10.2	57
R[a]	$(H_2O)_5Cr^{3+}$	8.4	58
R[a]	$(NH_3)_5Co^{3+}$	1.1	11
V^{2+}	$(NH_3)_5Co^{3+}$	1.3	11
$Ru(NH_3)_6^{2+}$	$(NH_3)_5Co^{3+}$	1.5	11
Cr^{2+}	$(NH_3)_5Co^{3+}$	1.9	59
V^{2+}	$(NH_3)_5Ru^{3+}$	1.8	60
$Ru(bpy)_3^+$	$(H_2O)_5Cr^{3+}$	1.1	this work

[a]R represents the 2-hydroxy-2-propyl radical.

[b]The reducing species is the excited state of the bis(cyano)bis(bipyridyl)ruthenium(II) complex.

the electron is never bound to the ligand. The orbitals on the ligand only mediate the electron transfer between the donor and acceptor. Thus, a ρ value of 1.1 is consistent with direct transfer to the chromium and not to the pyridine ligand.

The small ρ could also be due to the reaction approaching the diffusion controlled limit[61,62]. This seems unlikely, however, since the diffusion rate limit for this system is calculated[63] to be greater than 10^{10} $M^{-1}s^{-1}$. In addition, there are calibration reactions, the 2-hydroxy-2-propyl radical reactions[58] with $(H_2O)_5CrNC_5H_4X^{3+}$, which have nearly the same driving forces and have rate constants, at the upper end of the reactions reported, similar to those obtained in this study. The ρ value, however, is 8.4, not 1. It was reported[64] that 2-hydroxy-2-propyl radical reacts only very slowly with $Cr(H_2O)_6^{3+}$ and thus, the reaction is forced to occur through the ligated pyridine.

Two other experimental findings lend support to the resonance mechanism for the reduction of the pyridine chromium complexes. First, a pyridyl radical bound to chromium was not observed. Second, the reductions of $C_5H_5NH^+$ and $C_5H_5NCH_3^+$ were not cleanly first order, whereas, the reactions of the chromium complexes followed good pseudo-first-order kinetics.

Reduction of $Ni(tmc)^{2+}$ The reduction of $Ni(tmc)^{2+}$ was studied because of the recent work[12] in this group on the reaction chemistry of the Ni(I) complex. Although this study

was performed in highly basic pHs, I noted an interesting possibility for future work. It would be possible to conduct the experiments in more acidic solutions. The nickel complex might then act as a relay catalyst for the generation of H_2 from solution since the $Ni(tmc)^{2+/+}$ reduction potential is -0.90 V[51]. The $Ru(bpy)_3^{+}$ ion reduces the $Ni(tmc)^{2+}$ to Ni(I) which in turn reacts with water to generate hydrogen gas[51]. A similar scheme has, in fact, been developed[65] using $Co^{II}(Me_6[14]dieneN_4)(H_2O)_2^{2+}$ as the relay catalyst.

Summary

The reduction of the pyridinechromium(III) complexes, $(H_2O)_5Cr(NC_5H_4X)^{3+}$ (X= H, 3-Cl, 3-CN, 4-Me), produces the Cr^{2+} ion and the protonated ligand, $XC_5H_4NH^{+}$. The metal center is thought to be directly reduced in these complexes. Thus, the pyridine acts as a mediator for electron transfer to the chromium(III), but does not exist, during the reduction process, as a distinct ligand radical. In other words, a resonance mechanism for electron transfer is favored over the chemical mechanism[54].

The other chromium(III) complexes also react with $Ru(bpy)_3^{+}$ yielding some interesting consequences. The reduced organochromium(2+) ion, CrR^{+}, may have a lifetime long enough to undergo redox reactions rather than aquation.

Another finding of interest is the nonreaction between the benzyl radical and Eu^{2+}. This radical is some 10^7 fold less reactive towards Eu^{2+} than it is toward Cr^{2+}.

Bibliography

1. Demas, J.N.; Adamson, A.W. J. Am. Chem. Soc. 1973, 95, 5159.
2. Sutin, N.; Creutz, C. Adv. Chem. Ser. No. 168, 1978, 1.
3. Leopold, K.R.; Haim, A. Inorg. Chem. 1978, 17, 1753.
4. Jonah, C.D.; Matheson, M.S.; Meisel, D. J. Am. Chem. Soc. 1978, 100, 1449.
5. Creutz, C.; Chou, M.; Netzel, T.L.; Okumura, M.; Sutin, N. J. Am. Chem. Soc. 1980, 102, 1309.
6. Kurimura, Y.; Endo, E. Bull. Chem. Soc. Jpn. 1983, 56, 3835.
7. Espenson, J.H.; Shimura, M.; Bakac, A. Inorg. Chem. 1982, 21, 2537.
8. McHatton, R.C.; Espenson, J.H. Inorg. Chem. 1983, 22, 784.
9. Muralidharan, S.; Espenson, J.H. Inorg. Chem. 1984, 23, 636.
10. Connolly, P.; Espenson, J.H. submitted to Inorg. Chem.
11. Bakac, A.; Butkovic, V.; Espenson, J.H.; Marcec, R.; Orhanovic, M. submitted to Inorg. Chem.
12. Bakac, A.; Espenson, J.H. submitted to J. Am. Chem. Soc.
13. Bakac, A.; Espenson, J.H. J. Am. Chem. Soc. 1981, 103, 2721.
14. Kirker, G.W.; Bakac, A.; Espenson, J.H. J. Am. Chem. Soc. 1982, 104, 1249.
15. Hoselton, M.A.; Lin, C.-T.; Schwarz, H.A.; Sutin, N. J. Am. Chem. Soc. 1978, 100, 2383.

16. Creutz, C.; Sutin, N. J. Am. Chem. Soc. 1976, 98, 6384.

17. Creutz, C. Inorg. Chem. 1978, 17, 1046.

18. The molar absorptivity for $Ru(bpy)_3^+$ at λ 510 nm is: a) $1.4x10^4$ $M^{-1}cm^{-1}$ Elliott, C.M.; Hershenhart, G.J. J. Am. Chem. Soc. 1982, 104, 7519; b) $1.1x10^4$ $M^{-1}cm^{-1}$ Yellowlees, L.J.; Braterman, P.S. J. Chem. Soc. Chem. Comm. 1981, 287; c) $1.2x10^4$ $M^{-1}cm^{-1}$ Baxendale, J.H.; Fiti, M. J. Chem. Soc. Dalton Trans. 1972, 1995. The molar absorptivity for the $Ru(bpy)_3^{2+}$ at λ 510 nm was measured to be $1.5x10^3$ $M^{-1}cm^{-1}$.

19. Coombes, R.G.; Johnson, M.D.; Winterton, N. J. Chem. Soc. 1965, 7029.

20. Kochi, J.K.; Davis, D.D. J. Am. Chem. Soc. 1964,86,5264.

21. Schmidt, W.; Swinehart, J.H.; Taube, H. J. Am. Chem. Soc. 1971, 93, 1117.

22. Bakac, A. Personal Communication, Ames Laboratory, Iowa State University, Ames, Ia.

23. Malic, S.K.; Schmidt, W.; Spreer, L.O. Inorg. Chem. 1974, 13, 2986.

24. Dodd, D.; Johnson, M.D. J. Chem. Soc.(A) 1968, 34.

25. Bakac, A.; Orhanovic, M. Croatica Chem. Acta 1977, 49, 57.

26. Pfeiffer, P. Z. Anorg. Allg. Chem. 1902, 31, 401.

27. Bakac, A.; Orhanovic, M. Inorg. Chem. 1971, 10, 2443.

28. Bakac, A.; Marcec, R.; Orhanovic, M. Inorg. Chem. 1974, 13, 57.

29. Orhanovic, M.; Avdagic, M. Inorg. Chem. 1973, 12, 492.

30. Marcec, R.; Orhanovic, M. J. Chem. Soc. Dalton Trans. 1975, 319.

31. Bjerrum, J.; McReynolds, J.P. Inorg. Synth. 1946, 2, 216.

32. Work, J.B. Inorg. Synth. 1946, 2, 221.

33. McDowell, M.S. Ph.D. Thesis, Iowa State University, Ames, Iowa, 1983.

34. Creaser, I.I.; Greer, R.J.; Harrowfield, J.M.; Herlt, A.J.; Sargeson, A.M.; Snow, M.R.; Springborg, J. J. Am. Chem. Soc. 1982, 104, 6016.

35. These solutions had been prepared approximately 15 years ago and were stored in ground glass stoppered reagent bottles.

36. Wagner, F.; Mocella, M.T.; D'Aniello, M.J., Jr.; Wang, A.H.-J.; Barefield, E.K. J. Am. Chem. Soc. 1974, 96, 2625.

37. Wagner, F.; Barefield, E.K. Inorg. Chem. 1976, 15, 408.

38. Mulazzani, Q.G.; Emmi, S.; Fuochi, P.G.; Hoffman, M.Z.; Venturi, M. J. Am. Chem. Soc. 1978, 100, 981.

39. The rate constant for the reaction of Eu^{2+} with $Co(sep)^{3+}$ is 0.12 M^{-1} s^{-1}. Creaser, I.I.; Sargeson, A.M.; Zanella, A.W. Inorg. Chem. 1983, 22, 4022.

40. Chou, M.; Creutz, C.; Sutin, N. J. Am. Chem. Soc. 1977, 99, 5615.

41. a) Timnick, A.; Glockler, G. J. Am. Chem. Soc. 1948, 70, 1347; b) Laitinen, H.A. J. Am. Chem. Soc. 1942, 64, 1133.

42. a) Hermolin, J.; Levin, M.; Ikegami, Y.; Sawayangi, M.; Kosower, E.M. J. Am. Chem. Soc. 1981, 103, 4795.

42. b) Cohen, H.; Gould, E.S.; Meyerstein, D.; Nutkovich, M.; Radlowski, C.A. Inorg. Chem. 1983, 22, 1374.

43. Brown, H.C.; Mihm, X.B. Inorg. Chem. 1971, 10, 2443.

44. Nohr, R.S.; Espenson, J.H. J. Am. Chem. Soc. 1975, 97, 3392.

45. Blau, R.J.; Espenson, J.H.; Bakac, A. Inorg. Chem. 1984, 23, 3526.

46. Saji, T.; Aoyagui, S. J. Electroanal. Chem. 1977, 99, 2468.

47. Dwyer, F.P.; Sargeson, A.M. J. Phys. Chem. 1961, 65, 1892.

48. Christensen, R.J.; Espenson, J.H.; Butcher, A.B. Inorg. Chem. 1973, 12, 564.

49. Candlin, J.P.; Halpern, J.; Trimm, D.L. J. Am. Chem. Soc. 1964, 86, 1019.

50. Taube, H. Adv. Chem. Ser. No.162 1977, 127.

51. Jubran, N.; Ginzburg, G.; Cohen, H.; Koresh, Y.; Meyerstein, D. Inorg. Chem. 1985, 24, 251.

52. a) Herron, A.; Moore, P. Inorg. Chim. Acta 1979, 36, 89. b) Moore, P.; Sachinidis, J.; Willey, G.R. J. Chem. Soc. Dalton Trans. 1984, 1323.

53. Anderson, A.; Bonner, N.A. J. Am. Chem. Soc. 1954, 76, 3826.

54. Haim, A. Prog. Inorg. Chem. 1983, 30, 273.

55. The reaction of 2-hydroxy-2-propyl radical with $(H_2O)_5Cr(NC_5H_4X)^{3+}$ is thought to proceed by an "inner-sphere" mechanism (see ref 58).

56. Shimura, M.; Espenson, J.H. Inorg. Chem. 1983, 22, 334.

57. Nagle, J.K.; Dressick, W.J.; Meyer, T.J. J. Am. Chem. Soc. 1979, 101, 3993.

58. Bakac, A.; Butkovic, V.; Espenson, J.H.; Marcec, R.; Orhanovic, M. unpublished results, communicated to me by JHE, Iowa State University, Ames, Ia.

59. Nordmeyer, F.; Taube, H. J. Am. Chem. Soc. 1968, 90, 1162.

60. Brown, G.M.; Krentzien, H.J.; Abe, M.; Taube, H. Inorg. Chem. 1979, 18, 3374.

61. I thank H.B. Gray, California Institute of Technology, Pasadena, Ca., for calling this matter to my attention.

62. The reduction of pyridinium ions by several excited state complexes show two ρ values. Large values of ρ (> 10) are obtained when the reactions are activation controlled. Small values (about 1) are obtained as the reactions reach the diffusion controlled limit. See ref 57 and Marshall, J.L.; Stobart, S.R.; Gray, H.B. J. Am. Chem.Soc. 1984, 106, 3027.

63. Bock, C.R.; Connor, J.A.; Gutierrez, A.R.; Meyer, T.J.; Whitten, D.G.; Sullivan, B.P.; Nagle, J.K. J. Am. Chem. Soc. 1979, 101, 4815.

64. Muralidharan, S.; Espenson, J.H. Inorg. Chem. 1984, 23, 636.

65. Brown, G.M.; Brunschwig, B.S.; Creutz, C.; Endicott, J.F.; Sutin, N. J. Am. Chem. Soc. 1979, 101, 1298.

Appendix I

Table AI-1. Rate Constants for the Reduction of $Co(NH_3)_6^{3+}$ Ion by $Ru(bpy)_3^{+}$ [a]

10^4 x [Co(III)]/M	10^4 x $[Co(III)]_{av}$/M	10^{-5} x k/s^{-1}
3.08	2.92	7.64
2.49	2.33	6.14
2.05	1.89	4.55
1.47	1.31	3.41
1.03	0.87	2.08
0.51	0.36	0.69

[a] $T = 23(\pm 1)$ °C and I = 1.00 M. $[Ru(bpy)_3^{2+}] = 40.1\ \mu M$.

Table AI-2. Rate Constants for the Reduction of $Co(en)_3^{3+}$ Ion by $Ru(bpy)_3^{+}$ [a]

10^4 x [Co(III)]/M	10^4 x $[Co(III)]_{av}$/M	10^{-5} x k/s^{-1}
3.70	3.54	8.06
3.24	3.08	6.94
2.78	2.62	5.74
2.31	2.15	4.75
1.85	1.69	3.79
1.39	1.23	2.69
0.92	0.77	1.66

[a] $T = 23(\pm 1)$ °C and I = 1.00 M. $[Ru(bpy)_3^{2+}] = 40.1$ μM.

Table AI-3. Rate Constants for the Reduction of $Co(sep)^{3+}$ Ion by $Ru(bpy)_3^{+}$ [a]

10^4 x [Co(III)]/M	10^4 x $[Co(III)]_{av}$/M	10^{-5} x k/s^{-1}
3.00	2.85	6.58
2.75	2.60	4.67
2.50	2.35	4.71
2.00	1.85	3.69
1.50	1.35	2.19
1.00	0.85	1.26

[a] $T = 23(\pm 1)$ °C and I = 1.00 M. $[Ru(bpy)_3^{2+}] = 39.4\ \mu M$.

Table AI-4. Rate Constants for the Reaction of $Ru(bpy)_3^{+}$ with $MeCo(dmgBF_2)_2$ [a]

10^4 x [MeCo]/M	10^4 x $[MeCo]_{av}$/M	10^{-5} x k/s^{-1}
0	0	0.58
0.23	0.14	1.57
0.47	0.38	2.45
1.03	0.97	4.22

[a] 0.124 M Ascorbate ion used as the reductive quencher. $[Ru(bpy)_3^{2+}] = 5.13 \times 10^{-5}$ M. T = 23(± 1) °C.

Table AI-5. Rate Constants for the Reaction of $Cr(H_2O)_6^{3+}$ with $Ru(bpy)_3^{+}$ [a]

10^2 x [Cr]/M	$[H^+]$/M	$[Cl^-]$/M	$[ClO_4^-]$/M	10^{-3} x k/s^{-1}
4.48	0.25	0.539	0.134	218.0
3.36	0.25	0.585	0.134	164.0
3.08	0.25	0.592	0.134	140.0
2.80	0.25	0.600	0.134	132.0
2.24	0.25	0.629	0.134	114.0
2.24	0.336	0.629	0.134	111.0
1.68	0.352	0.650	0.134	90.2
1.40	0.25	0.652	0.134	72.8
1.12	0.25	0.672	0.134	63.0
0.84	0.25	0.680	0.134	44.4
0.56	0.0675	0.372	0.452	32.9
0.56	0.0675	0.530	0.293	36.0
0.56	0.0675	0.689	0.134	31.0
0.28	0.25	0.698	0.134	19.9

[a] $T = 23(\pm 1)$ °C and I = 1.00M. $[Ru(bpy)_3^{2+}] = 35.4\ \mu M$.

Table AI-6. Rate Constants for the Reduction of $(H_2O)_5Cr(CH_2Ph^{2+})$ by $Ru(bpy)_3^{2+}$ [a]

10^3 x $[CrR^{2+}]$ / M	10^{-4} x k_{obs} / s^{-1}
2.14	7.46
1.71	6.51
1.50	3.24
1.28	5.00
1.07	2.24
0.86	3.44
0.73[b]	3.13
0.64	1.62
0.43	1.12
0.36[b]	1.74
0.36[b]	1.55
0.18[b]	1.20

[a] $T = 23(\pm 1)$ °C and I = 1.00 M. $[Ru(bpy)_3^{2+}] = 35.4$ μM.

[b] $[Ru(bpy)_3^{2+}] = 38.1$ μM.

Table AI-7. Rate Constants for the Reduction of $(H_2O)_5CrCHCl_2^{2+}$ Ion by $Ru(bpy)_3^{+}$ [a]

10^3 x $[CrR^{2+}]$ / M	10^{-4} x k_{obs} / s^{-1}
3.89	9.46
3.00	7.84
2.25	6.07
1.50	4.65
0.90	3.08
0.00	0.34

[a] $T = 23(\pm 1)$ °C and I = 1.00 M. $[Ru(bpy)_3^{2+}] = 36.0\ \mu M$.

Table AI-8. Rate Constants for the Reaction of $(H_2O)_5CrCF_3^{2+}$ Ion with $Ru(bpy)_3^{+}$ [a]

10^3 x $[CrR^{2+}]$ / M	10^{-4} x k_{obs} / s^{-1}
11.3	1.38
8.70	1.55
6.53	1.50
4.35	1.66
2.18	1.28
0.00	0.32

[a] $T = 23(\pm 1)$ °C and I = 1.00 M. $[Ru(bpy)_3^{2+}] = 36.1$ μM.

Table AI-9. Rate Constants for the Reaction of $(H_2O)_5Cr(CH_2OCH_3)^{2+}$ Ion with $Ru(bpy)_3^{+}$ [a]

10^3 x $[CrR^{2+}]$ / M	10^{-4} x k_{obs} / s^{-1}
7.80	3.21
7.02	4.56
6.24	2.67
5.46	3.15
4.68	2.42
3.90	3.95
3.90	3.04
3.90	4.32
3.12	1.96
1.56	2.11

[a] $T = 23(\pm 1)$ °C and I = 1.00 M. $[Ru(bpy)_3^{2+}] = 35.0$ μM.

Table AI-10. Rate Constants for the Reduction of 4-pyridiomethylchromium(III) Ion with $Ru(bpy)_3^{+}$ [a]

10^4 x [CrR]/M	10^4 x $[CrR]_{av}$/M	[b] $[Ru^+]_0/\mu M$	10^{-5} x k/s^{-1}
3.98	3.82	32.7	5.17
3.01	2.86	29.6	3.89
1.99	1.95	8.1	2.51
1.99	1.87	23.4	2.45
1.99	1.87	24.7	2.41
1.63	1.49	27.4	1.99
1.27	1.16	22.6	1.48
0.76	0.67	19.4	0.83

[a] $T = 23(\pm 1)$ °C and I = 1.00 M. $[Ru(bpy)_3^{2+}] = 37.4\ \mu M$.

[b] The initial $Ru(bpy)_3^{+}$ concentration, $[Ru^+]_0$, was determined from the change in absorbance at λ 510 nm. The molar absorptivity value for the $Ru(bpy)_3^{+}$ ion at 510 nm is $1.25 \times 10^4\ M^{-1}cm^{-1}$ [18].

Table AI-11. Rate Constants for the Reduction of Bis-(pyridine)chromium(III) Ion with $Ru(bpy)_3^{+}$ [a]

10^4 x $[Cr(py)_2]$/M	10^4 x $[Cr(py)_2]_{av}$/M	10^{-5} x k_{obs}/s^{-1}
4.84	4.67	7.16
4.04	3.83	6.18
3.23	3.06	4.98
2.42	2.26	3.70
1.61	1.47	2.38
0.81	0.68	1.14
0.40	0.30	0.60

[a] $T = 23(\pm 1)$ °C and I = 1.00 M. $[Ru(bpy)_3^{2+}] = 39.4$ μM.

Table AI-12. Rate Constants for the Reaction of Pyridine-chromium(III) Ion with $Ru(bpy)_3^{+}$ [a]

10^4 x [Cr(py)]/M	10^4 x $[Cr(py)]_{av}$/M	10^{-5} x k_{obs}/s^{-1}
6.12	5.98	3.37
5.10	4.96	2.84
4.08	3.94	2.30
3.06	2.92	1.70
2.04	1.90	1.24
1.63	1.49	0.88
1.22	1.08	0.62

[a] $T = 23(\pm 1)$ °C and I = 1.00 M. $[Ru(bpy)_3^{2+}] = 39.4$ μM.

Table AI-13. Rate Constants for the Reduction of (4-methyl-pyridine)chromium(III) Ion by $Ru(bpy)_3^{+}$ [a]

10^4 x [Cr(py)]/M	10^4 x $[Cr(py)]_{av}$/M	10^{-5} x k_{obs}/s^{-1}
3.69	3.58	1.52
2.92	2.81	1.23
1.94	1.83	0.81
0.97	0.86	0.38

[a] $T = 23(\pm 1)$ °C and I = 1.00 M. $[Ru(bpy)_3^{2+}] = 35.4$ μM.

Table AI-14. Rate Constants for the Reduction of (3-chloropyridine)chromium(III) Ion by $Ru(bpy)_3^{+}$ [a]

10^4 x [Cr(py)]/M	10^4 x $[Cr(py)]_{av}$/M	10^{-5} x k_{obs}/s^{-1}
4.50	4.42	6.44
4.50	4.42	6.60
3.82	3.74	5.82
3.00	2.92	4.79
2.73	2.65	4.38
2.32	2.24	3.91
2.32	2.24	4.28
1.91	1.83	3.32
1.91	1.83	3.46
1.50	1.42	2.62
1.50	1.42	2.88
1.02	0.94	1.97
1.02	0.94	2.02
0.00	0.00	0.12

[a] $T = 23(\pm 1)$ °C and I = 1.00 M. $[Ru(bpy)_3^{2+}] = 41.4$ μM.

Table AI-15. Rate Constants for the Reduction of (3-cyanopyridine)chromium(III) Ion by $Ru(bpy)_3^{+}$ [a]

10^4 x [Cr]/M	10^4 x $[Cr]_{av}$/M	[Ru][b]/μM	10^{-5} x k_{obs}/s^{-1}
2.70	2.58	72.1	7.43
2.20	2.13	72.1	6.26
1.83	1.75	72.1	5.24
1.31	1.26	72.1	3.84
2.87	2.41	70.8	7.40
2.33	2.24	70.8	6.28
1.94	1.61	70.8	5.12
1.16	1.08	70.8	3.61
2.70	2.53	36.1	7.29
1.31	1.19	36.1	3.62
1.31	1.16	36.1	3.56
2.87	2.69	35.4	7.00
2.33	2.13	35.4	5.64
1.94	1.77	35.4	4.91
1.16	1.02	35.4	3.22
0.75	0.69	35.4	2.28
0.54	0.44	35.4	1.65
0.54	0.47	35.4	1.64
0.25	0.22	35.4	0.85
2.70	2.60	18.0	7.21
1.31	1.23	18.0	3.61
0.73	0.68	18.0	2.22

[a] $T = 23(\pm 1)$ °C and I = 1.00 M.

Table AI-16. Rate Constants for the Reduction of bipyridylchromium(III) Ion by $Ru(bpy)_3^{+}$ [a]

10^4 x [Cr(bpy)]/M	10^4 x $[Cr(bpy)]_{av}$/M	10^{-5} x k_{obs}/s^{-1}
4.49	4.37	8.29
3.37	3.25	7.01
2.92	2.80	5.54
2.25	2.13	4.67
1.68	1.56	3.41
1.12	1.00	2.32

[a] $T = 23(\pm 1)$ °C and I = 1.00 M. $[Ru(bpy)_3^{2+}] = 38.1$ μM.

Table AI-17. Rate Constants for the Reduction of Ni(tetramethylcyclam)$^{2+}$ by $Ru(bpy)_3^{+}$ Ion[a]

10^4 x $[Ni(tmc)^{2+}]$ / M	10^{-4} x k_{obs} / s^{-1}
4.04	21.7
2.69	14.9
1.35	8.1

[a] The quencher used was 0.20 M ascorbate anion at pH 11.1 and T = 23(±1) °C. $[Ru(bpy)_3^{2+}] = 38.7$ μM.

Table AI-18. Rate Constants for the Reduction of Ytterbium(III) and Samarium(III) Ions by $Ru(bpy)_3^{+}$ [a]

10^2 x [RE]/M	μ/M	10^{-3} x k_{obs}/s^{-1}	10^{-3} x k_{cor}[b]$/s^{-1}$
Yb^{3+}			
0	1.00	5.21	--
0.992	1.03	6.16	0.95
0	1.00	7.07	--
4.96	1.13	14.25	7.18
Sm^{3+}			
0	1.00	5.41	--
6.85	1.29	6.01	0.60
13.7	1.58	8.22	2.81
13.7	1.58	8.97	3.56

[a]These reactions were performed at T = 23(±1) °C and using $[H^+]$ = 0.25 M, $[Eu^{2+}]$ = 0.10 M and $[Ru(bpy)_3^{2+}]$ = 38.7 μM.

[b]k_{cor} is a corrected rate constant obtained by subtracting the "back reaction" rate constant from the observed rate constant.

CHAPTER II. THE CATALYZED PRODUCTION OF DIHYDROGEN FROM SOLUTIONS CONTAINING CHROMIUM(II) ION, HALIDE ION, AND (DIAQUO)BIS[DIFLUOROBORYLDIMETHYLGLYOXIMATO]COBALT(II)

Introduction

In the absence of a heterogeneous catalyst[1], the reduction of hydrogen ion by Cr^{2+}, Eu^{2+}, and V^{2+} to produce hydrogen gas occurs only very slowly, despite the rather large thermodynamic driving force for the reaction ($E°$= -0.415, -0.380, and -0.230 V for Cr^{2+}, Eu^{2+}, and V^{2+} respectively).[2,3] The problem, then, is a kinetic one. All of these metal ions are good <u>one</u> electron reductants. To produce H_2 by electron transfer, these metal ions would have to form hydrogen atoms in the first step, a process with an impossibly large energy change. Clearly, any practical route must proceed without hydrogen atom formation.

The present study reports what is, to my knowledge, the first example of a homogeneous[4] catalytic reduction of H^+ by Cr^{2+}, Eu^{2+}, and V^{2+}. The catalyst is $Co(dmgBF_2)_2$, and the reaction entails the production of a cobalt(I) intermediate, in the presence of a coordinating anion, such as Cl^- or Br^-, and the reducing metal ion. The decomposition of this intermediate leads to hydrogen evolution.

Of course, many macrocyclic cobalt(II) complexes can be reduced[4a-6] to cobalt(I) (the reduction potentials of various

cobalt(II) macrocycles occur in the range -0.5 to -1 V)[4b,7-9] using strong reductants, such as Zn metal or $NaBH_4$ in alkaline solutions. But, these reagents produce a high concentration of cobalt(I), and they produce it in an uncontrolled manner. The advantage of the system reported here is that the cobalt(I) is produced in acidic solutions and in a steady and controlled way.

One feature that most hydrogen evolution schemes have in common is the ability of a metal or metal complex to form hydridometal species. The formation of the metal hydride provides a low energy path for the production of hydrogen by eliminating the need for the hydrogen atom. These hydride species can react in two ways to produce hydrogen gas. The first involves a heterolytic cleavage of the metal-hydrogen bond by protic solvents.[10,11] The second mode of hydrogen production is by bimolecular reductive elimination; essentially a homolytic cleavage of the metal-hydrogen bond.[11,12]

These modes of metal hydride decomposition to H_2 have a direct bearing on a topic of considerable interest, that of homogeneous H_2 activation.[13-16] The evolution of hydrogen from these metal complexes is simply the microscopic reverse of the H_2 uptake process.

The use of Cr^{2+} to reduce cobalt(II) macrocycles is not unique. $Co(Me_6[14]\text{-}4,11\text{-}dieneN_4)(OH_2)_2^{2+}$ in aqueous $HClO_4$ acts as a catalyst for the reduction[7,17] of $Co(Me_6[14]\text{-}4,11\text{-}$

dieneN$_4$)(NH$_3$)$_2^{3+}$. There was no report in that study of a hydridocobalt species or hydrogen gas evolution; the cobalt(I), produced from the diaquocobalt(II) complex, reacted rapidly with the diamminecobalt(III) complex rather than with a H^+. In the same study, it was reported that aquocobalamin could also act as a catalyst for the reduction of the diamminecobalt(III) complex. However, the reduced cobalamin reacted competitively with H^+. No mention of a gaseous product was made.

In a similar system,[18] Co(Me$_6$[14]dieneN$_4$)(H$_2$O)$_2^{2+}$ and EuCl$_2$ are combined with Ru(bpy)$_3^{2+}$ in aqueous HCl to produce H_2 photochemically. Thermal generation of H_2 was not observed.

Experimental

Materials (Diaquo)bis(difluoroboryldimethylglyoximato)cobalt(II) was prepared by a method similar to that used for bis(difluoroboryldiphenylglyoximato)cobalt(II).[19] To

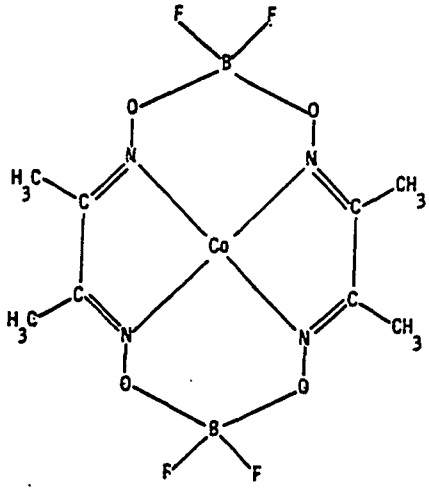

a deaerated suspension of dimethylglyoxime in diethyl ether, 0.5 equivalents of $Co(O_2CCH_3)_2\ 4H_2O$ were added. This mixture was stirred for 1 hour before an excess of freshly distilled boron trifluoride etherate was added. A brown solid was filtered from the mixture, washed twice with diethyl ether, three times with ice cold methanol, and again with diethyl ether. The UV-visible spectrum of the complex, in agreement with the literature values[20], exhibited absorption maxima at λ 456 nm (ε 4.06×10^3 $M^{-1}cm^{-1}$) and 328 (1.92×10^3).

Solutions of $Cr(ClO_4)_2$ and $EuCl_2$ were prepared by the reduction of the corresponding MX_3 solutions by zinc amalgam. The other materials were reagent grade and were used as received. The solvent used in this study was water, purified by a Millipore-Q water system.

Methods The reaction kinetics were studied by either of two spectrophotometric techniques, depending on the time scale of the reaction. The instruments used were a Varian Cary 219 recording spectrophotometer and a Durrum stopped flow instrument, equipped with an OLIS computerized data collection system. Kinetic determinations were done under an argon atmosphere at 25.0($\pm$0.1) °C and an ionic strength of 1.00 M.

In certain experiments, the visible absorption spectrum was scanned rapidly and repeatedly; these measurements were made using the Durrum stopped flow instrument modified with an OLIS Rapid Scan Spectrophotometer.

The loss of $[Cr^{2+}]$ during the reaction was determined by direct chemical analysis. At known time intervals during the reaction, an aliquot of the reaction solution was injected into a solution containing a known excess of $[(NH_3)_5CoBr](ClO_4)_2$. This Co(III) complex immediately reacted with the Cr^{2+} to produce Co^{2+}. The Co^{2+} was then analyzed spectrophotometrically by conversion to the $Co(NCS)_4^{2-}$ complex (λ 623 nm, ε 1842 $M^{-1}cm^{-1}$).

Analysis of the kinetic data was done by standard techniques, often assisted by a least-squares fitting program. Some aspects of the interpretation were facilitated by the use of numerical methods to simulate concentration-time profiles. These kinetic simulations were performed on a VAX computer using a program named KINSIM.[21]

The identification of the evolved gas as molecular hydrogen was confirmed by its reaction with $PdCl_2$.[22] The volumes of liberated gas were measured with a buret. The reaction products were separated on Sephadex SP C-25 cation exchange resin.

Results

Product Analyses When 0.024 M Cr^{2+} and 2.3 x 10^{-4} M $Co(dmgBF_2)_2$ are combined in deaerated 0.26 M HCl, a gas is evolved. Following the complete evolution of the gas, the reaction solution was ion-exchanged. The yellow $Co(dmgBF_2)_2$ was washed off the resin with water leaving a green band which

eluted with 0.5 M NaCl. The UV-visible spectrum of the green band matched that of $(H_2O)_5CrCl^{2+}$ with absorption maxima at λ 428 nm (ε 20.8 $M^{-1}cm^{-1}$) and 609 (16.4). This green band constituted the only chromium product found. The gas evolved was proved to be H_2.

Stoichiometry The quantity of H_2 produced was determined by measuring the volume of the gas and applying the necessary corrections for the temperature, the atmospheric pressure, and the water vapor pressure. The ratio, $[H_2]/[Cr^{2+}]_0$, was found to be 0.40 and 0.48 in two trials. The ratio, $[CrCl^{2+}]/[Cr^{2+}]_0$, was found to be 0.9(±0.1).

The reaction is clearly catalytic in the cobalt(II) complex, since the conversion to chromium(III) product is nearly 100 percent at chromium(II) ion concentrations some 10-1000 fold greater than the $Co(dmgBF_2)_2$ concentration.

The quantitative analyses just described establish the following to be the equation for the overall reaction.

$$Cr^{2+} + H^+ + Cl^- = CrCl^{2+} + \frac{1}{2} H_2 \qquad (1)$$

Mechanism of Hydrogen Evolution A mechanism consistent with the experimental data is presented in Scheme I. This is shown at the outset, since the relatively complex analysis is more clearly appreciated by reference to this model. The following sections will be presented in light of this scheme.

Scheme I

$$Cr^{2+} + Cl^- + Co(dmgBF_2)_2 \underset{k_{-2}}{\overset{k_2}{\rightleftharpoons}} INT \qquad (2)$$

$$INT \xrightarrow{k_3} CrCl^{2+} + Co(dmgBF_2)_2^- \qquad (3)$$

$$Co(dmgBF_2)_2^- + H^+ \underset{}{\overset{K_4}{\rightleftharpoons}} HCo(dmgBF_2)_2 \qquad (4)$$

$$HCo(dmgBF_2)_2 + H^+ \xrightarrow{fast} H_2 + Co(dmgBF_2)_2^+ \qquad (5)$$

$$Co(dmgBF_2)_2^+ + Cr^{2+} + Cl^- \xrightarrow{fast} CrCl^{2+} + Co(dmgBF_2)_2 \qquad (6)$$

Scheme II

$$E + S \rightleftharpoons ES$$

$$ES \longrightarrow E + P$$

Note that the kinetic implications of Scheme 1 are analogous to those of the Michaelis-Menten mechanism for enzyme catalysis, shown in Scheme II.

Michaelis-Menten Kinetics Pre-steady-state Phase In the Michaelis-Menten scheme, the intermediate, INT, is rapidly formed in a reaction between the catalyst and the substrate(s). In the system described here, $Co(dmgBF_2)_2$ is the catalyst. The substrates are Cr^{2+} and Cl^-, or more likely the $CrCl^+$ complex. The rapid buildup of INT continues until the intermediate has reached its maximum steady-state concentration. The period of rapid intermediate buildup is known as the pre-steady-state phase,[23] and follows pseudo-first-order kinetics. As the substrate is converted to product, the steady-state concentration of INT decreases. The equations pertinent to a Michaelis-Menten treatment of the data are presented in the Appendix II.

Pre-steady-state Phase -- Kinetics of the Reaction in the Presence of Chromium(II) and Chloride Ions The catalytic reaction of Cr^{2+}, H^+, Cl^-, and $Co(dmgBF_2)_2$ to produce H_2 and $CrCl^{2+}$ occurs in two observable stages. The first stage is marked by a fast increase in absorption, with the maximum change occurring at λ 770 nm. This fast stage corresponds to the pre-steady-state phase. Several difference spectra, recorded during the pre-steady-state, reveal some interesting features, and are presented in Figure I-1. The spectra were

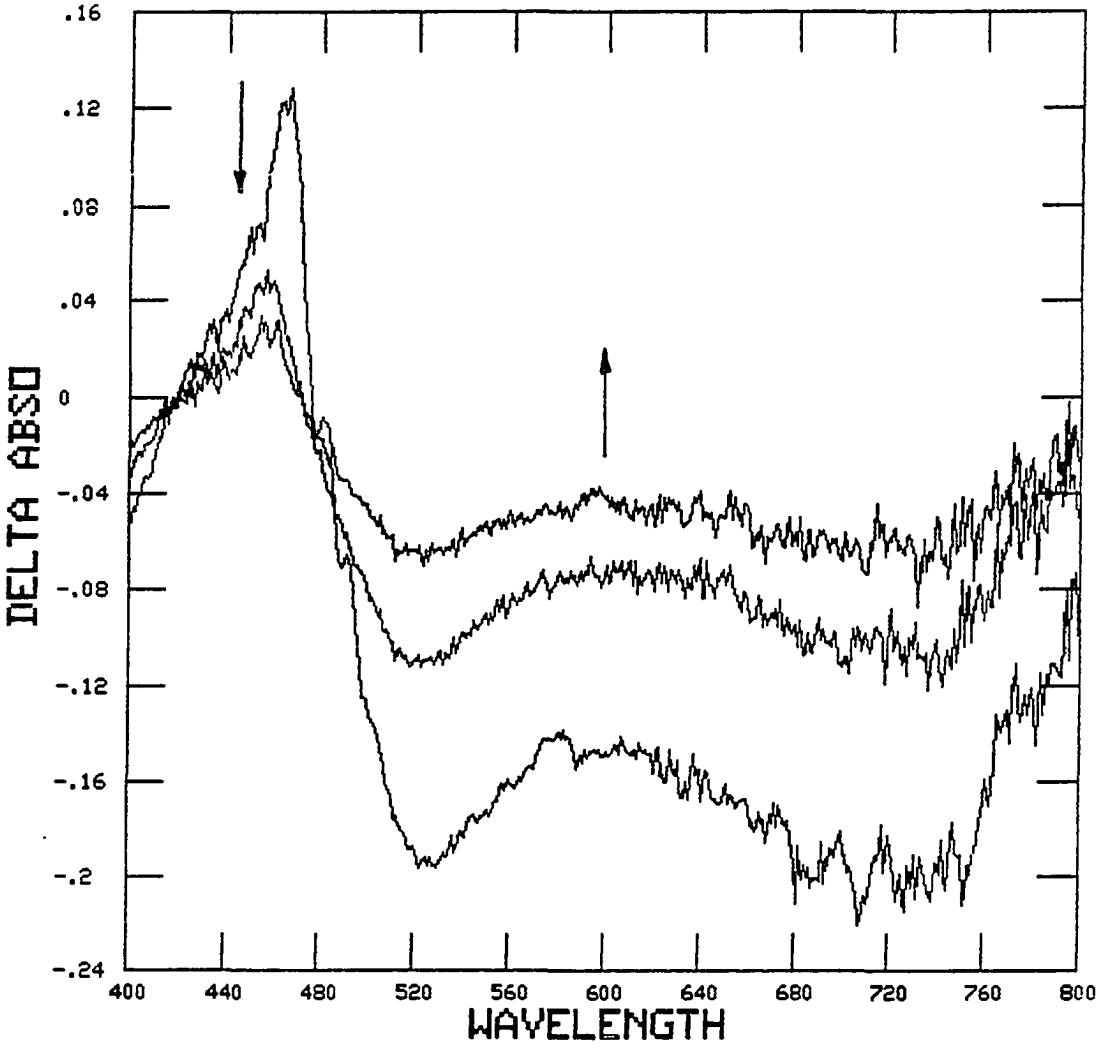

Figure II-1. Several difference spectra recorded during the pre-steady-state phase. The spectra were taken at 0.06, 0.39, and 0.72 s and referenced to the absorbance at 3 s. The concentrations of the reagents were $[Cr^{2+}]$ = 0.015 M, $[Cl^{-}]$ = 0.25 M, and $[Co(dmgBF_2)_2]$ = 1.2 x 10^{-4} M. The interpretation of these spectra are in the main text (p 95)

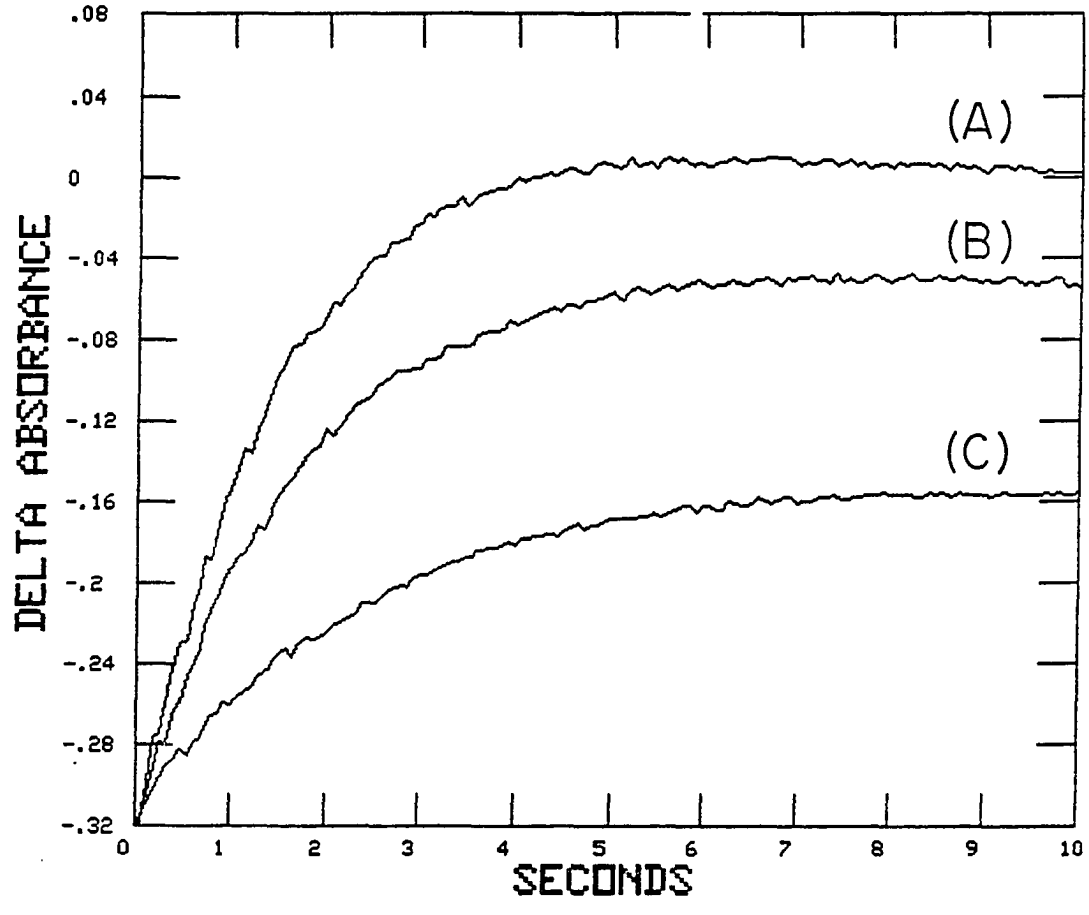

Figure II-2. An example of the absorbance changes that occur during the pre-steady-state as monitored at λ 770 nm. The concentrations of the reagents were $[Co(dmgBF_2)_2]$ = 1.1 x 10^{-4} M, $[Cl^-]$ = 0.25 M, and $[Cr^{2+}]$ = (A) 7.5 mM, (B) 5.0 mM, (C) 2.5 mM

Table II-1. Kinetic Data for the Formation of the Intermediate in a Chloride Medium[a]

$[Cr^{2+}]^b$	$[Cl^-]^b$	$10^4x[Co]^b$	$10^3x[Cr^{2+}][Cl^-]^c$	k/s^{-1}	ΔD^d
0.054	0.25	1.47	13.5	2.98	0.445
0.03	0.75	1.20	22.5	5.85	0.513
0.03	0.50	1.43	15.0	3.97	0.566
0.03	0.25	1.43	7.5	1.85	0.521
0.02	0.75	1.20	15.0	3.90	0.502
0.02	0.50	1.43	10.0	2.84	0.585
0.02	0.25	1.43	5.0	1.10	0.462
0.02	0.25	1.43	5.0	1.31	0.463
0.01	0.75	1.20	7.5	2.00	0.470
0.01	0.50	1.43	5.0	1.53	0.514
0.01	0.25	1.43	2.5	0.79	0.424
0.0054	0.75	1.20	4.0	1.10	0.455
0.0054	0.50	1.43	2.7	0.85	0.461
0.0054	0.25	1.43	1.4	0.56	0.332
0.0020	0.50	1.50	1.0	0.43	0.228
0.0020	0.50	1.50	1.0	0.40	0.233
0.0020	0.25	1.50	0.5	0.34	0.128
0.0020	0.25	1.50	0.5	0.34	0.128
0.0010	0.50	1.50	0.5	0.32	0.139
0.0010	0.50	1.50	0.5	0.37	0.129
0.0010	0.25	1.50	0.25	0.36	0.057
0.0010	0.25	1.50	0.25	0.47	0.054

[a]The kinetics and delta absorbance data were recorded at 770 nm in a 2 cm cell. T = 25.0(±0.1) °C, $[H^+]$ = 0.25 M, and I = 1.00 M adjusted with $LiClO_4$.

[b]Units of M.

[c]Units of M^2.

[d]ΔD is the change in absorbance during the pre-steady-state, and represents the maximum $[INT]_{ss}$.

taken at 0.06, 0.39, and 0.72 s, and are the differences between the absorbance values at these times and the absorbances at 3 s (when the maximum steady-state concentration of INT, $[INT]_{max}$, has been reached). Two isosbestic points, at 420 and 470 nm, occur. There are also two absorption maxima at 530 and 700 nm. These spectra are discussed more fully later in this thesis (p 95).

Figure II-2, depicting the data from kinetic runs at constant $[Cl^-]$ and varying $[Cr^{2+}]$, reveals two important points concerning the pre-steady-state phase. First, the rate of the intermediate buildup is dependent on the initial concentration of Cr^{2+}. Second, the extent of intermediate formation, as measured by ΔD, is also dependent on the initial Cr^{2+} concentration. Analogous results are obtained if $[Cr^{2+}]$ is held constant, while $[Cl^-]$ is varied.

The kinetic data for the pre-steady-state phase are given in Table II-1. The intermediate buildup conformed to pseudo-first-order kinetics. A plot of the apparent rate constant, k_{app}, vs. the concentration product, $[Cr^{2+}][Cl^-]$, is shown in Figure II-3. The data were analyzed by a least-squares program using eq 7, where $k_a = 220(\pm 11)\ M^{-2}s^{-1}$ and $k_b = 0.25(\pm 0.02)\ s^{-1}$. The parameters k_a and k_b correspond to k_2

$$k_{app} = k_a[Cr^{2+}][Cl^-] + k_b \qquad (7)$$

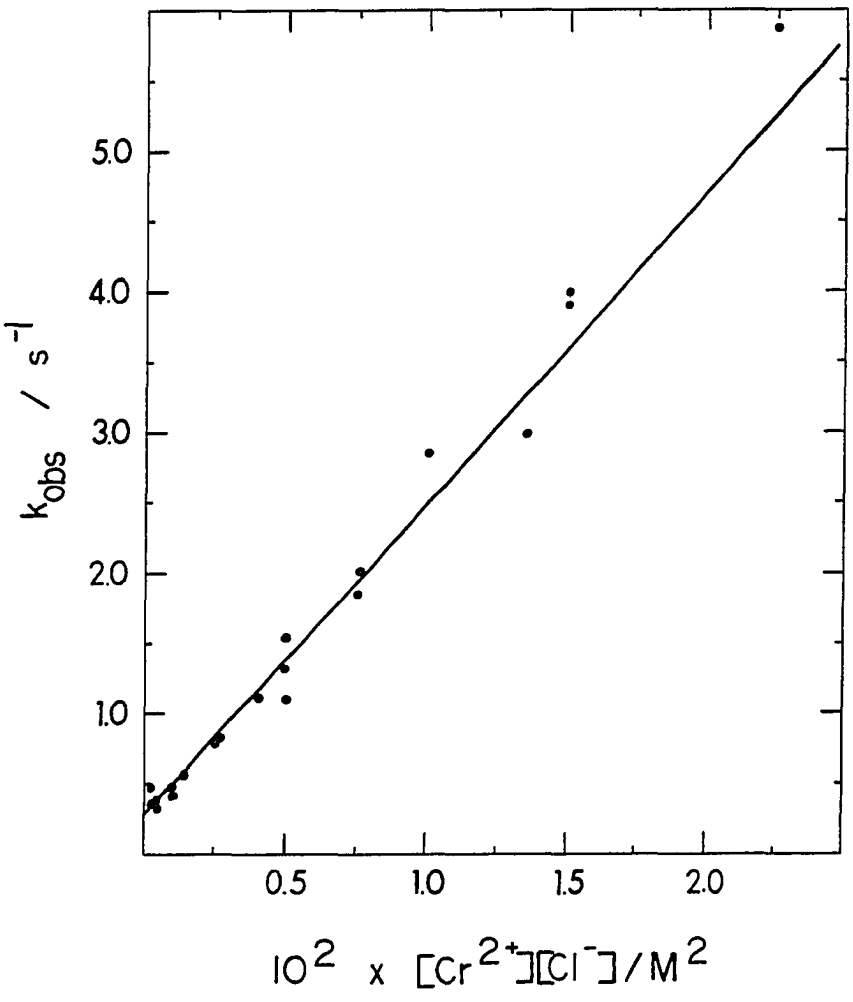

Figure II-3. Plot of the apparent rate constant for INT buildup vs. the product, $[Cr^{2+}][Cl^-]$. The slope and intercept, as determined by a least squares analysis of the data, are 220(±11) $M^{-2}s^{-1}$ and 0.25(±0.02) s^{-1}, respectively

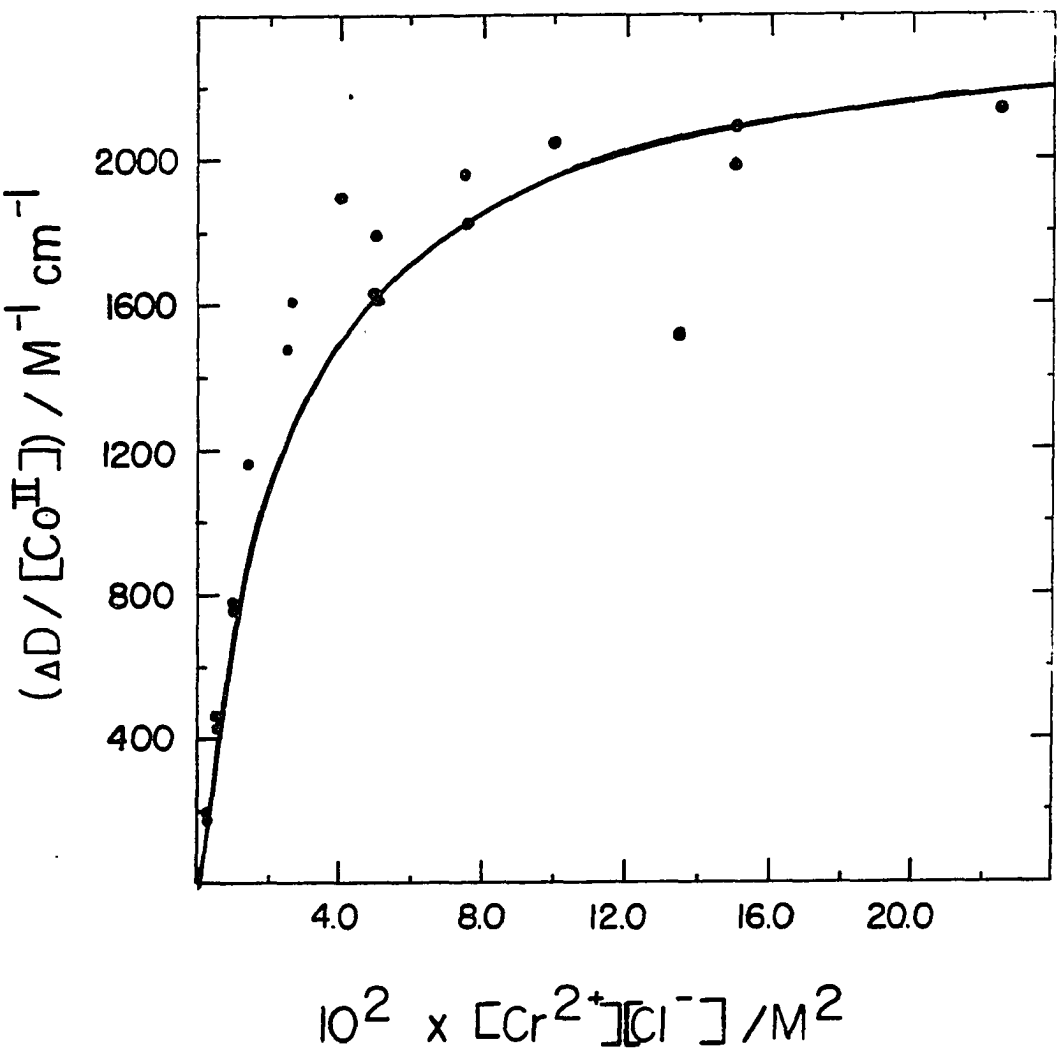

Figure II-4. Plot of the change in absorbance at 770 nm, normalized by the initial $[Co(dmgBF_2)_2]$ and divided by the path length (2 cm) of the reaction cell, vs. the product, $[Cr^{2+}][Cl^-]$. The line drawn was calculated by a least-squares analysis of the data according to eq 8

and the sum, $k_{-2} + k_3$, respectively, according to the mechanism in Scheme I.

The concentration of the intermediate, as determined by the total absorbance change ($\Delta D = D_{max} - D_0$) in the pre-steady-state data, came to a plateau at high concentrations of Cr^{2+} and Cl^-. Figure II-4 shows a plot of the absorbance change, normalized for the initial $[Co(dmgBF_2)_2]$, vs. the product, $[Cr^{2+}][Cl^-]$. These data were analyzed by a non-linear least-squares program according to eq 8. The values of parameters A and B are 2250($\pm$90) $M^{-1}cm^{-1}$ and (1.6$\pm$0.2) x 10^{-3} M^2 respectively.

$$\frac{\Delta D}{[Co(dmgBF_2)_2]_0} = \frac{A[Cr^{2+}][Cl^-]}{B + [Cr^{2+}][Cl^-]} \qquad (8)$$

The kinetic treatment (see the Appendix II) identifies the parameters A and B. A is equivalent to the molar absorptivity, $\Delta\varepsilon$, and B is equivalent to the Michaelis constant, K_s. In terms of the constants in Scheme I, $K_s = (k_{-2} + k_3)/k_2$, as also derived in the appendix.

Pre-steady-state Phase -- Kinetics of the Reaction in the Presence of Chromium(II) and Bromide Ions Many of the foregoing observations on the Cl^- system are applicable to the formation of an intermediate in the presence of the bromide ion. Figure II-5 presents several difference spectra obtained

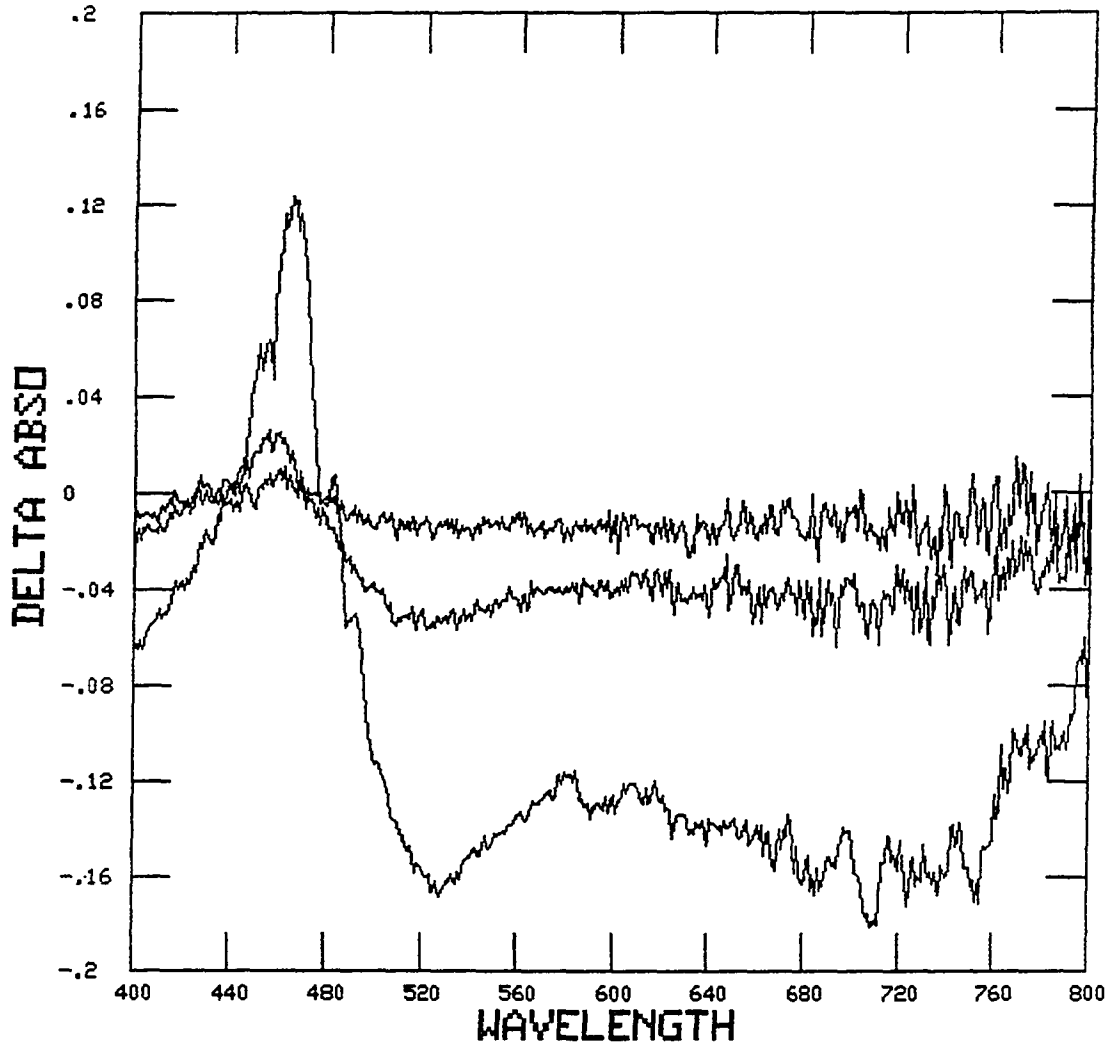

Figure II-5. Difference spectra recorded during the pre-steady-state phase at 0.06, 0.39, and 0.72 s. The spectra are referenced to the absorbance at 3 s. The concentrations of the reagents are $[Cr^{2+}]$ = 0.015 M, $[Br^-]$ = 0.25 M, and $[Co(dmgBF_2)_2]$ = 1.2 x 10^{-4} M. The interpretation of these spectra is given in the main text (p 95)

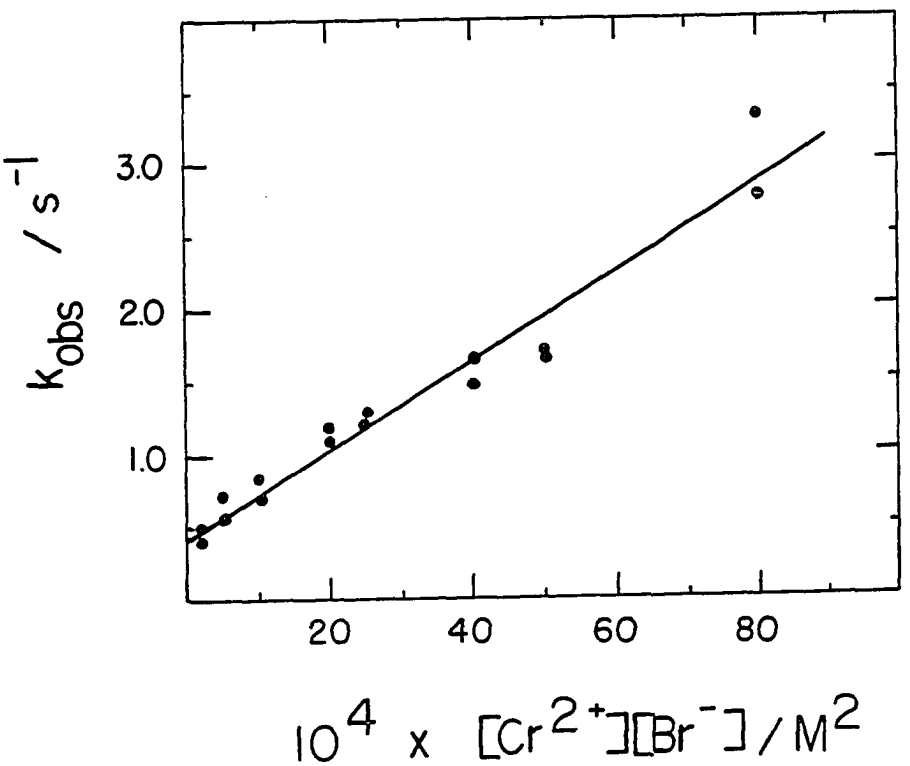

Figure II-6. Plot of the apparent rate constant for the buildup of the intermediate in a Br^- solution vs. the product, $[Cr^{2+}][Br^-]$. The values of the slope and intercept, determined by a least-squares analysis of the data, are 304(±19) $M^{-2}s^{-1}$ and 0.43(±0.07) s^{-1}, respectively

Table II-2. Kinetic Data for the Formation of the Intermediate in a Bromide Medium[a]

$[Cr^{2+}]^b$	$[Br^-]^b$	$10^4 x[Co]^b$	$10^3 x[Cr^{2+}][Br^-]^c$	k/s^{-1}	ΔD^d
0.02	0.50	1.11	80.0	3.32	0.400
0.02	0.50	1.11	80.0	2.76	0.410
0.02	0.20	1.34	40.0	1.66	0.420
0.02	0.20	1.34	40.0	1.46	0.410
0.01	0.50	1.11	50.0	1.68	0.350
0.01	0.50	1.11	50.0	1.64	0.350
0.01	0.20	1.34	20.0	1.08	0.320
0.01	0.20	1.34	20.0	1.20	0.320
0.005	0.50	1.11	25.0	1.28	0.300
0.005	0.50	1.11	25.0	1.20	0.300
0.005	0.20	1.34	10.0	0.82	---
0.005	0.20	1.34	10.0	0.70	0.220
0.001	0.50	1.11	5.0	0.72	0.120
0.001	0.50	1.11	5.0	0.56	0.140
0.001	0.20	1.34	2.0	0.50	0.056
0.001	0.20	1.34	2.0	0.40	0.055

[a]The kinetics and delta absorbance data were recorded at 760 nm in a 2 cm cell. T = 25.0(±0.1) °C, $[H^+]$ = 0.25 M, and I = 1.00 M adjusted with $LiClO_4$.

[b]Units of M.

[c]Units of M^2.

[d]ΔD is the change in absorbance during the pre-steady-state, and represents the maximum steady-state concentration of INT.

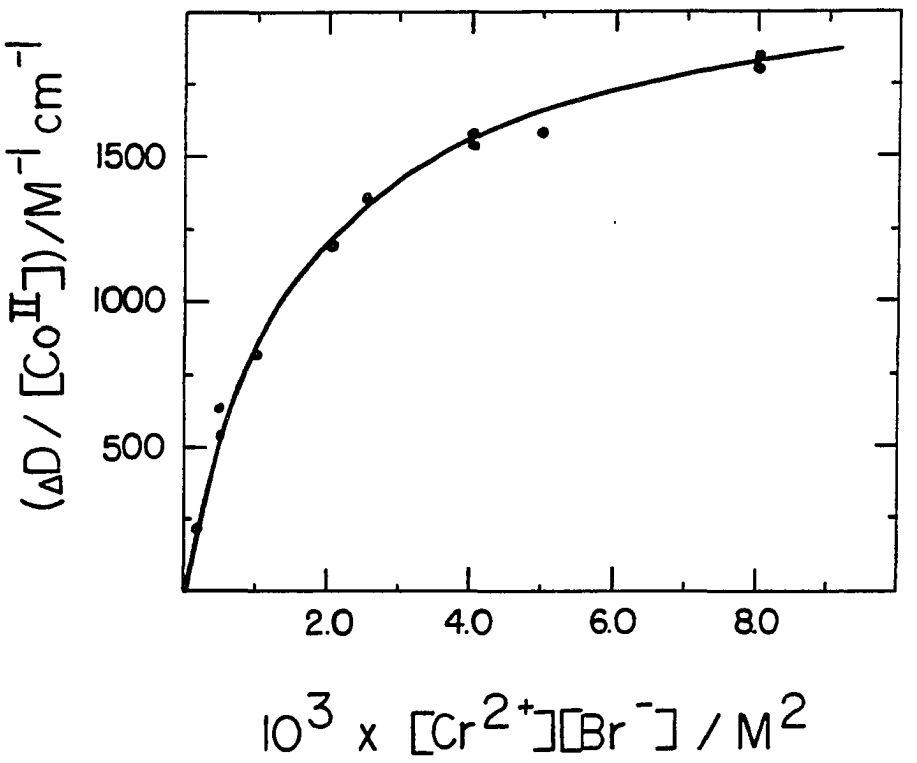

Figure II-7. Plot of the change in absorbance at 760 nm, normalized by the initial $[Co(dmgBF_2)_2]$ and divided by the path-length (2 cm) of the reaction cell, vs. the product $[Cr^{2+}][Br^-]$. The line drawn was calculated by a least-squares analysis of the data according to eq 8

during the pre-steady-state phase. The kinetics of this phase were pseudo-first-order. The data are contained in Table II-2 and presented in Figure II-6. The apparent rate constant has the same functional form as eq 7, and the parameters, k_a and k_b, calculated by a least-squares analysis of the data, are 304(±19) $M^{-2}s^{-1}$ and 0.43(±0.07) s^{-1}, respectively.

Figure II-7 shows that the change in absorbance at 760 nm reaches a plateau at high $[Cr^{2+}]$ and $[Br^-]$ in a manner that is analogous to the chloride ion system. The parameters A and B, derived from a nonlinear least-squares analysis of the ΔD data (normalized for the initial $[Co(dmgBF_2)_2]$) according to eq 8, are 2120(±50) $M^{-1}cm^{-1}$ and (1.52 ± 0.09) x 10^{-3} M^2 respectively.

Steady-state Phase -- Loss of Chromium(II) Ion The concentration of Cr^{2+} ion during the course of the reaction ($[NaCl] = 0.25$ M and $[H^+] = 0.52$ M) was determined by direct chemical analysis of samples withdrawn at intervals and rapidly quenched. Table II-3 contains the kinetic data for the loss of $[Cr^{2+}]$. Figure II-8 displays the initial rates for the loss of the Cr^{2+} (normalized for the initial $[Co(dmgBF_2)_2]$) vs. the initial Cr^{2+} concentration. The line drawn through the points was calculated by a least-squares analysis of the data according to eq 9. The calculated

$$\frac{v_i}{[Co(dmgBF_2)_2]_0} = \frac{\alpha[Cr^{2+}][Cl^-]}{\beta + [Cr^{2+}][Cl^-]} \qquad (9)$$

Table II-3. The Concentration of Chromium(II) Ion at Various Times and the Initial Rate for the Loss of the Chromium(II) Ion[a]

$[Cr^{2+}]_0$/M	10^2 x $[Cr^{2+}]_t$/M	t/s	10^5 x ν_{int}/M s^{-1}
0.05	4.16	24	
	4.08	46	
	3.88	64	
	3.68	83	8.33
0.03	2.40	45	
	2.12	87	
	1.91	118	
	1.67	147	7.09
0.01	0.74	32	
	0.65	59	
	0.51	91	
	0.43	119	3.63
0.004	0.27	30	
	0.25	53	
	0.20	79	
	0.17	102	1.40

[a]The reaction was performed at T = 25($\pm$0.5) °C with $[H^+]$ = 0.52 M, $[Co(dmgBF_2)_2]$ = 1.16 x 10^{-4} M, and $[Cl^-]$ = 0.25 M. The ionic strength of the reaction solution was 1.00 M and was adjusted using $LiClO_4$.

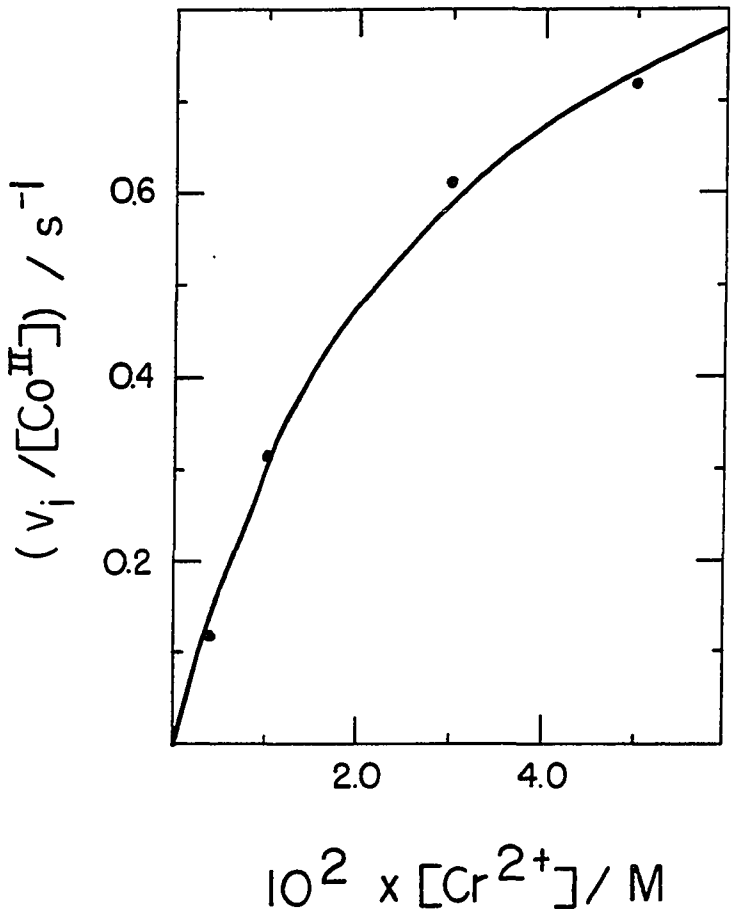

Figure II-8. Plot of the initial rate for $[Cr^{2+}]$ loss, normalized by the initial $[Co(dmgBF_2)_2]$, vs. the initial $[Cr^{2+}]$. The reaction was performed with $[Cl^-]$ = 0.25 M. The line drawn through the points was calculated by a least-squares analysis of the data according to eq 9

parameters, α and β, are 1.08($\pm$0.04) s^{-1} and (5.4 $\pm$ 0.6) x 10^{-3} M^2 respectively. Interpretation of the data according to the mechanism in Scheme 1 identifies α as $2k_3$ and β as the Michaelis constant, K_s or $(k_{-2} + k_3)/k_2$.

Steady-state Phase -- Loss of the Intermediate At longer times (> 10 s), the steady-state concentration of INT begins to decrease, as shown in Figure II-9. Table II-4 contains the kinetic data for the decrease of $[INT]_{ss}$, determined from the loss in absorbance at 770 nm. The kinetic traces at higher concentrations of Cr^{2+} (> 0.01 M) were somewhat noisy due to the evolution of the H_2 gas.

$$\frac{V}{[Co(dmgBF_2)_2]^2} = \frac{A[Cr^{2+}][Cl^-]}{(B + [Cr^{2+}][Cl^-])^3} \qquad (10)$$

Figure II-10 displays the rate, V (the initial rate for the loss in absorbance at λ 770 nm), for the loss of $[INT]_{ss}$ (normalized by the square of the initial $[Co(dmgBF_2)_2]$) vs. the initial $[Cr^{2+}]$. An interesting feature is readily apparent in this plot; a maximum in V occurs as the initial Cr^{2+} concentration is increased. The line drawn through the points is calculated by a least-squares analysis of the data according to eq 10 (see the appendix for the

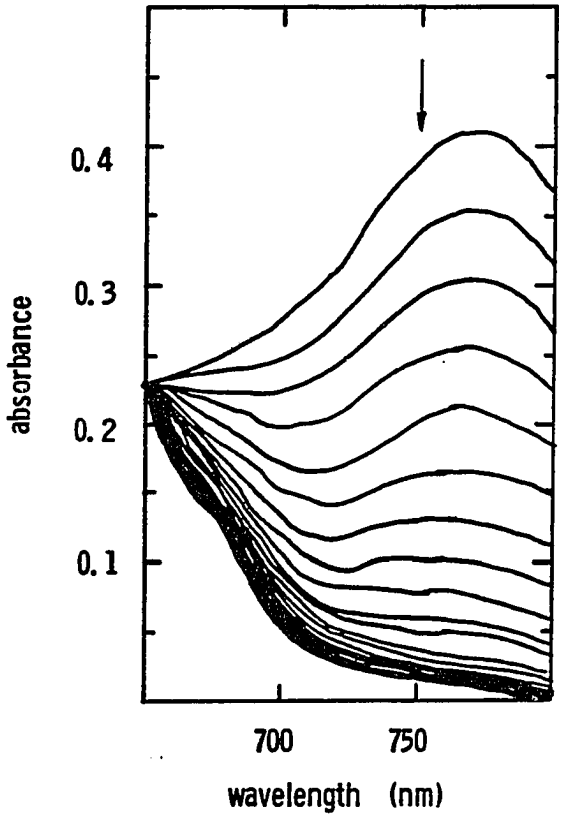

Figure II-9. Loss of INT absorbance with time. The spectra were recorded at 20 s intervals. The concentrations of the reagents were $[Cr^{2+}]$ = 0.024 M, [HCl] = 0.26 M, and $[Co(dmgBF_2)_2]$ = 1.9×10^{-4} M

Table II-4. Rate Data from the Decrease in the Steady-state Concentration of the Intermediate[a]

10^3 x $[Cr^{2+}]$/M	10^4 x [Co]/M	10^4 x V[b]	$t_{1/2}$/s	D_{max}
40.0	1.56	11.8	246	0.481
30.0	1.16	8.77	230	0.314
20.0	1.56	12.9	148	0.354
15.0	1.16	10.4	121	0.214
10.0	1.56	15.0	86	0.262
10.0	1.16	11.2	112	0.186
7.0	1.16	8.82	91	0.145
4.0	1.16	6.16	84	0.0882
3.0	1.16	6.58	63	0.0710
2.0	1.16	4.76	67	0.0496
1.5	1.16	4.07	49	0.0340
1.0	1.16	2.34	65	0.0245
20.0[c]	3.13	29.3	114	0.686
20.0[c]	1.56	11.4	178	0.393
20.0[c]	0.78	5.47	304	0.241
20.0[d]	1.56	14.3	124	0.343

[a]The rates were measured at λ 770 nm by following the loss in absorbance during the first 40 s of the reaction. T = 25.0(±0.1) °C, $[Cl^-]$ = 0.25 M, $[H^+]$ = 0.52 M, and I = 1.00 M adjusted with $LiClO_4$.

[b]Units of M^{-1} s^{-1} cm^{-1}.

[c]$[H^+]$ = 0.27 M.

[d]$[H^+]$ = 0.77 M.

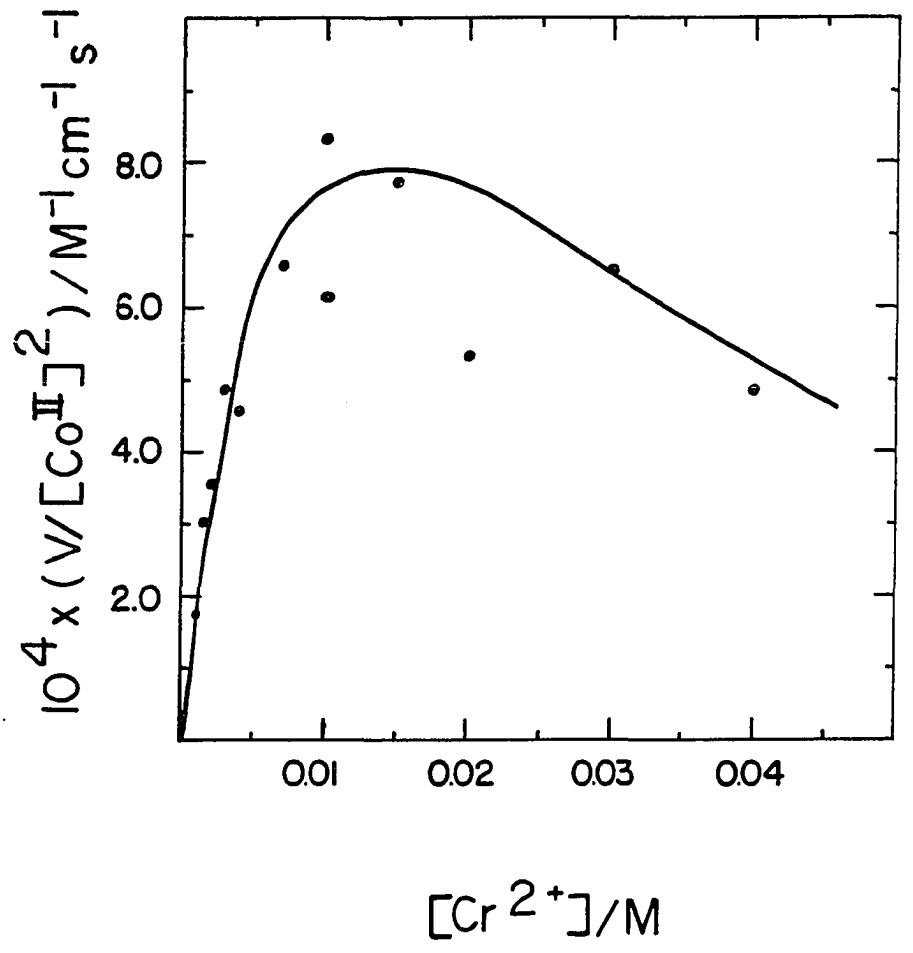

Figure II-10. Plot of the initial rate for the loss of [INT], normalized by the square of the $[Co(dmgBF_2)_2]$, vs. the initial $[Cr^{2+}]$. The concentration of Cl^- was 0.25 M in all of the runs. The line drawn through the points was calculated by a least-squares analysis of the data according to eq 10

derivation of this equation). The parameters derived from the least-squares analysis must be regarded as approximate due to the difficulty in measuring the initial rates for the loss of absorbance. The value of the parameters, A and B, are 19(±4) M s^{-1} cm^{-1} and 6.1(±0.6) x 10^{-3} M^2, respectively. A and B are equivalent to the constants $2\Delta\varepsilon K_s k_3$ and K_s using Scheme I as the model. Although this treatment is not quantitative, the qualitative agreement between observed and calculated results is quite good.

The kinetics for the loss of the absorbance at 770 nm can be treated in another manner (see Appendix II). Equations 11 and 12 relate $t_{1/2}$ (the time in which the absorbance at 770 nm declines to half of its maximum value) values with the concentration product $[Cr^{2+}][Cl^-]$. Figure II-11 displays the

$$(t_{1/2})[Co(dmgBF_2)_2] = \frac{(K_s)}{2k_3[Cl^-]} + (2k_3[Cl^-])^{-1}[Cr^{2+}][Cl^-] \qquad (11)$$

$$(t_{1/2})(D_{max}) = \Delta\varepsilon(2k_3[Cl^-])^{-1}[Cr^{2+}][Cl^-] \qquad (12)$$

plots of the data according to eq 11 and 12. The values of the parameters, $K_s/2k_3[Cl^-]$ and $1/2k_3[Cl^-]$, determined from a least-squares analysis of the data according to eq 11 are

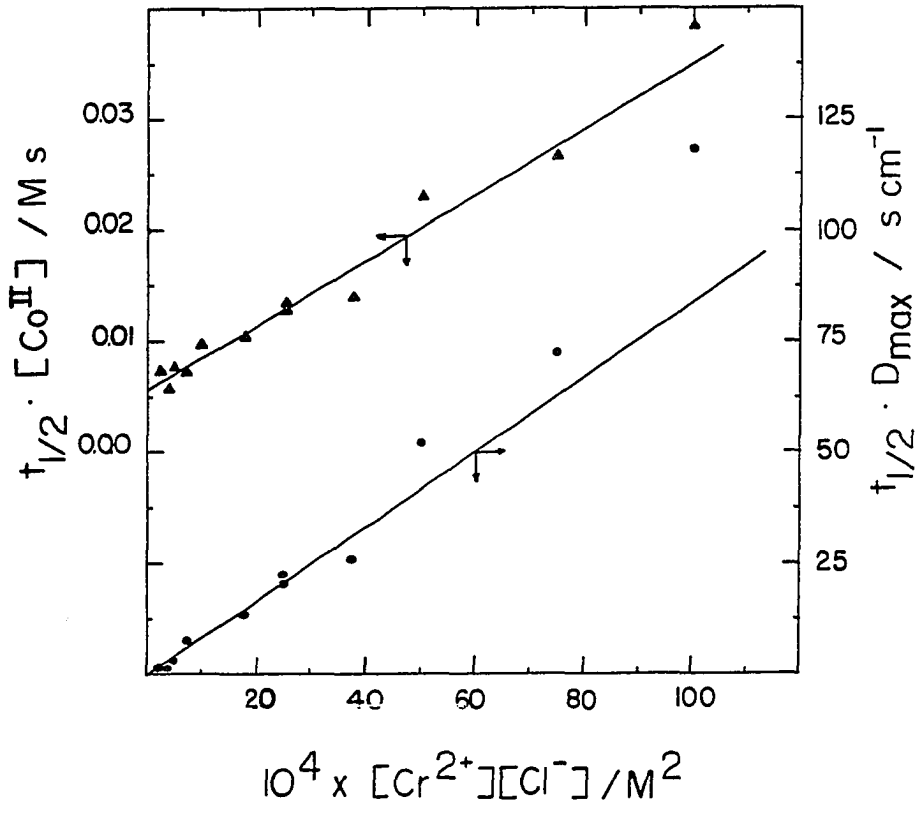

Figure II-11. Plots representing the variation of $t_{1/2}$ for the loss of absorbance of the intermediate as function of the concentration product $[Cr^{2+}][Cl^-]$. ▲ data plotted according to eq 11. ● data plotted according to eq 12

$5.6(\pm 0.4) \times 10^{-3}$ M^2 and $2.9(\pm 0.2)$ M^{-1} s respectively. The calculated value of $\Delta\epsilon/2k_3[Cl^-]$ is $6900(\pm 500)$ M^{-2} s cm^{-1}. Note that eq 11 predicts that $t_{1/2}$ should be inversely proportional to $[Co(dmgBF_2)_2]$. This behavior is observed (see Table II-4).

Formation of an Intermediate Using Eu^{2+}or V^{2+} The reducing metal ions, Eu^{2+} and V^{2+}, both react with $Co(dmgBF_2)_2$ and Cl^- to form an intermediate which absorbs at 770 nm. A plot of ΔD, for the formation of INT, vs. the product, $[Eu^{2+}][Cl^-]$, begins to show curvature at high $[Eu^{2+}]$ and $[Cl^-]$, as can be seen in Figure II-12. This curvature is not as pronounced as that seen in the Cr^{2+} system. The ΔD and concentration data for the Eu^{2+} reaction are contained in Table II-5. A least-squares analysis of the data, according to an equation with the same functional form as eq 8, yields the values $(3 \pm 1) \times 10^3$ $M^{-1}cm^{-1}$ and $0.2(\pm 0.1)$ M^2 for the parameters A and B respectively.

Miscellaneous Experimental Results To test for the intermediacy of cobalt(I) species, several experiments were performed. First, phenylacetylene, a known trap[24] for $HCo(dmgH)_2$ and $Co(dmgH)_2^-$, was included in the Cr^{2+}, Cl^-, and $Co(dmgBF_2)_2$ reaction. The ratio of $[H_2]/[Cr^{2+}]_0$ dropped dramatically to 0.08 from about 0.44. The reaction mixture became cloudy as a white precipitate formed. Second, if some nonreducing metal ion, such as Fe^{2+} or Zn^{2+}, is added to $Co(dmgBF_2)_2$ and Cl^- in the place of Cr^{2+}, Eu^{2+}, or V^{2+} ions,

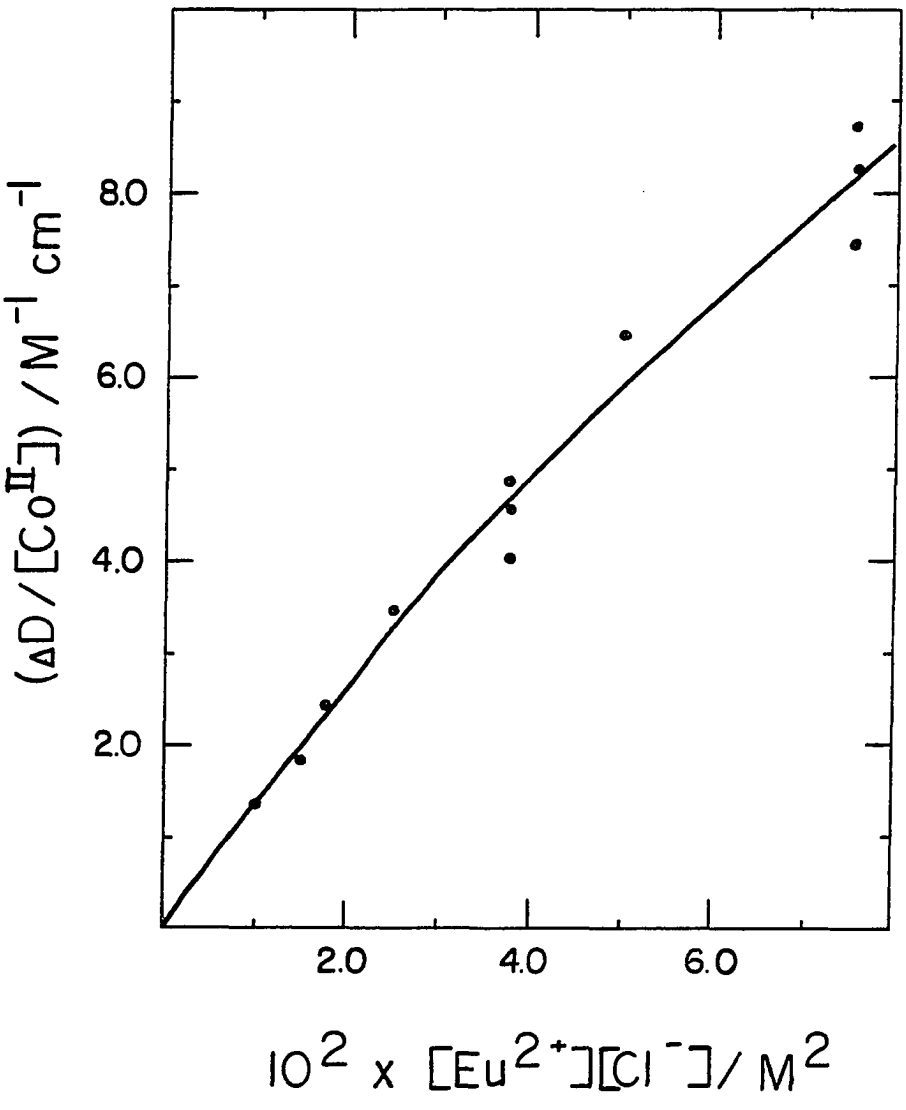

Figure II-12. Plot of the change in absorbance at 770 nm, normalized by the initial $[Co(dmgBF_2)_2]$, vs. the product, $[Eu^{2+}][Cl^-]$. The line drawn through the points was calculated by a least-squares analysis of the data according to eq 8

Table II-5. The Absorbance Change Due to Intermediate Formation in the Eu^{2+}, Cl^-, $Co(dmgBF_2)_2$ System[a]

$[Eu^{2+}]$ / M	$[Cl^-]$ / M	10^4 x [Co] / M	ΔD
0.10	0.75	2.99	0.246
0.10[b]	0.75	2.10	0.182
0.10	0.75	0.99	0.0734
0.10	0.50	2.99	0.194
0.075	0.50	1.49	0.0725
0.05	0.75	2.99	0.136
0.05	0.75	0.99	0.040
0.05	0.50	2.99	0.104
0.035	0.50	1.49	0.036
0.02	0.75	2.99	0.0545
0.02	0.50	2.99	0.0405

[a]The delta absorbance was obtained in a 1 cm cell at λ 772 nm. The reaction was done at T = 23(±1) °C, $[H^+]$ = 0.25 M, and I = 1.00 M adjusted with $LiClO_4$.

[b]This run had 0.05 M Eu^{3+} added.

no absorbance above 700 nm is formed and no H_2 is evolved.

The reaction between Cr^{2+} and $Co(dmgBF_2)_2$ was conducted in ClO_4^- solution. Cr^{3+} was formed, but only very slowly (about 1 hr), compared with the reaction in the presence of some coordinating ligand. Also, the evolution of a gas was not observed.

A slight $[H^+]$ dependence is observed on the loss of the steady-state concentration of INT (see Table II-4). Since the kinetics for the loss of this intermediate are quite complicated, the $[H^+]$ dependence was not studied quantitatively. The rate for the loss of the intermediate did, however, increase with increasing $[H^+]$. No dependence on $[H^+]$ was observed in the pre-steady-state phase.

Collection of Experimental Results The kinetic experiments described can be divided into four types. Type I experiments are the kinetics of INT buildup. Type II experiments are the measurements of the changes in visible absorption for the buildup of $[INT]_{ss}$ to its maximum value. Experiments of types I and II were performed during the pre-steady-state phase of the reaction. An experiment of type III is the measurement of the initial rate for the loss of Cr^{2+}. Finally, the type IV experiment is the kinetics for the loss of INT visible absorption. The values of the rate constants and the experimental types from which they were derived are summarized in Table II-6.

Table II-6. A Collection of Rate and Other Constants and the Experimental Types from which There were Derived[a]

Type	k_2	$(k_{-2} + k_3)$	k_3	$10^3 \times K_s$	$\Delta\varepsilon$
Cr^{2+}, Cl^- [b]					
I	220(±11)	0.25(±0.02)	---	1.1(±0.1)	---
II	---	---	---	1.6(±0.2)	2250(±90)
III	---	---	0.54(±0.02)	5.4(±0.6)	---
IV[c]	---	---	0.69(±0.04)	1.9(±0.2)	---
IV[d]	---	---	0.52(±0.04)	---	---
IV[e]	---	---	0.7 (±0.2)	6.1(±0.6)	---
Cr^{2+}, Br^- [f]					
I	304(±19)	0.43(±0.07)	---	1.4 (±0.2)	---
II	---	---	---	1.52(±0.09)	2120(±50)
Eu^{2+}, Cl^- [g]					
II	---	---	---	0.2(±0.1)	3000(±1000)

[a]These constants were calculated from the experimental parameters using Scheme 1 as a model. The units for the constants, beginning with k_2 and ending with $\Delta\varepsilon$, are $M^{-2}s^{-1}$, s^{-1}, s^{-1}, M^2, $M^{-1}cm^{-1}$ respectively.

[b]The Cr^{2+}, Cl^-, and $Co(dmgBF_2)_2$ reaction.

[c]These constants were calculated using eq 11.

[d]This constant was calculated using eq 12.

[e]This constant was calculated from the parameter, $2\Delta\varepsilon K_s k_3$, derived from eq 10 using the $\Delta\varepsilon$ value from the type II experiment and the K_s value from this experiment.

[f]The Cr^{2+}, Br^-, and $Co(dmgBF_2)_2$ reaction.

[g]The Eu^{2+}, Cl^-, and $Co(dmgBF_2)_2$ reaction.

Discussion

Intermediacy of Cobalt(I) The presence of cobalt(I) intermediates in the reaction between M^{2+}, X^-, and $Co(dmgBF_2)_2$ is well-supported by several experimental observations. First, the reaction requires the presence of a reducing M^{2+}, like Cr^{2+}, Eu^{2+}, or V^{2+}. Second, the addition of phenylacetylene, a specific trapping agent[24] for $Co(dmgH)_2^-$ and $HCo(dmgH)_2$, dramatically reduces the quantity of H_2 evolved. Third, the absorption spectrum of INT suggests that it is a cobalt(I) species.

Figures II-1 and II-5 show difference spectra for the buildup of INT. These difference spectra at any time, t, can be calculated using eq 15. Equation 15 was derived from eq 13

$$D_t = \varepsilon_{Co(II)}[Co(II)]_t + \varepsilon_{Cr(II)}[Cr(II)]_t + \varepsilon_{int}[INT]_t \quad (13)$$

$$D_{max} = \varepsilon_{Co(II)}[Co(II)]_{max} + \varepsilon_{Cr(II)}[Cr(II)]_{max} + \varepsilon_{int}[INT]_{max} \quad (14)$$

$$\Delta D_t = D_t - D_{max} = (\varepsilon_{Co(II)} - \varepsilon_{int})([INT]_{max} - [INT]_t) \quad (15)$$

and 14, using the mass balance for the cobalt species and the approximation that the change in absorbance due to Cr^{2+} is negligible. D_{max} is the value of the absorbance when the maximum steady-state concentration of INT is reached. The

absorption values at wavelengths greater than 500 nm in Figures II-1 and II-5 are, to a good approximation, equivalent to those of INT. The molar absorptivity of $Co(dmgBF_2)_2$ is about 280 $M^{-1}cm^{-1}$ at 520 nm and drops to below 60 $M^{-1}cm^{-1}$ at 600 nm, whereas those of the intermediate, in this wavelength range, are > 2 x 10^3 $M^{-1}cm^{-1}$.

Absorption maxima occur at 525 and 720 nm in both Figures II-1 and II-5. These correspond quite well with a number of known spectra for cobalt(I) macrocycles[25-28]. In fact, the spectrum[27,28] of $[Co(dmgBF_2)_2C_5H_5N]^-$ in basic methanol shows maxima at 625 and 526 nm.

Mechanistic Role of the Halide Ion The presence of the halide ion is clearly necessary for the evolution of H_2, as the result of the experiment done in ClO_4^- solution attests. The halide ion acts as a bridge for inner-sphere electron transfer between the reducing metal ion and the cobalt(II). This result is particularly evident by the fact that only $CrCl^{2+}$ is formed and not the thermodynamically favored[29] $Cr(H_2O)_6^{3+}$.

The exact path for the involvement of the halide ion can not be distinguished kinetically, but the presence of a termolecular reaction (eq 2) is unlikely. Two kinetically indistinguishable paths can be considered, and are presented in Schemes III and IV. The binding of anions to macrocyclic cobalt(II) species has been established.[30,31] The equilibrium

constants[30] for the binding of Cl^- and Br^- to $Co(dmgH)_2$ are about 1, although more recent work[32] suggests that this value may be too large. No binding constants for Cl^- or Br^-

Scheme III

$$Co(dmgBF_2)_2 + X^- \underset{}{\overset{K_{16}}{\rightleftharpoons}} XCo(dmgBF_2)_2^- \qquad (16)$$

$$XCo(dmgBF_2)_2^- + Cr^{2+} \underset{k_{-2}}{\overset{k_2'}{\rightleftharpoons}} INT \qquad (17)$$

Scheme IV

$$Cr^{2+} + X^- \underset{}{\overset{K_{18}}{\rightleftharpoons}} CrX^+ \qquad (18)$$

$$Co(dmgBF_2)_2 + CrX^- \underset{k_{-2}}{\overset{k_2''}{\rightleftharpoons}} INT \qquad (19)$$

to Cr^{2+} have been measured, but they are not expected to be large[33,34]. Since the binding constants for the Cr^{2+} and $Co(dmgBF_2)_2$ are comparable, no arguments can be advanced to select one scheme over the other.

Is the Intermediate a Dead-end? An alternative mechanism to the one presented in Scheme I is given in Scheme V. In this scheme, INT is a dead-end intermediate. The kinetic equations take the same form as those used in Scheme I, but the experimental parameters have a different significance (see

Scheme V

$$Cr^{2+} + Cl^- + Co(dmgBF_2)_2 \underset{k_{-2}}{\overset{k_2}{\rightleftharpoons}} INT \qquad (2)$$

$$Cr^{2+} + Cl^- + Co(dmgBF_2)_2 \xrightarrow{k_3^*} CrCl^{2+} + Co(dmgBF_2)_2^- \qquad (3)$$

$$Co(dmgBF_2)_2^- + H^+ \underset{}{\overset{K_4}{\rightleftharpoons}} HCo(dmgBF_2)_2 \qquad (4)$$

$$HCo(dmgBF_2)_2 + H^+ \xrightarrow{fast} H_2 + Co(dmgBF_2)_2^+ \qquad (5)$$

$$Co(dmgBF_2)_2^+ + Cr^{2+} + Cl^- \xrightarrow{fast} CrCl^{2+} + Co(dmgBF_2)_2 \qquad (6)$$

the Appendix II). These two mechanisms cannot be distinguished from the kinetic data. The likelihood of the reaction taking two inner-sphere electron transfer paths with the same components is, however, small, and the generation of

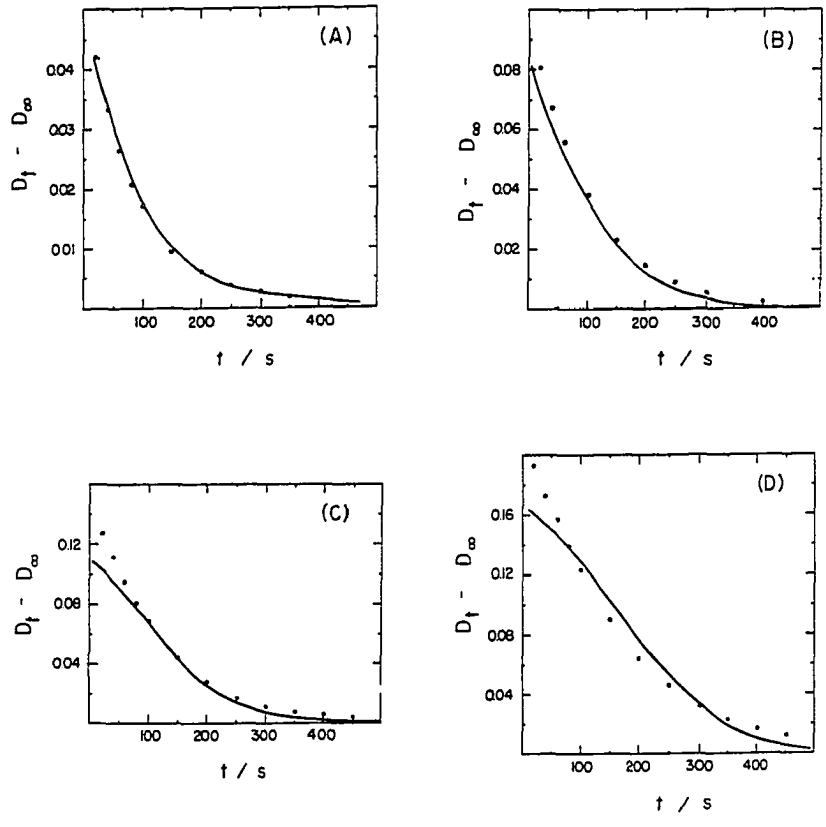

Figure II-13. Comparisons of the experimental data with the numerically simulated data according to Scheme I. The concentrations of the reagents are $[Cl^-]$ = 0.25 M, $[Co(dmgBF_2)_2]$ = 1.16 x 10^{-4} M, and $[Cr^{2+}]$ = (A) 2.0 mM, (B) 4.0 mM, (C) 7.0 mM, and (D) 15 mM. The values of the rate constants, k_2, k_{-2}, and k_3, used were 220 $M^{-2}s^{-1}$, 0.001 s^{-1}, and 0.54 s^{-1}, respectively

the products, $CrCl^{2+}$ and H_2, probably occurs via the intermediate.

Kinetic Simulations The values of the rate constants used in the numerical simulations were a compromise of several experimental results. The values of k_2 and k_3, 220 $M^{-2}s^{-1}$ and 0.54 s^{-1}, were taken from experiments types I and III. The value of k_{-2} was more difficult to obtain. In accordance with Scheme I, k_{-2} can be calculated from several of the experimental parameters. The intercept in the plot of the apparent rate constant vs. the concentrations of the substrates (type I experiment) is equal to the sum, $k_{-2} + k_3$. Since the value of k_3 is larger than the value of the intercept (0.25 s^{-1}), the value of k_{-2} would be negative. Thus a small value of k_{-2}, 0.001 s^{-1}, was chosen for the numerical analysis.

Figure II-13 shows the numerically simulated, and experimental, loss of the absorbance at 770 nm. The kinetic simulation was performed with k_2 = 220 $M^{-2}s^{-1}$, k_{-2} = 0.001 s^{-1}, k_3 = 0.54 s^{-1} for $[Cl^-]$ = 0.25 M, $[Co(dmgBF_2)_2]$ = 1.16 x 10^{-4} M, and Cr^{2+} concentrations of 0.002, 0.004, 0.007, and 0.015 M. The simulated concentration-time profile, according to Scheme I, fits the experimental data very well at low concentrations of Cr^{2+}. At the higher Cr^{2+} concentrations, the fit becomes less good, with most of the deviation occurring at the beginning of the reaction. If the value of k_{-2} is increased the loss of $[INT]_{ss}$ becomes slower.

Likewise, a decrease in the value of k_3 slows the loss of $[INT]_{ss}$.

The simulated line, according to the mechanism shown in Scheme V, overlaps the line calculated for Scheme I. The values of k_2, k_{-2}, and k_3^* used were 220 $M^{-2}s^{-1}$, 0.53 s^{-1}, and 225 $M^{-2}s^{-1}$, respectively.

The Hydrogen Evolution Step A heterolytic cleavage of the cobalt-hydrogen bond is proposed, although a bimolecular reductive elimination of H_2 cannot be ruled out. The evolution of H_2 from $HCo(dmgH)_2(PBu_3)$[11] was found to occur by the heterolytic path in acidic solution, but, as the H^+ concentration was lowered, the bimolecular path for the release of H_2 became dominant. Considering the highly acidic solutions ($[H^+]$ = 0.25 - 0.75 M) used in this study, it seems reasonable that H^+ reacts directly with the $HCo(dmgBF_2)_2$ to form H_2.

Summary

The reaction between M^{2+} (M = Cr, Eu, and V), X^- (Cl^- or Br^-), and $Co(dmgBF_2)_2$ produces H_2 catalytically. The numerical data can be analyzed in terms of the Michaelis-Menten mechanism for enzyme catalysis. There are two well-defined stages to the reaction; a buildup of a strongly absorbing intermediate, and its subsequent decay to a hydridocobalt complex. The intermediate is a Co(I) species, as characterized by its visible spectrum.

Work is continuing on the Co(II) catalyzed generation of H_2 from Cr^{2+} and Cl^- solutions. $[Co(Me_4[14]\text{-}1,4,8,11\text{-}tetraeneN_4)](Br)_2$ has been found to also act as a catalyst toward H_2 evolution. Of course, the use of Cr^{2+} to generate Co(I) for the purpose of H_2 evolution is not practical. However, Co(I) can undergo other reactions, such as the hydrogenation of alkenes and alkynes[24,27]. The catalytic reactions described provide a controlled means for the production of Co(I), an important intermediate.

Bibliography

1. Spiro, M.; Ravno, A.B. J. Chem. Soc. 1965, 78.
2. Yee, E.L.; Cave, R.J.; Kendall, L.G.; Tyma, P.D.; Weaver, M.J. J. Am. Chem. Soc. 1979, 101, 1131.
3. Weaver, M.J.; Yee, E.L. Inorg. Chem. 1980, 19, 1936.
4. It has been reported that Cr^{2+} in EDTA solutions reduces vitamin B_{12r} to vitamin B_{12s}. The B_{12s} slowly reacts with water to produce B_{12r} and H_2. a) Johnson, A.W.; Mervyn, L.; Shaw, N.; Smith, E.L. J. Chem. Soc. 1963, 4146. b) Schrauzer, G.N.; Deutsch, E.; Windgassen, R.J. J. Am. Chem. Soc. 1968, 90, 2441.
5. Schrauzer, G.N.; Holland, R.J. J. Am. Chem. Soc. 1971, 93, 1505.
6. Schrauzer, G.N. Inorg. Syn. 1968, 11, 61.
7. Rillema, D.P.; Endicott, J.F. Inorg. Chem. 1972, 11, 2361.
8. Dodd, D.; Johnson, M.D. Organomet. Chem. Rev. 1973, 52, 1.
9. Murakami, Y. Adv. Chem. Ser. No. 191 1980, 179.
10. Ryan, D.A.; Espenson, J.H. Inorg. Chem. 1981, 20, 4401.
11. Chao, T.-H.; Espenson, J.H. J. Am. Chem. Soc. 1978, 100, 129.
12. Evans, J.; Norton, J.R. J. Am. Chem. Soc. 1974, 96, 7577.
13. Halpern, J. Inorg. Chim. Acta 1983, 77, L105.
14. Halpern, J. J. Organomet. Chem. 1980, 200, 133.
15. Simandi, L.I.; Budo-Zahonyi, E.; Szeverenyi, Z. Inorg. Nucl. Chem. Lett. 1976, 12, 237.

16. Labinger, J.A. Adv. Chem. Ser. No. 167 1978, 149.

17. Rillema, D.P.; Endicott, J.F. Inorg. Chem. 1976, 15, 1459.

18. Brown, G.M.; Brunschwig, B.S.; Creutz, C.; Endicott, J.F.; Sutin, N. J. Am. Chem. Soc. 1979, 101, 1298.

19. Tovrog, B.S.; Kitko, D.J.; Drago, R.S. J. Am. Chem. Soc. 1976, 98, 5144.

20. Bakac, A.; Espenson, J.H. J. Am. Chem. Soc. 1984, 106, 5197.

21. Barshop, B.A.; Wrenn, R.F.; Frieden, C. Anal. Biochem. 1983, 130, 134.

22. Burns, D.T.; Townshend, A.; Carter, A.H. "Inorganic Reaction Chemistry"; Halsted Press: New York, N.Y., 1981; Vol. 2, p 191.

23. Hiromi, K. "Kinetics of Fast Enzyme Reactions"; Halsted Press: New York, N.Y., 1979.

24. Naumberg, M.; Duong, K.N.V.; Gaudemer, A. J. Organomet. Chem. 1970, 25, 231.

25. Tait, A.M.; Hoffman, M.Z.; Hayon, E. J. Am. Chem. Soc. 1976, 98, 86.

26. Espenson, J.H.; Chao, T.-H. Inorg. Chem. 1977, 16, 2553.

27. Schrauzer, G.N.; Weber, J.H.; Beckham, T.M. J. Am. Chem. Soc. 1970, 92, 7078.

28. Ramasami, T.; Espenson, J.H. Inorg. Chem. 1980, 19, 1523.

29. $K_{eq} = [CrCl^{2+}]/[Cr^{3+}][Cl^{-}] = 0.11\ M^{-1}$.

30. Burger, K.; Pinter, B. J. Inorg. Nucl. Chem. 1967, 29, 1717.

31. Marov, I.N.; Panfilov, A.T.; Ivanova, E.K. Koord. Khim. 1976, 2, 948.

32. Brynildson, M.; Espenson, J.H.; Bakac, A. unpublished observations, Iowa State University, Ames, Ia.

33. The binding constant, K_B, for Cl^- to Cr^{2+} can be estimated from two reactions: $Cr^{2+} + CrCl^{2+} \rightarrow CrCl^{2+} + Cr^{2+}$ (k_a = 500 M^{-1} min^{-1}) and $Cr^{2+} + {}^*Cl^- + CrCl^{2+} \rightarrow Cr{}^*Cl^{2+} + Cr^{2+} + Cl^-$ (k_b= 31 M^{-2} min^{-1}). Since $k_b = K_B k'$ and if k' is approximately = k_a, then, K_B = 0.06 M^{-1}. The data were taken from: Taube, H.; King, E.L. J. Am. Chem. Soc. 1954, 76, 4053.

34. An empirical equation for calculating the binding constants of various ligands for Cr^{2+} has been developed (Cannon, R.D. J. Inorg. Nucl. Chem. 1976, 38, 1222), $\log K_{Cr} = \alpha \log K_{Cu} + (1/5)(6-\alpha)\log K_{Mn} - (1/5)(1+4\alpha)\log K_{Zn}$ where $\alpha = 0.55$. This expression yields, after substitution of the known binding constants of Cl^- for Cu^{2+}, Mn^{2+}, and Zn^{2+} (logK = 0.15, -0.33, -0.06 respectively), a value of -0.24 for $\log K_{Cr}$. The binding constants for Cu^{2+}, Mn^{2+}, and Zn^{2+} were obtained from Smith, R.M.; Martell, A.E. "Stability Constants of Metal Ion Complexes"; Plenum Press: New York, N.Y., 1976; Vol 4.

Appendix II

The Michaelis-Menten mechanism for a reaction between an enzyme and its substrate (Scheme II) is repeated here in Scheme AII-1. The kinetic expressions for this mechanism has been covered quite well in the literature[23]. Nevertheless, the mechanism and the rate expressions are given here for quick reference. There are two time regimes in this

Scheme AII-1

$$E + S \underset{k_{-a}}{\overset{k_a}{\rightleftharpoons}} ES \qquad (a)$$

$$ES \xrightarrow{k_b} P + E \qquad (b)$$

$$[ES]_{ss} = \frac{[E]_0[S]}{\frac{k_{-a} + k_b}{k_a} + [S]} \qquad (c)$$

mechanism. They are designated the pre-steady-state and steady-state phases. The pre-steady-state is the time prior to the buildup of ES to its steady-state value. The buildup of ES follows pseudo-first-order kinetics with the apparent rate constant, $k_{app} = k_a[S] + (k_{-a} + k_b)$. The value of the steady-state concentration of ES is given by eq c, where the

collection of rate constants, $(k_{-a} + k_b)/k_a$, is known as the Michaelis constant, K_s.

The rate for product formation is given by eq d and becomes eq e after substitution of the expression for $[ES]_{ss}$. As [S] increases, the rate begins to plateau and a limiting rate, $k_b[E]_0[S]$ is reached.

The rate for the loss of [ES], following the pre-steady-state, is given by eq f. The [S] does not remain constant with time, unlike during the pre-steady-state, as [ES] is lost. Differentiation of eq e with respect to time yields eq g.

$$d[P]/dt = -d[S]/dt = k_b[ES] \qquad (d)$$

$$d[P]/dt = \frac{k_b\,[E][S]}{(K_s + [S])} \qquad (e)$$

$$-d[ES]/dt = -(k_b)^{-1}\, d^2[P]/dt^2 \qquad (f)$$

$$-d[ES]/dt = \frac{k_b K_s [E]_0{}^2 [S]}{(K_s + [S])^3} \qquad (g)$$

[ES] should increase, go through a maximum, and then decrease, with increasing [S].

The rate for the loss of ES can be related to the loss of absorbance of ES by eq h.

$$-d[ES]/dt = -(\varepsilon)^{-1}(dD/dt) \qquad (h)$$

Integration of eq d between the limits 0 and ∞ gives the area beneath the [ES]-time curve. Substitution of eq c into eq j and rearrangement yields eq k. Alternatively, $[ES]_{max}$ can be substituted by $D_{max}/\Delta\varepsilon$, yielding eq l upon rearrangement.

$$\int_o^\infty d[P] = k_b \int_o^\infty [ES]dt \qquad (i)$$

$$[P]_\infty - [P]_o = [S]_o = k_b \int_o^\infty [ES]dt = k_b[ES]_{max}\ t_{1/2} \qquad (j)$$

$$(t_{1/2})[Co(dmgBF_2)_2] = K_s/k_b + k_b^{-1}[S]_o \qquad (k)$$

$$(t_{1/2})D_{max} = (\Delta\varepsilon/k_b)[S]_o \qquad (l)$$

Scheme AII-2 shows the case where ES is a deadend intermediate. The kinetic equations have the same form as those obtained using Scheme AII-1, however, the specific meanings of the parameters are different. The value of

Scheme AII-2

$$E + S \underset{k_{-a}}{\overset{k_a}{\rightleftharpoons}} ES$$

$$E + S \xrightarrow{k_b} P + E$$

the apparent rate constant becomes $k_{app} = k_a + k_{-a}$. The value of the Michaelis constant, K_s, is k_{-a}/k_a. The rate for product formation becomes $d[P]/dt = k_b K_s [ES]_{ss}$.

CHAPTER III. A FLASH PHOTOLYTIC STUDY OF THE REDUCTION OF HALOCOBALOXIMES BY 1-HYDROXY-1-METHYLETHYL RADICAL

Introduction

The reduction of Co(III) complexes by hydroxyalkyl radicals has been a subject of recent interest[1-3]. Such studies were conducted by following the decay of the radical absorbance in the ultra-violet region of the spectrum. This poses two limitations: (a) the UV absorbance change is relatively small, in a region of the spectrum where absorptions are nonspecific, owing to the small molar absorptivities of aliphatic radicals; and (b) the necessary use of higher initial concentrations of radical, which leads to a greater proportion of the nonproductive self-reactions (bimolecular radical disproportionation or dimerization) at the expense of the desired reaction. In addition, these traditional methods rely on the very specialized technique of pulse radiolysis which is available at only a few installations. The methods reported here were developed to overcome these various complications and to offer data for the reduction of the previously unexplored cobalt(III) complexes known as cobaloximes[a].

---

[a]Cobaloxime is a trivial name for bis(2,3-butanedione dioxime)cobalt also known as bis(dimethylglyoximato)cobalt.

The use of cobalt(III)cobaloxime compounds as substrates for electron transfer reactions with aliphatic radicals is particularly advantageous, as the cobaloxime(II) formed in the reaction has a large molar absorptivity in the visible[4]. Use of this visible absorption maximum thus avoids the nonspecificity of following a small UV absorption change in a region where the substrate absorbs. The reaction of $BrCo(dmgH)_2(H_2O)$ and $ClCo(dmgH)_2(H_2O)$ with photochemically

$$BrCo(dmgH)_2(H_2O) + (CH_3)_2COH = Co(dmgH)_2 + CH_3C{=}O + H^+ + Br^-$$

produced 1-hydroxy-1-methylethyl radical, trivially the hydroxyisopropyl radical, is the subject of this paper.

Experimental

Reagents The $BrCo(dmgH)_2(H_2O)$ and $ClCo(dmgH)_2(H_2O)$ complexes were prepared by the literature method[5]. All of the

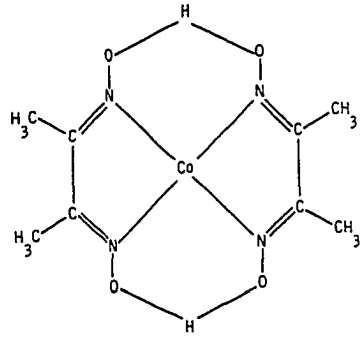

other material used in this study were reagent grade and were used as received.

Kinetics The flash photolysis experiments were performed on a Xenon Corporation Model 710 xenon flash lamp unit described previously[6]. Data from the photomultiplier tube were digitized and collected using a Nicolet model 2090-3A digital oscilloscope with a model 206-1 plug-in unit, which was interfaced with an Apple II computer. The reactions were monitored by measuring, in 5 cm quartz cylindrical cells, the growth in absorbance at the absorption maximum of the cobaloxime(II): λ 462 nm (ε 3400 $M^{-1}cm^{-1}$)[4].

Data Analysis The flash photolysis system can monitor events approximately 70 μs after the initiation of the light flash. Since the reactions of the hydroxyisopropyl radical with cobalt(III) complexes have high reaction rate constants (about 10^8 $M^{-1}s^{-1}$), the concentration of the cobalt(III) substrate must be kept low. In so doing, however, the

Scheme 1

$$R = (CH_3)_2\dot{C}\text{-}OH$$

$$R\cdot + Co(III) \xrightarrow{k_1} Co(II) + R^+$$

$$R\cdot + R\cdot \xrightarrow{k_2} (CH_3)_2C{=}O + (CH_3)_2CHOH$$

self-reaction of the radical can not be avoided, because the rate constant[7] for disproportionation of the hydroxyisopropyl

radical is 7×10^8 $M^{-1}s^{-1}$. Scheme 1 describes the reaction sequence.

A simple pseudo-first order treatment of the data can not be made for this reaction sequence, even though the absorbance growth of the cobalt(II) is monitored. A mixed first and second-order kinetic analysis is required. The rate laws for scheme 2 are shown in eq 1 and eq 2.

$$\frac{d[Co(II)]}{dt} = k_1[R\cdot][Co(III)] \qquad (1)$$

$$-\frac{d[R\ ]}{dt} = k_1[R\cdot][Co(III)] + 2k_2[R\cdot]^2 \qquad (2)$$

Integration of eq 2 leads to the concentration of the radical at any time. Substitution of [R·] into eq 1, followed by integration, yields eq 3, the time dependent expression for [Co(II)], where $P = k_\psi = k_1[Co(III)]$, $D = 2k_2$, and $C = [R\cdot]_0$.

$$[Co(II)]_t = \frac{P}{D}\left\{\ln\left[\frac{(P + DC)e^{(Pt)} - DC}{P}\right] - Pt\right\} \qquad (3)$$

The calculated value of the pseudo-first order rate constant, $k_1[Co(III)]$, hereafter referred to as k_ψ, can be

determined by using a nonlinear least squares analysis of the data according to eq 3. The initial concentration of the radical, $[R\cdot]_0$, must be known, however, in order to obtain a good estimate of k_Ψ. Since $[R\cdot]_0$ could not be measured directly, an iterative process was used to obtain k_Ψ and ultimately k_1.

The initial radical concentration can be expressed in terms of two factors as seen in eq 4[8]. The second factor

$$[R\cdot] = (\psi I_0 t)\{[10^{-\varepsilon[BrCo]}][1- 10^{-\varepsilon[A]}]\} \qquad (4)$$

depends on the concentrations and molar absorptivities of the acetone and halocobaloxime. This factor thus varies in a known way, from run to run, with the concentration conditions chosen. The first factor, $\psi I_0 t$, designated Q, depends upon the efficiency of the acetone photolysis, the light flash intensity and duration, and the geometric design of the system. The constant Q is thus a characteristic of a particular reaction system; it is however unknown and is thus refined during the iterative process to obtain $[R\cdot]_0$ and k_1.

To obtain the value of the rate constant, an initial estimate of Q is chosen (this in effect chooses $[R\cdot]_0$ by using eq 4), and k_Ψ is then calculated using eq 3. The reaction

rate constant, k_1, is then calculated from the least squares slope of a plot of k_ψ vs. $[XCo(III)]_{av}$. Using the

$$[Co(II)]_\infty = \frac{P}{D}\left[\ln\left(\frac{P + DC}{P}\right)\right] \qquad (5)$$

calculated value of k_1, $[R\cdot]_0$, and eq 5 (where $P = k_\psi$; $D = 2k_2$; and $C = [R\cdot]_0$), the final concentration of the cobalt(II) cobaloxime, $[Co(II)]_\infty$, is calculated. A correlation diagram between the observed yield and the calculated yield of the cobaloxime(II) is then constructed. A slight change is then made in Q, observing the result on the agreement between observed and calculated values of $[Co(II)]_\infty$. This process is continued until the correlation is virtually 1:1.

Results

The hydroxyisopropyl radical can be conveniently prepared by the UV irradiation of acetone in the presence of 2-propanol[9]. This represents the first reported use of this method to follow the kinetics of the radical produced.

Scheme 2

$$(CH_3)_2C{=}O \xrightarrow{h\nu} (CH_3)_2\dot{C}{-}\dot{O}$$

$$(CH_3)_2\dot{C}{-}\dot{O} + H{-}C(CH_3)_2OH \longrightarrow 2\ (CH_3)_2\dot{C}{-}OH$$

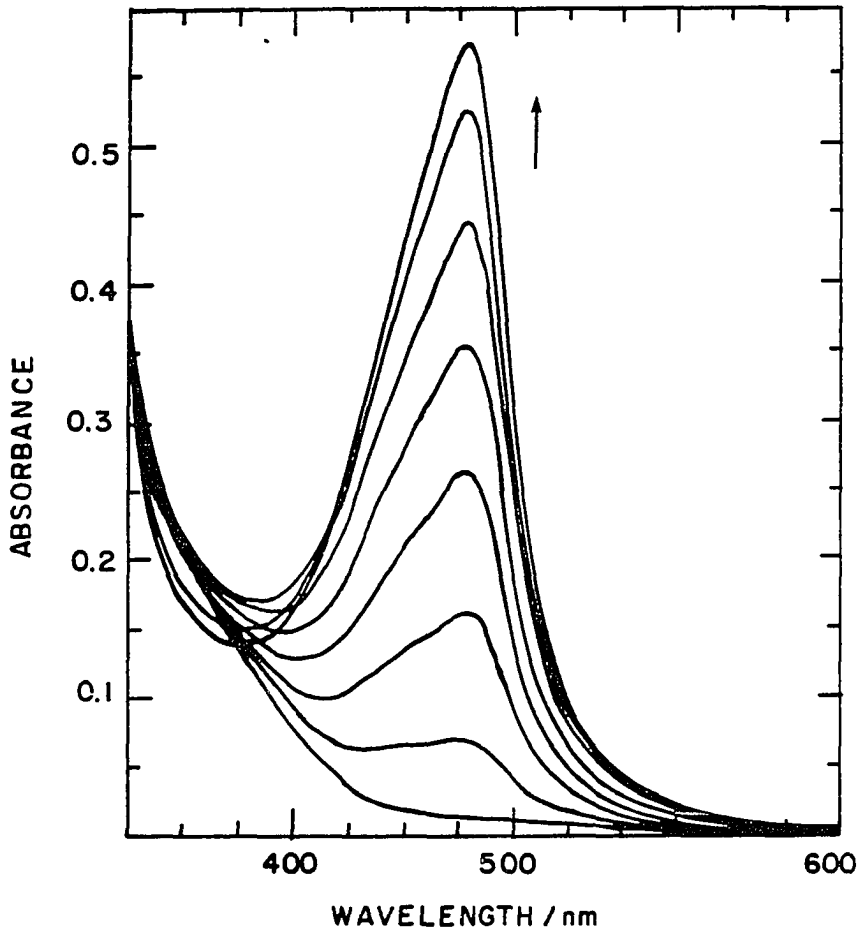

Figure III-1. Spectral changes during the photolysis of 1.9×10^{-4} M chlorocobaloxime in a pH 7.5, phosphate buffered, 1 M 2-propanol solution containing 1 M acetone. Each Scan was taken after 15 s of photolysis with a 275 W sun lamp

The triplet state of the excited acetone abstracts a hydrogen atom from the 2-propanol, producing two molecules of the hydroxyisopropyl radical.

Steady-state photolysis of a 1 M solution of 2-propanol, buffered by phosphate at pH 7.5, containing acetone and the desired cobalt(III) complex, efficiently produces cobaloxime(II). This can be seen in Figure III-1, which shows the growth in the Co(II) absorbance at 460 nm with photolysis time. Photolysis of the halocobaloxime in a solution containing only 2-propanol or only acetone does not produce the cobalt(II) cobaloxime. The reaction between the hydroxyisopropyl radical, produced by the flash photolysis of an acetone/2-propanol solution, and a given cobalt(III) complex can be easily monitored on a fast time scale (< 200 μs) by following the growth in the cobalt(II) cobaloxime absorbance with time.

Numerical Results The yield of cobaloxime(II) for the steady-state photolysis experiment shown in Figure III-1 is 87 percent. Close inspection of the spectrum shows that at the end of the photolysis the cobalt(II) concentration begins to decline. This is probably due to the reaction of the hydroxyisopropyl radical with the ligands of the cobaloxime(II) near the end of the reaction when [Co(II)] >> [Co(III)]. Since the yield of the cobalt(II) is 87 percent, the reaction of the strongly reducing radical with the

Table III-1. Kinetic Data for the Reaction of Hydroxyisopropyl Radical with Bromocobaloxime[a]

$10^5 \times [BrCo]_{av}$/M	[Acetone]/M	$10^6 \times [R\cdot]_0$/M
0.898	0.0054	11.2
0.915[b]	0.0025	5.23
1.39	0.0029	5.22
1.42[b]	0.0012	2.22
1.49[b]	0.0031	5.39
1.83	0.0076	10.9
2.35	0.0038	5.04
2.39[b]	0.0021	2.82
2.44[b]	0.0042	5.39
2.49[b]	0.0044	5.39
2.77	0.0107	10.7
2.97[b]	0.0079	7.85
3.31	0.0058	5.48
3.72	0.0157	10.5
3.88[b]	0.0033	2.84
4.67	0.0243	10.7

[a]The refined (iterative) value of the factor Q (eq 4) is 7.5×10^{-5}; pH 7.5 phosphate buffer, except as noted. T = 23 (±1)° C.

[b]These values were determined in a pH 8 acetate medium.

10^6x[Co(II)]$_\infty$/ M			
Calc	Obs	k_ψ/s^{-1}	$10^{-8}xk_\psi/[BrCo]_{av}$ /$M^{-1}s^{-1}$
2.66	2.04	960	1.07
1.92	1.70	1400	1.53
2.35	2.26	1910	1.37
1.41	1.42	2660	1.87
2.47	2.43	1660	1.11
3.93	3.40	2160	1.18
2.86	3.01	3650	1.55
1.94	2.26	4440	1.86
3.02	2.82	2400	0.98
3.07	3.93	3880	1.56
4.77	4.65	3760	1.36
4.13	4.66	4900	1.65
3.41	3.80	5450	1.65
5.37	5.57	5390	1.45
2.19	2.30	5190	1.34
5.94	6.66	8420	1.80
			1.46 ± 0.28

Figure III-2. Graphical display of the data for the reduction of bromocobaloxime by the hydroxyisopropyl radical. (A) Plot of k_ψ vs. $[BrCo]_{av}$ for bromocobaloxime, using Q = 7.5×10^{-5} M to calculate k_ψ. The line drawn is the least-squares fit line. (B) Plot of the calculated values of $[Co(II)]_\infty$ (eq 5) vs. the observed values of $[Co(II)]_\infty$ for the bromocobaloxime reaction. The line shown has a slope of 1.00. ■ denotes the runs using pH 7.5 phosphate buffer. ▲ correspond to runs using a pH 8.0 acetate medium

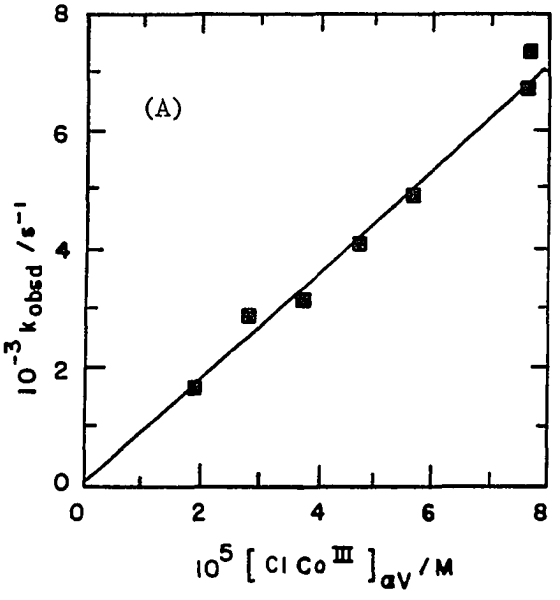
(A)
$10^{-3}\, k_{obsd}\ /s^{-1}$
$10^{5}\,[\,Cl\,Co^{III}\,]_{av}\ /M$
0
2
4
6
8

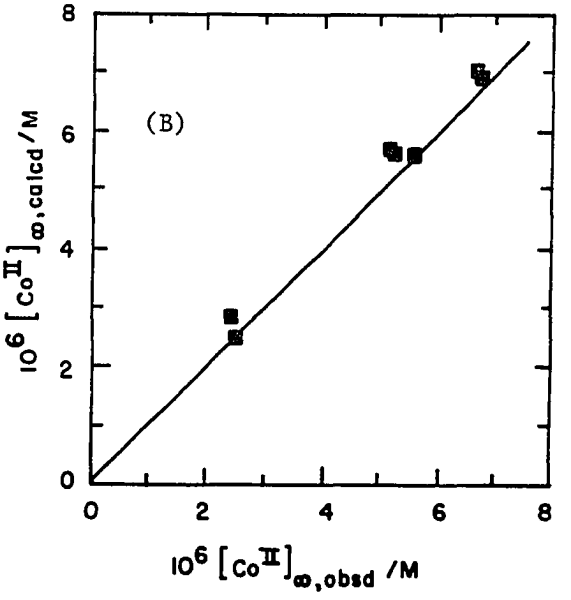
(B)
$10^{6}\,[Co^{II}]_{\omega,calcd}\ /M$
$10^{6}\,[Co^{II}]_{\omega,obsd}\ /M$
0
2
4
6
8

cobaloxime(II) is almost negligible in comparison to the reaction with the halocobaloxime(III) and only becomes important near the end of the steady-state photolysis. This result is not unexpected as the cobaloxime(III) is a much better oxidant than the cobaloxime(II)[10]. Consequently, one need not consider the reaction of the hydroxyisopropyl radical with the cobaloxime(II) in the flash photolysis experiments, which were conducted in the presence of excess Co(III).

The values of $[R\cdot]_0$ and k_ψ for the reaction of the hydroxyisopropyl radical with bromocobaloxime are given in Table III-1. The bromocobaloxime concentrations used ranged from 1×10^{-5} M to 5.00×10^{-5} M. This reaction was performed in a pH 8 acetate medium and a pH 7.5 phosphate buffer; there was no difference in the results obtained. The average bromocobaloxime concentration was calculated by subtracting half of the observed $[Co(II)]_\infty$ from the initial [BrCo(III)]. The value of k_1 for the bromocobaloxime is $(1.5\pm0.3)\times10^{8}M^{-1}s^{-1}$ and was determined using $Q = 7.5\times10^{-5}$ M. A least squares analysis of the final correlation between observed and calculated $[Co(II)]_\infty$ yielded a value of 0.95($\pm$0.03) for the slope. Figure III-2 shows the k_ψ vs. $[Co(III)]_{av}$ plot and the $[Co(II)]_{calc}$ vs. $[Co(II)]_{obs}$ plot for the bromide complex.

Table III-2 gives the values of $[R\cdot]_0$ and k_ψ for the chlorocobaloxime complex. This complex was only studied in the pH 7.5 phosphate buffered medium with a concentration

Table III-2. Kinetic Data for the Reaction of Hydroxyisopropyl Radical with Chlorocobaloxime[a]

$10^5 \times [ClCo]_{av}$/M	[Acetone]/M	$10^6 \times [R\cdot]_0$/M
1.88	0.0028	9.36
2.87	0.0019	5.08
3.74	0.0117	19.9
4.74	0.0115	15.2
5.66	0.0243	19.9
7.66	0.0376	15.0
7.72	0.0183	9.99

[a]The refined (iterative) value of the factor Q (eq 4) is 1.5×10^{-4} M; pH 7.5 phosphate buffer. T= 23 ($\pm$1)° C.

10^6x[Co(II)]$_\infty$/ M			
Calc	Obs	k_ψ/s^{-1}	$10^{-7}xk_\psi/[ClCo]_{av}/M^{-1}s^{-1}$
2.71	2.50	1630	8.67
2.48	2.55	2880	10.0
5.55	5.26	3180	8.50
5.59	5.24	4060	8.57
6.99	6.72	4870	8.60
7.01	6.82	6650	8.68
5.53	5.57	7300	9.46
			8.92 ± 0.57

Figure III-3. Graphical display of the data for the reduction of chlorocobaloxime by hydroxyisopropyl radical. (A) Plot of k_ψ vs. $[ClCo]_{av}$ for chlorocobaloxime, using $Q = 1.5 \times 10^{-4}$M to calculate k_ψ (B) Plot of the calculated values of $[Co(II)]_\infty$ (eq 5) vs. the observed values of [Co(II)] for the chlorocobaloxime reaction. The line drawn has a slope of 1.00

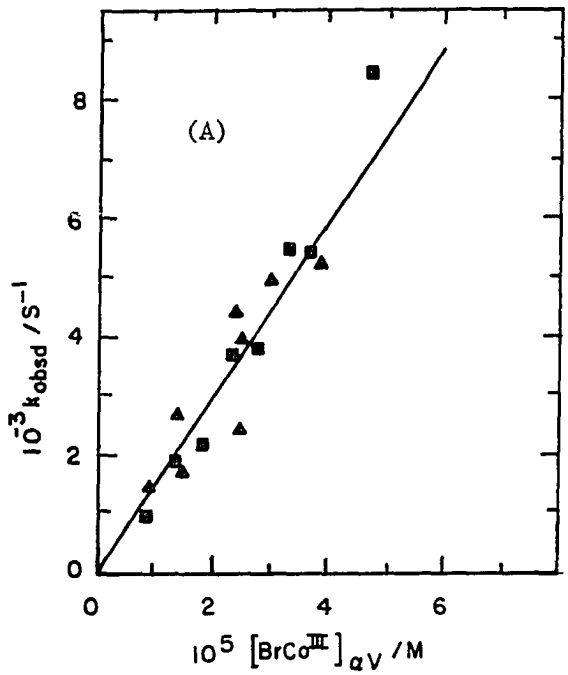
(A)
$10^{-3} k_{obsd} / S^{-1}$
$10^{5} [BrCo^{III}]_{aV} / M$
0
2
4
6
8

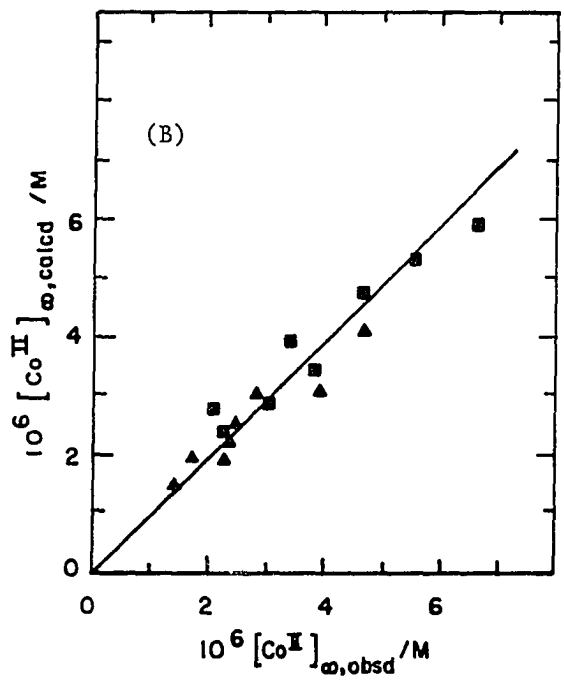
(B)
$10^{6} [Co^{II}]_{\infty,calcd} / M$
$10^{6} [Co^{II}]_{\infty,obsd} / M$
0
2
4
6

range of 2.0 to 8.0×10^{-5} M. As before, the average [ClCo(III)] during a run was calculated by subtracting half of the observed $[Co(II)]_\infty$ from the initial chlorocobaloxime concentration. The rate constant for the reaction between the chloro complex and the hydroxyisopropyl radical is $(8.9 \pm 0.6) \times 10^7$ $M^{-1}s^{-1}$ and was determined using $Q = 1.5 \times 10^{-4}$ M. The value of the final cobalt(II) concentration correlation, determined from a least squares analysis of the data, is $1.03(\pm 0.01)$. Figure III-3 shows plots of k_ψ vs. $[ClCo(III)]_{av}$ and of observed vs. calculated values of $[Co(II)]_\infty$.

Discussion

The reactions of alkyl radicals with metal complexes can proceed by an inner-sphere electron-transfer (or atom abstraction) pathway. Cyclopentyl radical and isopropyl radical are both known[11,12] to react with $BrCo(NH_3)_5^{2+}$ to yield the corresponding alkyl bromides. The reaction of alkyl radicals with $Ir(Cl)_6^{2-}$ also gives the atom abstraction product[13]. Concurrent with this reaction, however, is an outer-sphere mechanism which forms an alcohol product. In addition, copper(II) complexes show an increasing tendency toward direct atom transfer to an alkyl radical as opposed to direct attack at the metal center as the radical changes from methyl to ethyl to isopropyl[14].

The reduction of metal complexes with hydroxyalkyl radicals cannot, however, be as easily described in terms of

an outer-sphere or inner-sphere mechanism. The products in both cases would be the same: reduced metal complex, halide, proton, and an aldehyde (if the parent alcohol is primary) or a ketone. The formation of the products in the inner-sphere case can occur by two possible paths, since the bridged transition state can decompose two ways as shown in Scheme 3. The first, P_1, involves the formation of the reduced metal complex and an α-haloalcohol which would subsequently yield the aldehyde or ketone,

Scheme 3

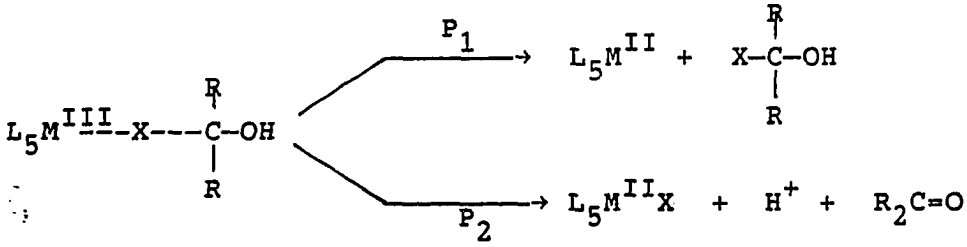

the halide, and the proton. The second path, P_2, is the formation of the aldehyde or ketone and the proton directly, leaving a reduced metal halide complex. If the reduced metal is labile, this complex would decompose to the halide and reduced metal ion.

Evidence cited[1] in favor of a bridged transition-state involved the large rate changes encountered upon changing the bridging ligand. It was also found that the reaction of

hydroxymethyl radical with $(NH_3)_6Co^{3+}$ did not proceed by a simple outer-sphere mechanism.

The results of this work and some selected values from the work of Cohen and Meyerstein[1] are presented in Table III-3. They found a reactivity pattern similar to the halocobaloximes (BrCo>ClCo), although there were much larger differences between their values of the rate constants.

Table III-3. Rate Constant Comparisons for Several Hydroxyalkyl Radicals With Some Complexes of Cobalt(III)[a]

	$10^{-7}x\ k_1\ /\ M^{-1}s^{-1}$				
Radical	A_5CoF^{2+}	A_5CoCl^{2+}	A_5CoBr^{2+}	$(dmgH)_2CoCl$	$(dmgH)_2CoBr$
$HOCH_2$	0.8	3.0	18	----	----
$(CH_3)_2COH$	0.22[b]	4.0	30	8.9	15

[a]The rate constants for the pentaamminecobalt(III) complexes were taken from ref 1.

[b]This value was taken from ref 15.

The relative insensitivity of the reaction rate constant to the bridging ligand in this work suggests the possibility of an outer-sphere electron-transfer. This is not unusual since α-hydroxyradicals have been suggested to react

predominantly by o.s. electron transfer[13]. In addition, the cobaloximes have low lying π^* orbitals[16] which could facilitate electron transfer to the cobalt. These π^* orbitals, which arise from the unsaturated oxime ligands, are unavailable to the halopentaamminecobalt(III) complexes. Finally, reductions of some similar cobalt(III) macrocycles, $XCo(Me_4[14]tetraeneN_4)$ and $XCo(Me_4[14]4,11\text{-}dieneN_4)$[17], also showed small changes in reactivity with the change of the axial ligand.

Summary

A convenient method for the generation of 1-hydroxy-1-methylethyl radical by flash photolysis for kinetic studies has been described. The rates of electron-transfer from this radical with several cobalt(III) reagents were studied, aided by the large absorption growth of the cobalt(II) product in the visible. The small change in reaction rate as the axial ligand on the cobalt(III) cobaloxime is consistent with an outer-sphere electron transfer as is the availability of low lying π^* orbitals on the macrocyclic ligand.

Bibliography

1. Cohen, H.; Meyerstein, D. J. Chem. Soc. Dalton 1977, 1056.
2. Papaconstantinou, E. J. Inorg. Nuc. Chem. 1981, 43, 115.
3. (a) Campano, D.D.; Kantrowitz, E.R.; Hoffman, M.Z.; Weinberg, M.S. J. Phys. Chem. 1974, 78, 686. (b) Olson, K.R.; Hoffman, M.Z. J. Chem. Soc. Chem. Commun. 1974, 938.
4. Heckman, R.A.; Espenson, J.H. Inorg. Chem. 1979, 18, 38.
5. Costa, G.; Tauzher, G.; Puxeddu, A. Inorg. Chim. Acta 1969, 3, 45.
6. Ryan, D.A. Ph.D. Dissertation, Iowa State University, Ames, Iowa, 1981.
7. Simic, M.; Neta, P.; Hayon, E. J. Phys. Chem. 1969, 73, 3794.
8. Calvert, J.G.; Pitts, J.N., Jr. "Photochemistry"; John Wiley and Sons Inc.: New York, 1966; Chapter 7.
9. Kirker, G.W.; Bakac, A.; Espenson, J.H. J. Am. Chem. Soc. 1982, 104, 1249.
10. Dodd, D.; Johnson, M.D. Organomet. Chem. Revs. 1973, 52, 1.
11. Espenson, J.H.; Connolly, P.; Meyerstein, D.; Cohen, H. Inorg. Chem. 1983, 22, 1009.
12. Ryan, D.A.; Espenson, J.H. J. Am. Chem. Soc. 1982, 104, 704.

13. (a) Chen, J.Y.; Kochi, J.K. J. Am. Chem. Soc. 1976, 98, 6150. (b) Steenken, S.; Neta, P. J. Am. Chem. Soc. 1982, 104, 1244.

14. Kochi, J.K. In "Free Radicals"; Kochi, J.K., Ed.; John Wiley & Sons: New York, 1973; Vol. I, p 622.

15. McHatton, R.C.; Espenson, J.H. Inorg. Chem. 1983, 22, 784.

16. Schrauzer, G.N.; Lee, L.P.; Sibert, J.W. J. Am. Chem. Soc. 1970, 92, 2997.

17. Tait, A.M.; Hoffman, M.Z.; Hayon, E. Int. J. Radiat. Phys. Chem. 1976, 8, 691.

GENERAL SUMMARY

The reduction of pentaaquo(pyridine)chromium(3+) by tris-(bipyridyl)ruthenium(1+) ion occurs by direct electron transfer to the chromium(III). This result is supported by several findings including a Hammet correlation of the rates of reduction. The reduction of the pentaaquo(organo)-chromium(2+) ions reveals the possibility of a long-lived organochromium(1+) species.

The production of H_2 from chromium(II) or europium(II) ion solutions, using $Co(dmgBF_2)_2$ as a catalysts, proceeds by a mechanism that is analogous to the Michaelis-Menten mechanism for enzyme catalysis. The $Co(dmgBF_2)_2$ is reduced to a Co(I) intermediate in a reversible reaction. The electron transfer from Cr^{2+} to the Co(II) is inner-sphere occurring via a halide bridge. The Co(I) forms $HCo(dmgBF_2)_2$ in acidic solutions. It is the reaction of this hydridocobalt complex with H^+, that evolves the H_2 from the solution.

The ultra-violet photolysis of an aqueous acetone and 2-propanol solution produces 2-hydroxy-2-propyl radical. This radical reduces $XCo(dmgH)_2$ ($X = Cl^-$, Br^-) to $Co(dmgH)_2$. The $Co(dmgH)_2$ has a strong absorption maximum in the visible and thus provides an indicator for the reaction. This complex may also be useful as an indicator for the study of other reactions of this reducing radical.

ACKNOWLEDGMENTS

I would like to thank Dr. Espenson for his guidance during my graduate career. He maintained the right balance between directing the research in his group and allowing the student the expression of his/her thoughts. Very special thanks are also given to Dr. Andreja Bakac for supplying at times a needed compound or thought.

This acknowledgment would not be complete without also mentioning two people who had a strong influence on my development as a scientist. Mr. Mumford, my high school chemistry teacher, introduced and piqued my interest in the science through his enthusiastic and dedicated instruction. Dr. Wu, my organic chemistry professor at Southeastern Massachusetts University, helped me gain the self-confidence needed to continue my education towards this degree.